ANALYSES OF THE CLOUD CONTENTS OF MULTISPECTRAL IMAGERY FROM LANDSAT 2

ERTS Follow-on Programme Study No. 2962A
National Aeronautics & Space Administration,
Greenbelt, Md., U.S.A.

Final Report on

Mesoscale Assessments of Cloud and Rainfall over the British Isles

by

Eric C. Barrett

and

Colin K. Grant

2962A

Supported by the U.K. Department of Industry,
Monsanto House, 10-18, Victoria Street, London, SW1H 0NQ

June 1977

ANALYSES OF THE CLOUD CONTENTS OF MULTISPECTRAL IMAGERY FROM LANDSAT 2

ERTS Follow-on Programme Study No. 2962A

Final Report on

Mesoscale Assessments of Cloud and Rainfall over the British Isles

by

Eric C. Barrett

and

Colin K. Grant

Supported by the U.K. Department of Industry,
Monsanto House, 10-18, Victoria Street, London, SW1H 0NQ

June 1977

CONTENTS

I. INTRODUCTION

This investigation was conceived and proposed originally as a study of cloud and associated rainfall over south-western England and the western sea-approaches within the limits defined by latitudes 49° and 55°N, and longitudes 0° and 20°W, intimately associated with other proposals from the University of Bristol all relating to its Sabrina Project. This project is an inter-disciplinary study of the River Severn and its region, designed to consider many aspects of its natural science whether independent of, or affected by, the activities of man. Since the other proposals for a satellite component in the Sabrina Project dealt with evidences in Landsat 2 imagery of terrestrial and marine phenomena, involving their distributions and characteristics through space and time, it was decided that a complementary programme of work concerned with attendant atmospheric variables evidenced in the same Landsat imagery might contribute invaluable supporting information for use in analysis and interpretation of the surface phenomena.

In the event, since the related proposals were not accepted for the ERTS Follow-on Program, this study of cloud and rainfall had to stand alone as an independent investigation. Modifications to the study plan were inevitable, although efforts were made to follow the original intentions as far as possible.

The most significant basic change in the study plan involved the area to be investigated. Cut free from the need to focus exclusively upon south-western England it was proposed by the Principal Investigator, and agreed by NASA, that the whole of the British Isles be included in the study area, thereby increasing greatly the opportunities for comparisons with ground station data, though a large expanse of sea in the Western Approaches which had been included in the initial proposal was excluded from the study area, decreasing the chances that the data set might throw light on details of approaching systems of cloud and rain (see Barrett, 1973). The geographic co-ordinates of the study area finally approved by NASA were as follows:

Table 1

Effective co-ordinates for the revised study plan (clockwise order)

Corner	Latitude	Longitude
North-west	60°00'N	12°30'W
North-east	60°00'N	2°30'E
South-east	49°00'N	2°30'E
South-west	49°00'N	12°30'W

Once the flow of data from NASA had been established it became quickly apparent that the imagery were not being provided very completely for the study area, and worse still from the point of view of research design, were not being provided with any uniform or predictable distribution. In the Data Profile (Attachment B) sent by NASA to the Principal Investigator on the acceptance of his revised study proposals it was stated that NASA would make "best efforts to provide the Principal Investigator with the ERTS data described in the data profile" (NASA 1974). These were to cover the study region for the period from March

1975 - February 1976 for up to and including 100% cloud cover. Although it was anticipated that some short-fall from a complete coverage in space and time should be expected, no clear indication was received to the effect that the funds allocated to the cloud project would effectively limit the number of frames to only about one-third of the theoretical maximum. This large short-fall would, perhaps, have been less significant from the point of view of the redesign and development of the project as reported in this document had the coverage been reasonably complete in space and time for some pre-agreed sub-region within the British Isles. As remarked as early as the First Quarterly Report (Barrett & Grant, 1975), and as reiterated in subsequent reports, it was the fragmented nature of the coverage provided which ultimately affected most the programme of work which could be carried out. Correspondence on this point led to the assurance that efforts would be made to provide full Landsat coverage of the British Isles on the occasion of the last Landsat cycle falling within the study period (Cycle 23, 16 March - 2 April 1976): this was the only cycle for which arrangements could be made with other agencies for special support for the project, over and above that provided routinely by the British Meteorological Office in the form of maps of hourly weather observations for synoptic stations in the British Isles, and that provided in effect by other authorities routinely observing weather elements, especially rainfall.

For the most part, therefore, the studies described in the Final Report relate to treatment of the available Landsat 2 imagery of the British Isles as a total data set from which a range of general conclusions have been drawn concerning atmospheric phenomena observed by Landsat and from the ground in this mid-latitudinal region on the western edge of a major continental mass of land. Our image file, when complete, contained 491 Landsat scenes. Principal copies of this Final Report contain a computer tabulation of the image file in a pocket inside the back cover (q.v.). The geographic distribution of those scenes is summarised in Figs. 1 & 2. Their temporal distribution (time of day) is summarised in Fig. 3. One special study (see Sections II.5 & III 5) relates to investigations involving special radar and aircraft support facilities arranged in advance for Cycle 23; this exemplifies the type of study we had hoped might have been more frequently possible during the 12 months of the Landsat imagery exercise. Had these hopes been realised, we should have been able to have fulfilled the revised study plan much more completely than we were in fact able to do.

Notwithstanding our problems and their repercussions we feel that much has been learnt from the study we were able to carry out, and that the spirit, if not in all cases the precise letter, of the original proposals has been well satisfied. Clearly the Landsat 2 data file that has been built up for the British Isles from March 1975 - March 1976 has much more to offer the atmospheric scientist than we have been able to identify and appreciate through our 2-year study period. It is intended that further investigations be undertaken in the near future to extend the value of the Landsat 2 file as a unique source of meteorological information for this area. Such investigations will focus particularly on an extension of the work reported here relating to the multispectral characteristics of different classes of clouds, and on case studies of the more interesting mesoscale cloud structures which appear in the data file.

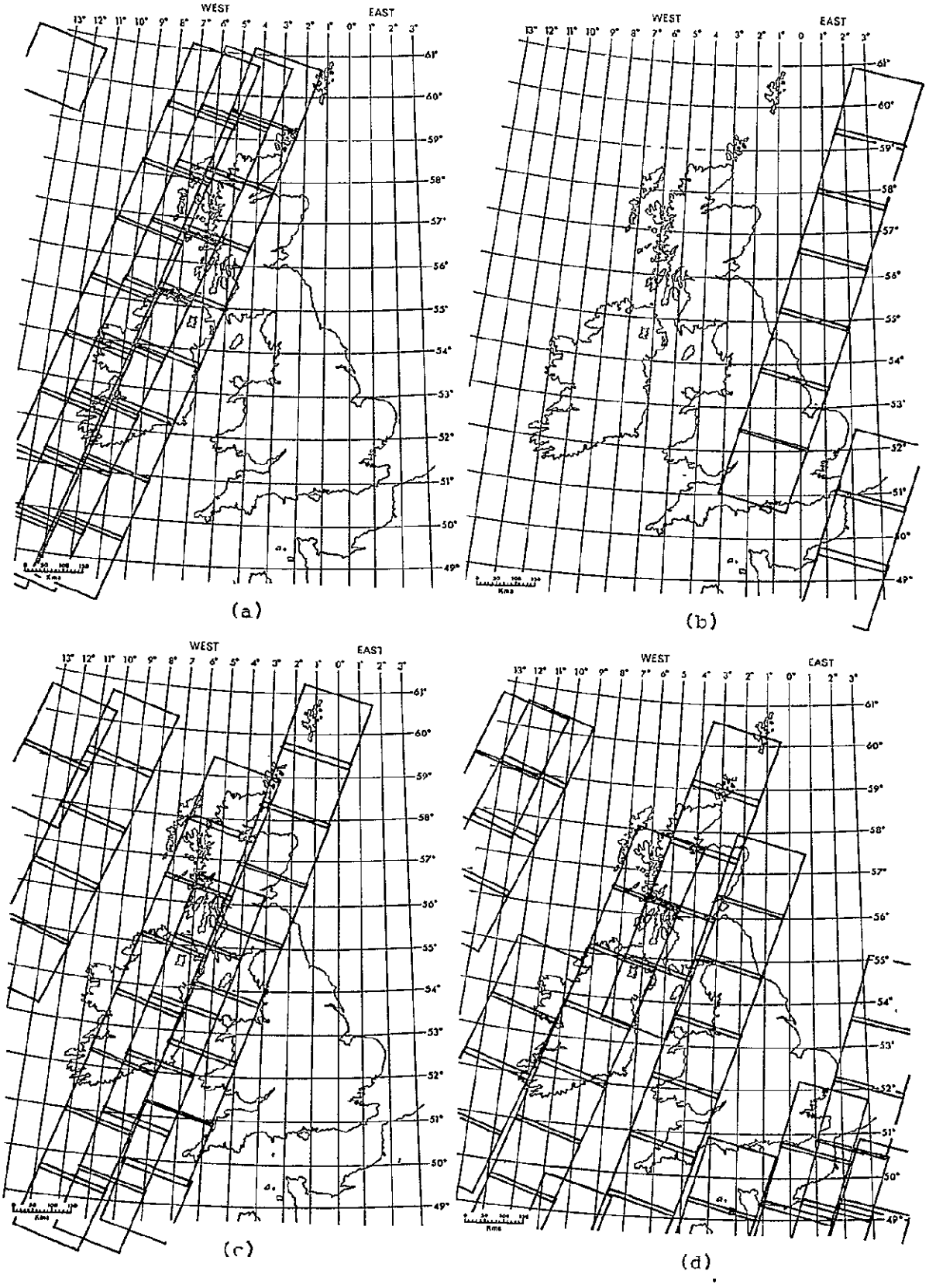

ORIGINAL PAGE IS
OF POOR QUALITY

Fig. 1 (a-d): Geographical distribution of images; Cycles 3,4,6 & 7.

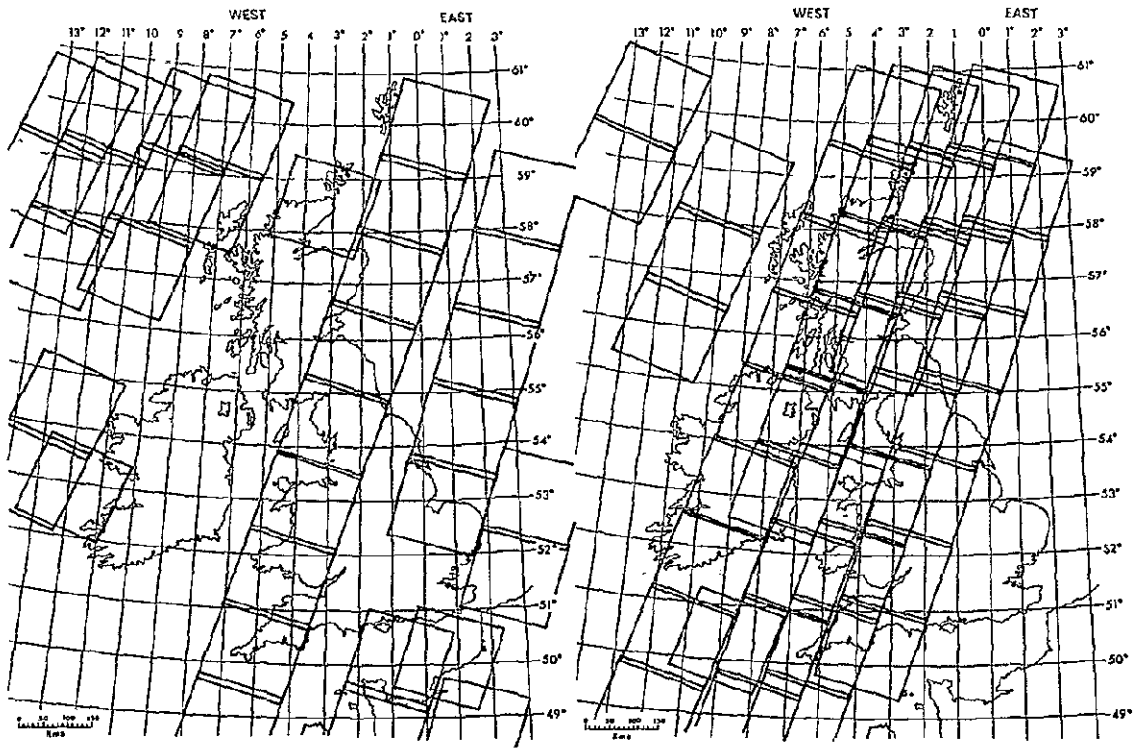

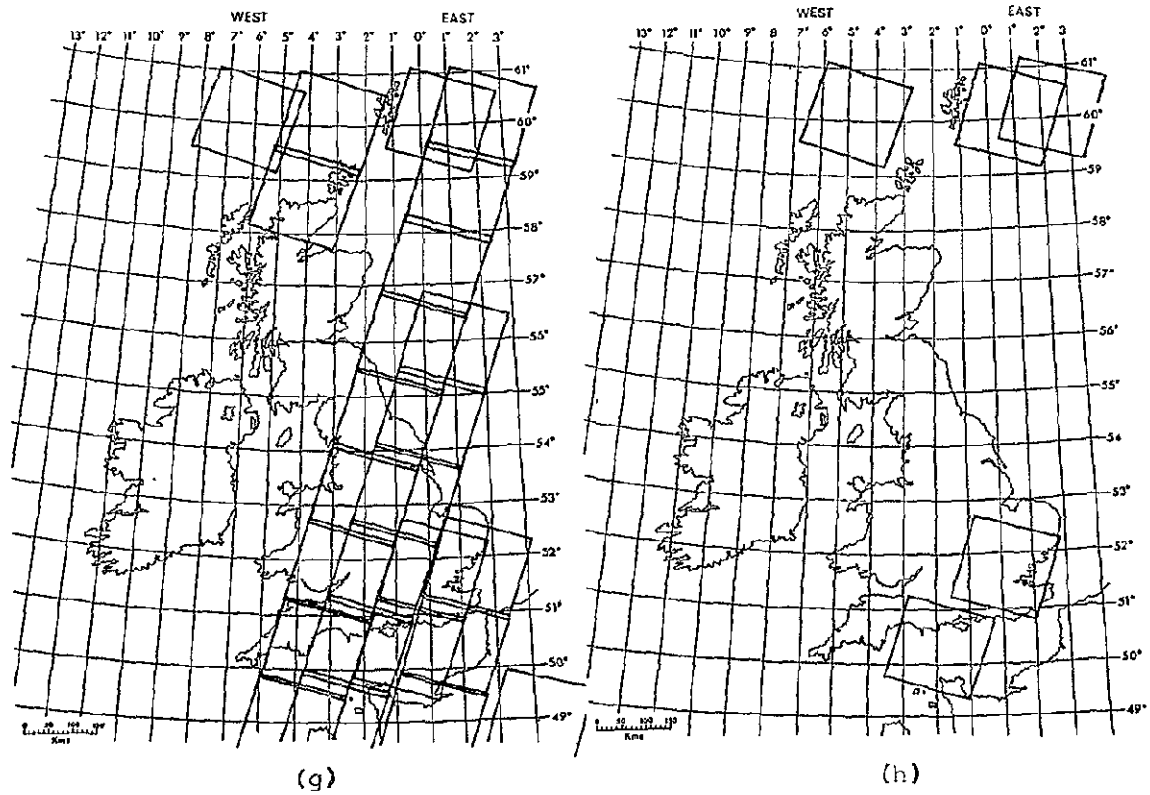

Fig. 1 (e-h): Geographical distribution of images: Cycles 8 to 11

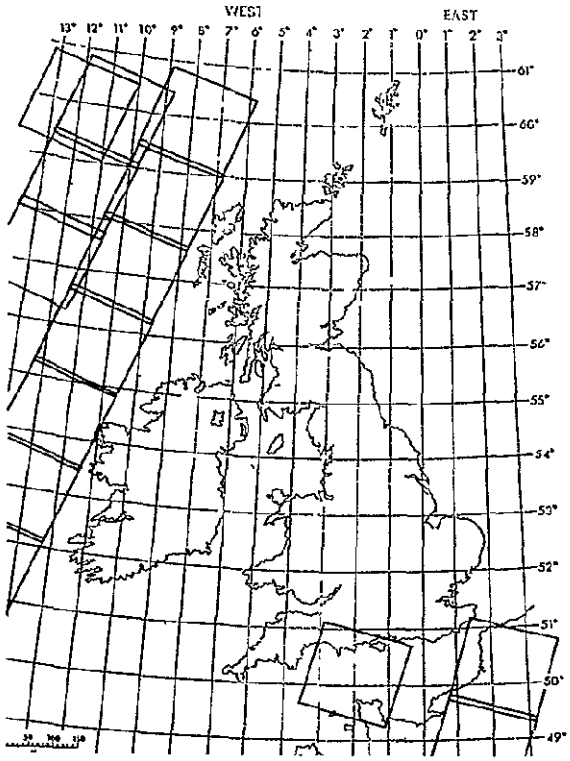

(i)

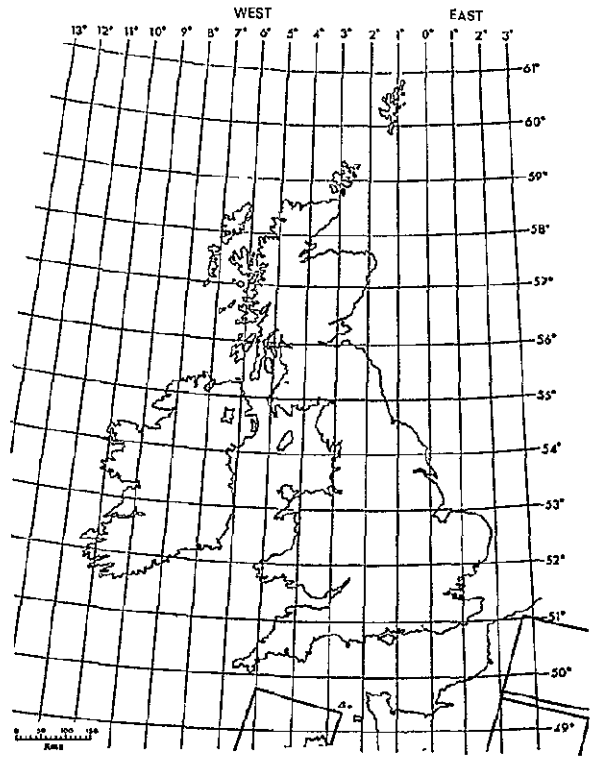

(j)

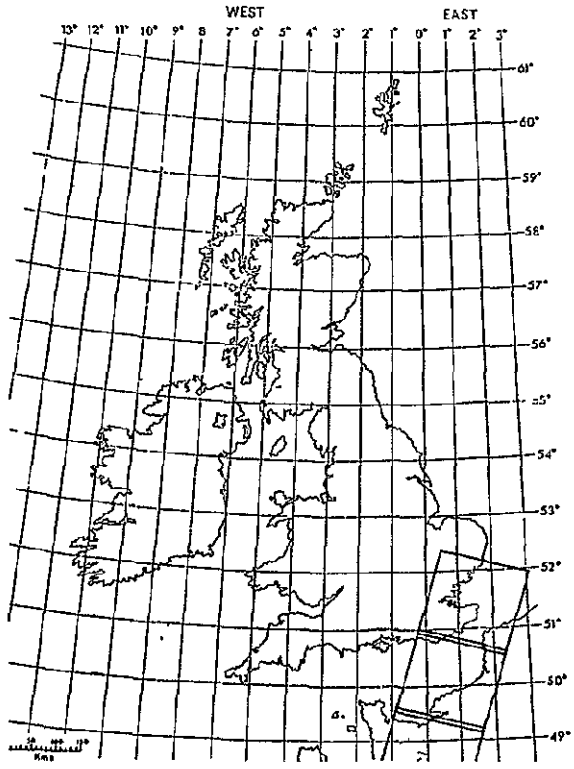

(k)

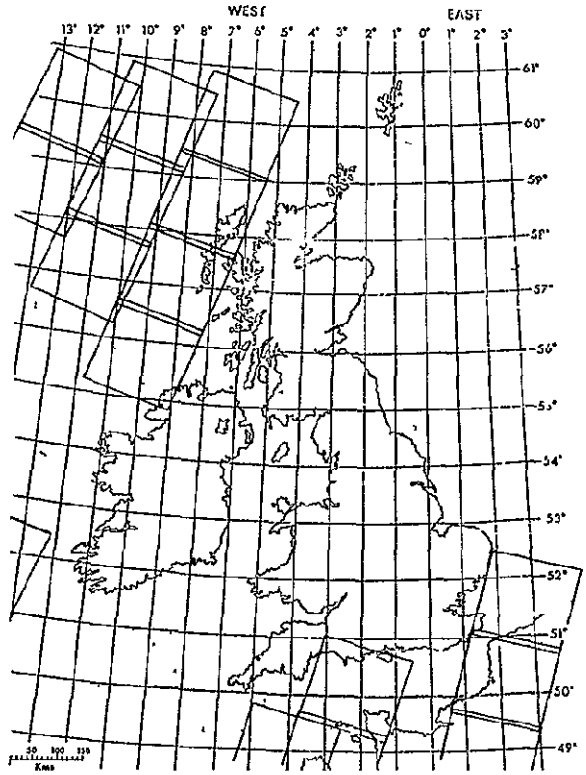

(l)

Fig. 1 (i-l): Geographical distribution of images: Cycles 12 to 15

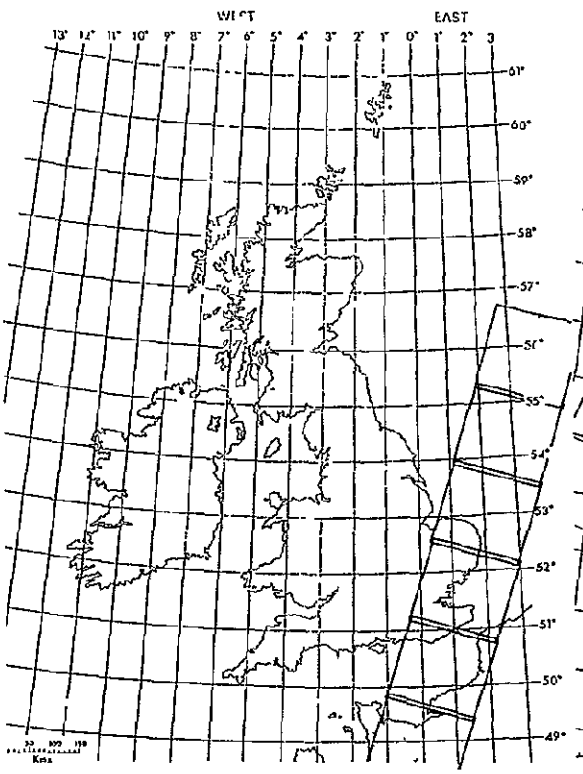

(m)

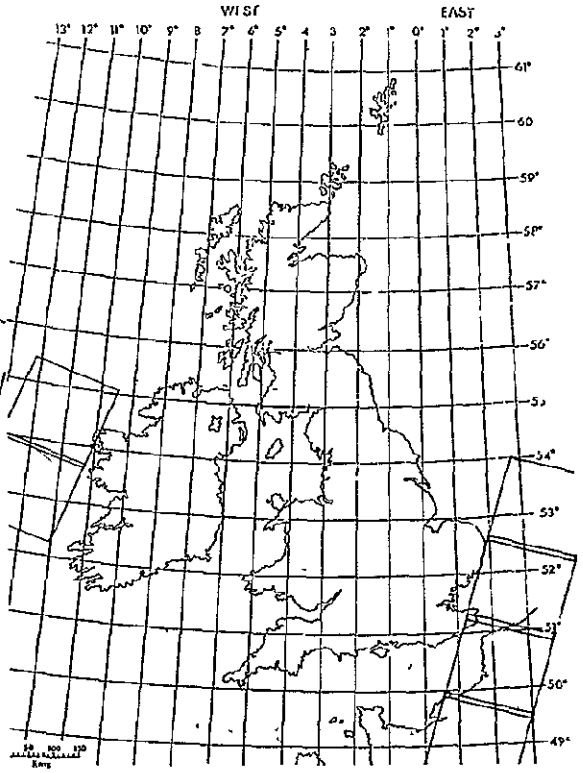

(n)

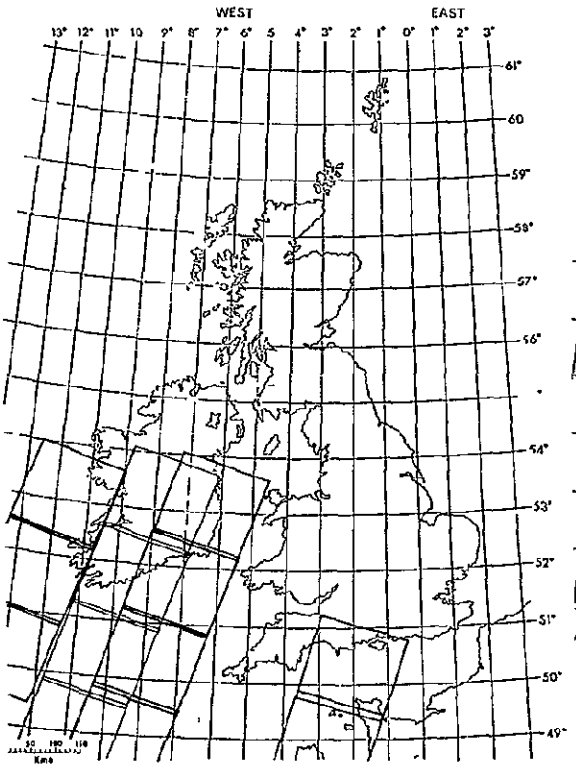

(o)

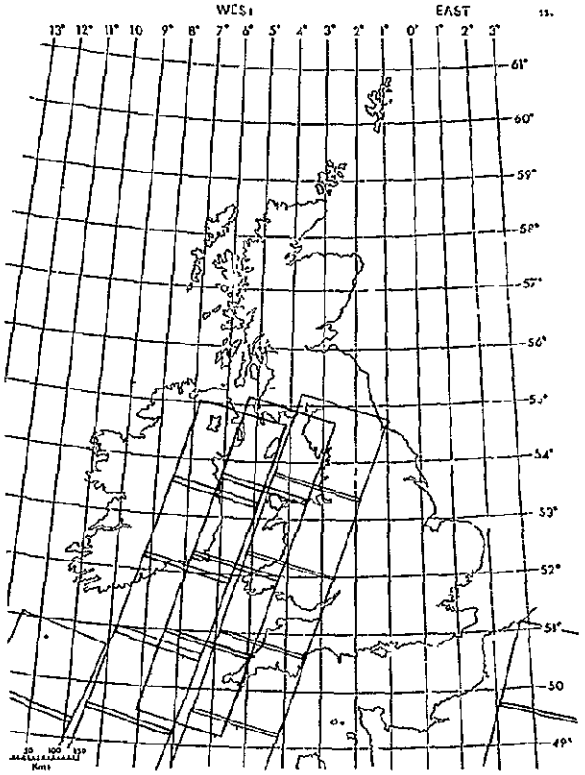

(p)

Fig. 1 (m-p): Geographical distribution of images: Cycles 16 to 19

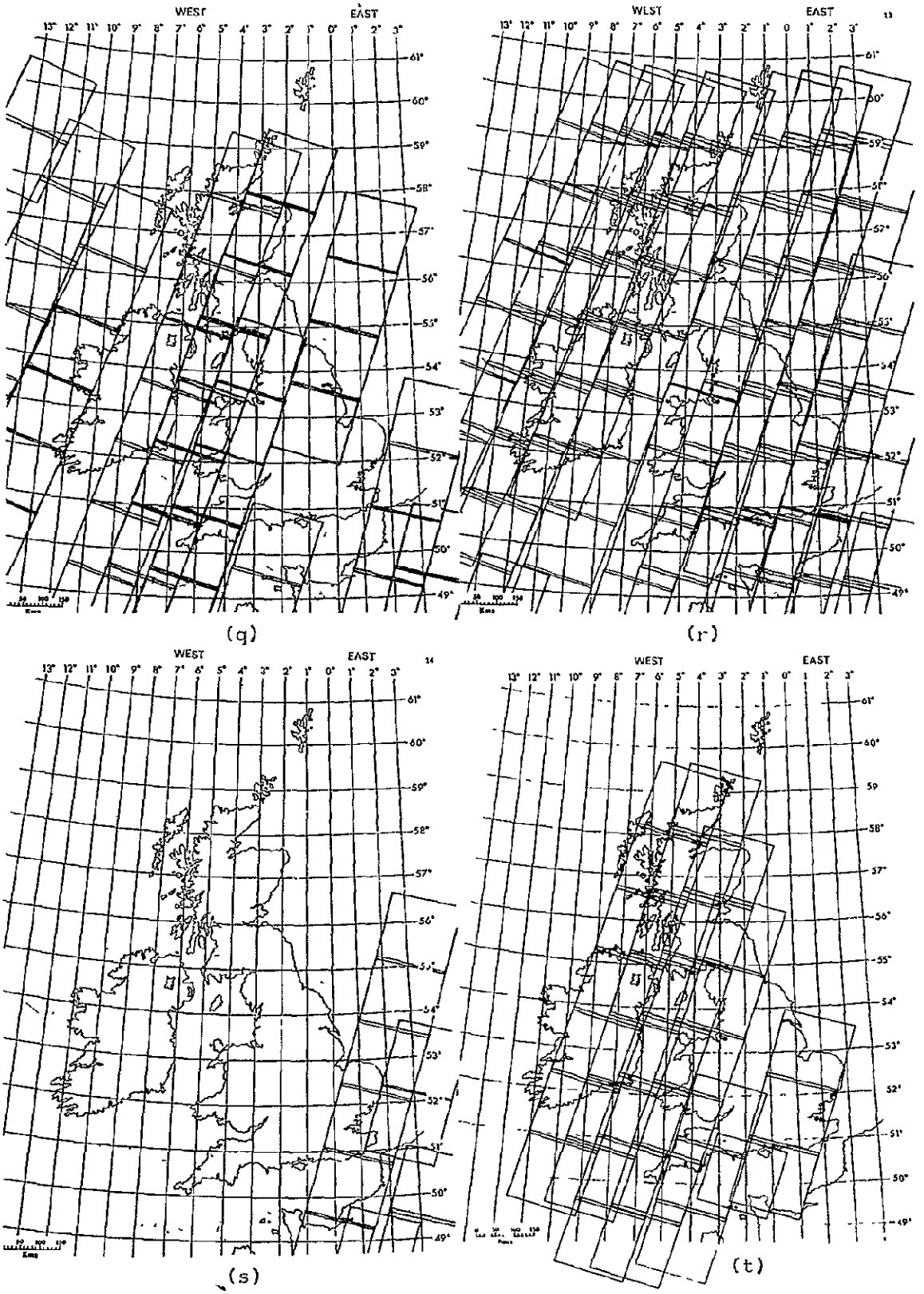

Fig. 1 (q-t): Geographical distribution of images: Cycles 20 to 23

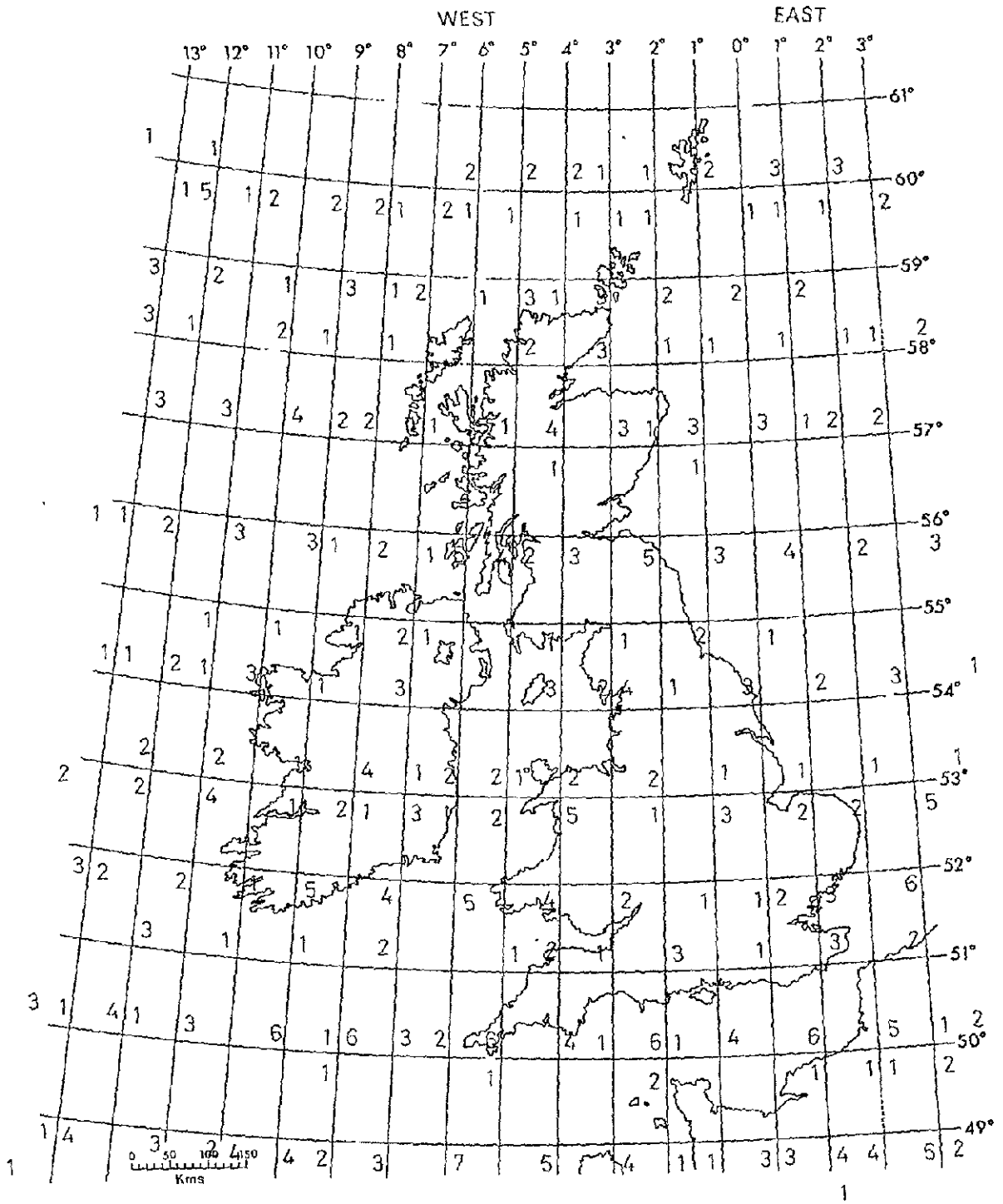

Fig. 2: Geographical distribution of imagery (total)

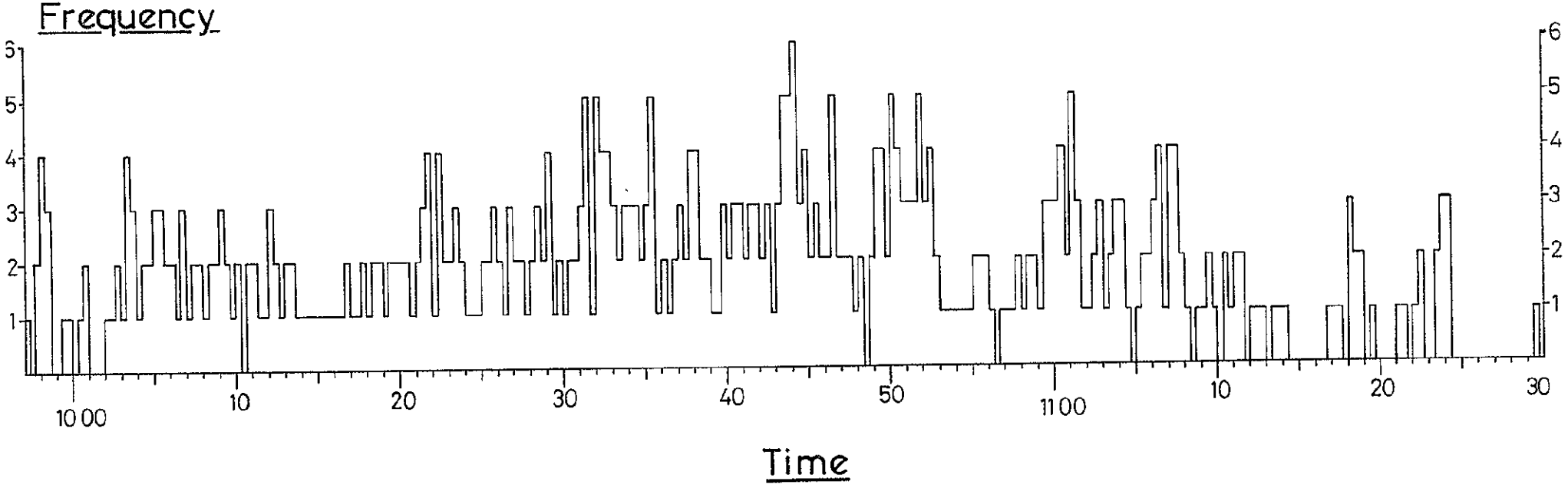

Fig. 3: Temporal distribution of imagery.

The purpose of this Final Report is, therefore, to report and discuss those findings which we have accumulated during the period covered by the tripartite agreement between NASA, the U.K. Department of Industry, and the University of Bristol, which expires in mid-1977. The structure of the Report follows the pattern required by NASA, a pattern perhaps better suited to projects with a more unitary structure than our own: it will be seen that in Sections II, III & IV "Techniques", their resulting "Accomplishments" and author-identified "Significant Results" are separated from one another. In conformity with NASA's advice and in order to achieve maximum clarity in terms of the relations between the various techniques adopted for different components of our work and the results which we obtained therefrom, we have broken Sections II, III & IV into 7 parallel sub-sections, in which the internal orders are the same.

II. TECHNIQUES

1. The compilation of a Landsat Cloud Photointerpretation Key

In the early stages of this ERTS Follow-on Study it was recognised that:

(a) The appearances of different cloud types would not be the same in Landsat imagery as in the meteorological satellite imagery with which we were more familiar. The higher resolution of the Landsat imagery (c. 80m, cf. previous best resolutions of 0.6km from the American DMSP satellites, 0.9km from the operational Noaa satellites) would reveal much more cloud detail, whilst the multi-spectral capability of the Landsat system (cf. the uni- or bispectral capability of most weather satellites) might be an aid to the correct identification of cloud types hard to separate in cloud images from other satellites.

&(b) Although detailed attention had been given earlier to the description and identification of clouds portrayed by images from meteorological satellites (e.g. Anderson et al, 1974; Barrett, 1974; Conover, 1962 & 1963; Hopkins, 1967; and Lee & Taggart, 1969) no similar analyses seemed to have been undertaken of Landsat MSS imagery.

We felt, therefore, that the compilation of a Landsat Cloud Photointerpretation Key was a task we should undertake urgently as a basis for our own subsequent Landsat cloud studies, and that the resulting identification scheme would be of interest and value to other members of the scientific community in any way concerned with the cloud contents of Landsat images. The method summary that follows is based on that which appeared in the Second Quarterly Report by Barrett & Grant (1976); the dependent Cloud Photointerpretation Key (see Section III.I) is reproduced from that source without modification.

In selecting "classic" examples of different cloud types for consideration in the compilation of the Landsat Cloud Photo-interpretation key, the following steps were taken:

(a) Numbers of Landsat 2 70mm positive transparencies were laid out on large light tables, and separated into sets on the basis of their dominant cloud contents. The family categories adopted were those commonly employed in meteorological satellite nephanalysis procedures (see Harris and Barrett, 1975), namely cumulonimbiform, cumuliform, stratiform, cirriform and stratocumuliform. Recourse was made to the hourly charts of meteorological observations made by stations within the synoptic reporting network of the U.K. Meteorological Office (see Fig. 4) to confirm that the dominant cloud categories had been correctly identified.

(b) The initial sets were examined separately so that a small number of images containing type examples of those different cloud families could be identified.

(c) The sets of type examples were viewed on a microfilm reader (E.Marshall Smith Ltd., Bournemouth), with X14 and X25 magnification in order that the finer details of the five basic cloud families might be examined closely and

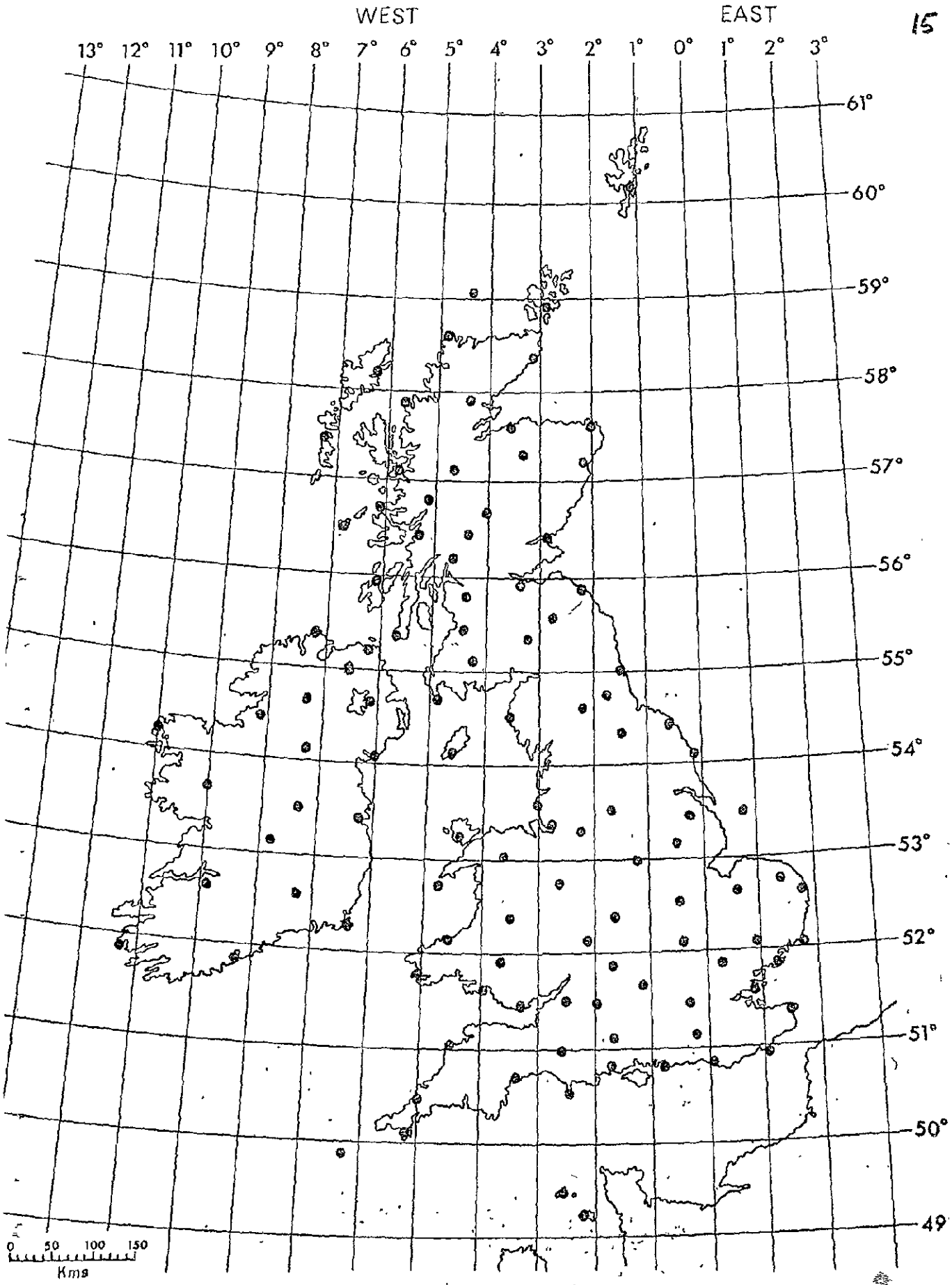

Fig. 4: Chart of hourly reporting stations.

(d) Representative examples of the five cloud families, and their more important members evident in the Landsat imagery, were selected for incorporation and description in the photo-key (see Plates 1-5).

At each stage in this procedure there was dependence upon previously-gained experience in cloud recognition using meteorological satellite imagery, and a knowledge and understanding of the principles upon which commonly-accepted cloud classifications from ground viewing positions are based.

2. The comparison of cloud cover evaluated from Landsat 2 imagery and conventional meteorological stations across the British Isles

Introduction

In the previous sub-section attention was paid to the compilation of cloud photointerpretation keys for application to Landsat imagery. This was a necessary undertaking in preparation for later stages of this ERTS Follow-on Programme Study, concerned as it was with aspects of mesoscale weather patterns over the British Isles.

In this sub-section our attention turns to comparisons between evaluations of cloud cover based on Landsat image analysis, and those observations of cloud recorded as part of the routine meteorological observing programme of stations reporting hourly to the British Meteorological Office (see Fig. 4). All previous studies of which we are aware, concerned with the reduction of satellite-derived cloud amounts to climatological information, have considered data from meteorological satellites, including members of the American Tiros, Nimbus, Essa, Noaa and DMSP families. Landsat is important because the scale of its data is larger than that of the highest resolution data from meteorological satellites by about one order of magnitude. Although the Landsat coverage is much less frequent (eighteen daily as against once or twice daily, geostationary and geosynchronous satellites excepted) Landsat-based studies of cloud cover may have important implications for the design of future environmental satellite systems, and for the joint practices of analysis and utilisation of cloud imagery for meteorological and climatological applications.

The earlier comparisons between satellite and conventional data are divisible into two groups, based on the nature of the analytical procedures applied to the satellite data. These are as follows:

(a) Eyeball (subjective) methods. In these not only are the ground observations made by eye (which is the standard practice in the United Kingdom, as described in the Meteorological Observer's Handbook (HMSO, 1969)), but also those assessments of cloud which are drawn from the satellite imagery. The products include schematized cloud charts (nephanalyses) which include an evaluation of cloud cover, whether the base data are visible (Harris and Barrett, 1975) or infrared images (Barrett and Harris, 1977), and tabulated cloud amount statistics prepared in analagous fashion to the conventional assessments of cloud amount by trained, experienced analysts. Examples of studies involving cloud amount mapping from neph-

analyses compiled for routine meteorological use are those reported by Clapp (1964), Godshall (1971) and Sadler (1969). Examples of statistical tabulations include those by Sherr et al., (1968) and Malberg (1973).

(b) Machine-assisted (partially objective) methods. Here the satellite image analyst is aided by some apparatus which reduces the reliance on human skill. Such methods have mostly involved some form of video processing or densitometry through which areas above a pre-selected brightness threshold are automatically summed. Examples of such studies include those by Miller (1971) (based on visible imagery) and Coburn (1971) (based on infrared imagery). Many factors complicate the selection of the brightness threshold. These include:

i) The waveband investigated;

ii) The characteristics and performance of the sensor system;

iii) The data path from sensor to display facility (including the passage through preprocessing and processing procedures);

iv) The characteristics of the display facility;

v) The time of year of each observation;

vi) The time of day of each observation;

vii) The dominant cloud type;

viii) Background brightness effects;

ix) User requirements; and

x) Operator performance.

Any or all of these may induce variance within a single set of results and/or differences between sets of results. In any operational scheme designed to run through extended periods of time very careful controls would be essential in every case.

With the experimental development of automatic devices for cloud cover assessment from the ground two other groups of techniques for the comparison of satellite and in situ ("ground truth") observations may become possible. These would relate the new objective surface observations to the satellite data evaluated by either eyeball or machine-assisted methods. Examples of studies of automated ground observation systems include the computer simulation exercises carried out by Duda et al., (1973) and the experimental use of a radiometer detector for cloud cover by Werner (1973).

Surface observations

As this study is concerned with comparisons of cloud cover statistics derived from Landsat 2 imagery with those from ground observations, a brief note is in order firstly concerning the surface observation technique.

In the U.K. cloud amount is reported in oktas (eighths), with the scale of values extending from 0, when the sky is completely cloudless, to 8 when the sky is completely overcast. The complete scale is listed below (HMSO, 1969).

Table 2

The U.K. code for reporting cloud amount

Code Figure	Amount of Cloud
0	Sky completely cloudless
1	Trace to 1/8
2	1/8+ to 5/16-
3	5/16 to 7/16-
4	7/16 to 9/16
5	9/16 to 11/16-
6	11/16 to 7/8-
7	7/8 to 8/8- (overcast with openings)
8	Sky completely overcast
9	Sky obscured or cloud amount impossible to estimate.

Note: (+) and (-) signs indicate "slightly more than", and "slightly less than", respectively.

The surface observer is instructed to estimate the cloud amount from a viewpoint which "commands the widest possible view of the sky", and he (she) should be "careful to give equal weight to the areas around the zenith and those at a lower angular elevation".

The Choice of Landsat imagery for cloud cover assessment studies

The Landsat MSS imagery consists of individual frames, each frame being comprised of 4 individual images, corresponding to the 4 separate wavebands of the multispectral scanner. It was decided that, for the purposes of this study, the examination of the imagery in a single waveband would suffice to provide estimates of satellite observed cloud amount. Band 5 imagery (0.6 - 0.7 μm) was chosen as this usually provides better contrast between background features and clouds than Band 4. The impression of improved contrast in Band 5 gained through simple eyeball observations is supported by a quantitative study by Danko (1974). He measured the contrast of a variety of cloud types against different land and water backgrounds in both Bands 4 and 5. The measured contrast in Band 5 was in each case more than one and a half times the contrast in Band 4.

The location of surface stations on Landsat imagery

One of the initial tasks in this study was to identify the positions of the surface observation stations on the Landsat imagery. The British Meteorological Office provided latitude and longitude coordinates for the stations concerned.

A map of the British Isles was prepared at the same scale as

that of the Landsat imagery (1 : 3,369,000). This was achieved by photographically reducing a map at a scale of 1 : 2,500,000 to the correct scale. The projection of the original map (and similarly the final, reduced product) was a Transverse Mercator, constructed by the U.K. Ordnance Survey. The surface stations were then marked on the final product.

It has been shown by Colvocoresses (1973) that the MSS bulk processed imagery has its own unique projection, termed the "Space Cylindrical Strip Perspective". However, it has been established that, in fitting the imagery to a Transverse Mercator projection, only small positional errors are introduced thereby (generally less than 1 : 1,000), and this was deemed sufficiently accurate for our purposes.

The Landsat MSS imagery is provided with latitude and longitude marks on the outside edge of the image writing area at intervals of 30 arc minutes. It has been noted that the latitude and longitude marks are often in error by up to 5 or 6 kms., sometimes more (e.g. Mott and Chismon, 1975). This could result in our station circles being displaced by up to about 20% of their areas. As the cloud cover in most of the images was substantial, it was not possible to use visible landmarks to improve the "fit" of the imagery to the map of surface station locations. However, it is felt that any errors incurred as a result should be randomly distributed and therefore not substantially affect the final results.

Using the latitude and longitude marks, it was possible to fit the images to the map of surface station locations. For each image, a thin sheet of clear plastic was overlayed, and the positions of the stations falling within the image area were marked on the plastic by small dots. To facilitate the accurate relocation of the overlay small dots were applied to the plastic, coincident with the centres of the four registration marks (crosses) provided at the corners of each image.

The choice of station circle size

The next phase of the study was to determine on the Landsat imagery, the size and shape of the area which would be used to extract cloud amount statistics. A circular area, centred at the station location, was felt to represent best on the image the surface observer's view of the sky. The surface observer has a very limited field of view in comparison with the satellite. The maximum radius of his vision is about 50 kilometres, depending on topography, visibility and local obstructions. However, this maximum value is rarely achieved in practice, and, frequently, a very much smaller field of view is observed. It had been hoped at an earlier stage in this study, that we would have been able to take account of factors such as obstructions to the fields of view from individual surface observation positions, and then to assess their effects on cloud amount estimation (Barrett and Grant, 1975). However, further consideration of the matter, including discussions with surface observers and senior officials at the U.K. Meteorological Office led us to abandon such a course. One of the major problems was that many surface stations are situated at, or near, military establishments. Permission for access to these for the purpose of sketching the silhouettes of buildings and other installations would not have been easily or rapidly obtained.

Having decided thus that the shape of the data extraction area was to be circular, we next considered the question of its size. Similar studies have utilised circles of various sizes to provide comparisons with surface observations.

Studies by Sherr et al. (1968), Glaser et al. (1968) and Greaves (1973) all used circles with a diameter of 1° of latitude (approximately 111 kilometres), to extract cloud amount statistics from Nimbus II and Essa imagery. A study by Barnes and Chang (1968) examined the effect of varying the circle diameter. They used circles with diameters of $\frac{1}{2}^{\circ}$, 1°, 2° and 3° of latitude. These diameters correspond to distances of 56, 111, 222 and 333 kilometres respectively on the ground. They found that the $\frac{1}{2}^{\circ}$ diameter circle provided the closest approximation to values of cloud amount registered by surface observers. They concluded that "... for climatological purposes, satellite cloud amounts extracted for circular areas of about $\frac{1}{2}^{\circ}$ latitude diameter can be considered to form a sample compatible with surface observations".

It was decided therefore to employ a circular area with a diameter of 50 kilometres to extract cloud amount statistics from the Landsat imagery.

The sample size

The total number of frames available at the time of preparation of the Third Quarterly Report (Barrett & Grant, 1976), when the method was first described and initial results presented, was 328 (Landsat cycles 1 - 20). However, many of the frames portrayed sea areas, with consequently no compatible surface observations. Therefore, the number of suitable frames was reduced to 131. The number of surface observations available for each frame varied, from one to a maximum of six. It was decided to include only those surface observations around which a complete circle of 25 km. radius could be drawn within the image area. In this way a number of additional problems were avoided. Thus the total number of satellite image observations available for comparison with surface observations was 288. At a later stage all occasions when code figure 9 was reported at the surface were withdrawn from the population on account of the ambiguity of this surface observation. This reduced the number of comparisons to 282. We are now able to present complete results for the whole study period, for which a total of 438 comparisons were available.

Methodology

As noted in the introduction, in similar studies of this type both eyeball and machine-assisted methods have been employed. This study included both approaches. The work was undertaken in two phases. The first phase was machine-assisted, using a Quantimet 720 Image Analysing Computer at ADAS, Cambridge (see Plate 6). The second phase was an eyeball investigation of the same images, using a microfilm reader to enlarge the 70mm images to a comfortable viewing size. The two sets of results were then compared with the corresponding surface observations of cloud amount extracted from the hourly charts provided by the Meteorological Office.

Phase I : Machine-assisted method

The Machine

The Quantimet 720 Image Analysing Computer used in this study was manufactured by Cambridge Instruments and is owned by the Air Photography Unit of the Agricultural Development Advisory Service (ADAS), Ministry of Agriculture. (see Plate 6)

The input peripheral of the instrument is an epidiascope connected to a vidicon camera. Illumination of the images was by fluorescent tubes with a diffuse screen intervening. The lens attached to the vidicon in this study had a focal length of 51 mm (f1.9), providing the largest magnification of the original image while retaining on the display screen a circular analysis area equivalent to a circle of 50 km diameter (see Plate 7). As large a magnification as possible was chosen (approximately 7 times the original) in order that as much of the original image detail should be retained. The vidicon in the system was specifically designed for image analysis purposes and incorporates a 720-line scan, with no interlacing, and a very slow scan rate of 10.6 scans per second.

The image is scanned, digitised and displayed on a cathode ray tube (CRT) screen. Image editing is possible on the machine used for this study, and, using a light-pen, the operator can interact with the machine in a variety of ways. The major advantage to this study of the image editing function was the possibility of outlining a circular analysis area on the CRT screen (corresponding to a 50 km diameter circle on the original image). Without the image editing function, the analysis area would have been restricted to a square or rectangular area.

The full CRT screen display contains 500,000 picture points (p.p.). All area measurements made in this study are therefore in terms of p.p. which were later transformed to give the correct cloud amount values in eighths of the area investigated. The circular analysis area drawn by the light pen was approximately 53 mm. in diameter, and consisted of some 106,072 p.p. Each p.p. therefore corresponds to an area of approximately 0.02 sq. km or approximately a square of sides 136 metres. The pixel size on the original image is approximately 79 metres square, and therefore some loss of resolution may have occurred through this system.

The other major component of the machine used for this study was the "ID Auto-Detector". This module selects or "detects" features displayed on the CRT screen, on the basis of differences in colour or contrast. Thus to detect the required features, they must have, in general, a grey-scale difference from everything not requiring detection.

A "whiter-than" detection mode was adopted in this study. This provides detection of all features brighter than the grey-scale level (or brightness threshold) selected. The grey scale is divisible into 1000 divisions, and is infinitely variable: threshold values are selected by turning a marked dial. The maximum resolution of the system is 1p.p.

Threshold setting is the most important source of systematic error in the 720 machine (Imanco, 1971). On reasonably well defined features the use of the "flicker" method (Fisher, 1971)

should not give a systematic error greater than 1p.p. in defining the feature perimeter, but the detection process may add to that a random error of ± 1p.p. (Imanco, 1971). This means that area measures, as used in this study, may have an error of 1p.p. multiplied by the feature perimeter. This could be quite large where many, small features (e.g. cumulus cells) are being detected. However, for the purposes of this study it was felt that these errors would be minimal in the majority of cases. In cases where many small features were detected, for example when small cumulus cells predominate, resulting errors should not be significant, as we are working finally to the nearest 1/8 of the detection circle (13,259 p.p).

Area measurement on the machine is defined as "the number of picture points in the field falling inside the detected features".

Detailed discussion of the machine and its various modules can be found in Fisher (1971) and Imanco (1971).

Operational Procedure

(a) Each time the machine was switched on, at the start of a working period, it was allowed at least half an hour to "warm up" to allow the vidicon time to settle down.

(b) After applying a shade correction (automatically executed by the machine), the images were placed in the same central optical paths in the focal plane of the vidicon. This ensured that any systematic errors remaining, after shading correction in the machine, would be similar for each image.

(c) The iris of the vidicon lens was set approximately half open, in order to achieve the best combination of dynamic range and sensitivity. The lens was manually focussed on the lettering of a Landsat image, this providing a sharply-defined, high contrast object.

(d) A brightness threshold reading was taken of step 8 on the 15-step grey scale on each Landsat image. This was to check for differences in photographic processing etc. undergone by each image. Two threshold values were taken, the first when any part of the step was just detected, the second when complete detection had been achieved.

(e) An area not coincident with that to be later analysed within a station circle(s) was chosen, and a cloud/no cloud brightness threshold value was obtained using the "flicker" method. Usually one value was adequate for all the clouds on a particular image. However, on certain occasions two or more different thresholds had to be established for application to different station circles. This was necessitated mainly by differences in background brightness over an image and/or changes in cloud type. As the solar elevation angle alters throughout the year, cloud brightness alters also; consequently it was not possible to select single threshold values for different cloud types to be used on all images.

(f) The plastic overlay providing station location information was then carefully aligned with the Landsat image, and each individual station location was centred on the circle displayed on the CRT screen. The overlay was removed before each area measurement was made.

(g) Using the "accept" mode on the image editor, and the cloud threshold value(s) established previously, an area measurement of the cloud amount in each circle on an image was made. The Quantimet 720 has memories which store the results from 16 separate measurements, from 16 successive scans. This allows the mean values to be taken. In this way errors resulting from noise are reduced. Each mean value was in p.p. The following conversions were applied to make the data compatible with surface observations:

Table 3

Quantimet p.p.-to-cloud okta conversion Table

Code No.	p.p.
0	1 - 13,259
2	13,260 - 33,147
3	33,148 - 46,406
4	46,407 - 59,666
5	59,667 - 72,925
6	72,926 - 92,812
7	92,813 -106,071
8	106,072

(h) At the completion of the initial data set, some replicate readings were taken in the same manner described above. Images were chosen at random and retested. In most cases both the step 8 and the cloud/no cloud brightness threshold values were different, usually within the range of 1 to 20 on the 1000 division scale. However, the calculated areas were usually similar, the maximum discrepancy being 1 okta in a few cases. Thus, although absolute brightness threshold values are difficult to obtain, broad-category area measurements can be replicated in an overwhelming majority of cases.

Phase II : Eyeball Study

The same sets of images used in Phase I of the study were examined some 10 days later by an eyeball technique. A time gap was left in order that the observer should not be biased by remembering previous results.

Each image was examined on a microfilm reader, with a magnification of 14 times. A circle corresponding to the 50 km - diameter circle representing the field of view of the surface observer was placed on the screen to provide the area inside which cloud amount would be estimated. Each station location on the image overlay of each image was placed so as to

coincide with the centre of that circle. An eyeball assessment of the cloud amount inside the circle was then made; the dominant cloud type was also noted. The dominant cloud type was assessed under the following categories:

(i) Cumulonimbiform
(ii) Cumuliform
(iii) Stratiform
(iv) Stratocumuliform
(v) Cirriform
(vi) No cloud
(vii) Mixed - when 2 or more cloud types were equally dominant

A number of replicate readings were taken (approx. 25%). Over 90% yielded identical results. No discrepancy was greater than 1 okta.

Finally, the values of cloud amount observed at the surface stations were extracted from the hourly charts provided by the Meteorological Office. As the time of the Landsat imagery used in this study varied from 09.57 G.M.T. to 11.29 G.M.T. both 10:00 and 11:00 charts were used, and the surface data extracted from the chart nearest in time to that of the imagery. In no case was the time difference greater than 30 minutes. This is probably smaller than in any previous satellite/ground truth comparison; it is certainly much smaller than in most. All 3 sets of results were then compiled into contingency tables.

3. Evaluations of relationships between clouds and their shadows in Landsat 2 imagery

Introduction

Catalogs of Landsat imagery published by NASA give estimates of the % cloud cover in each scene. These estimates are determined by two experienced interpreters, working independently, to produce a final estimate to the nearest 10% (Oseroff, personal communication, 1977). For most (surface-orientated) users the value of a particular Landsat image is reduced by its cloud cover. We were interested in the extent to which the shadow associated with this cloud might further reduce image utility. It seems possible that some images, although apparently acceptable for Earth resource studies so far as their stated cloud amounts indicate, might prove unacceptable in practice on account of the extents to which the areas portrayed by those images were obscured by cloud plus cloud shadow.

This study seeks to elucidate empirically the nature and scale of this problem.

Method

A number of images were selected to represent a wide range of different cloud/cloud shadow conditions. These were digitised using an Optronics P - 1000 Photoscan rotating drum microdensitometer (see Section II.4), and the values stored on magnetic tape. These data were sent to the Image Analysis Group of the U.K. Atomic Energy Authority (UKAEA), Harwell, Oxon. The data were put into a suitable format on an IBM 370/168 computer for processing on the Harwell Image Processing System (Fig. 5). The basic analysis procedure was as follows:

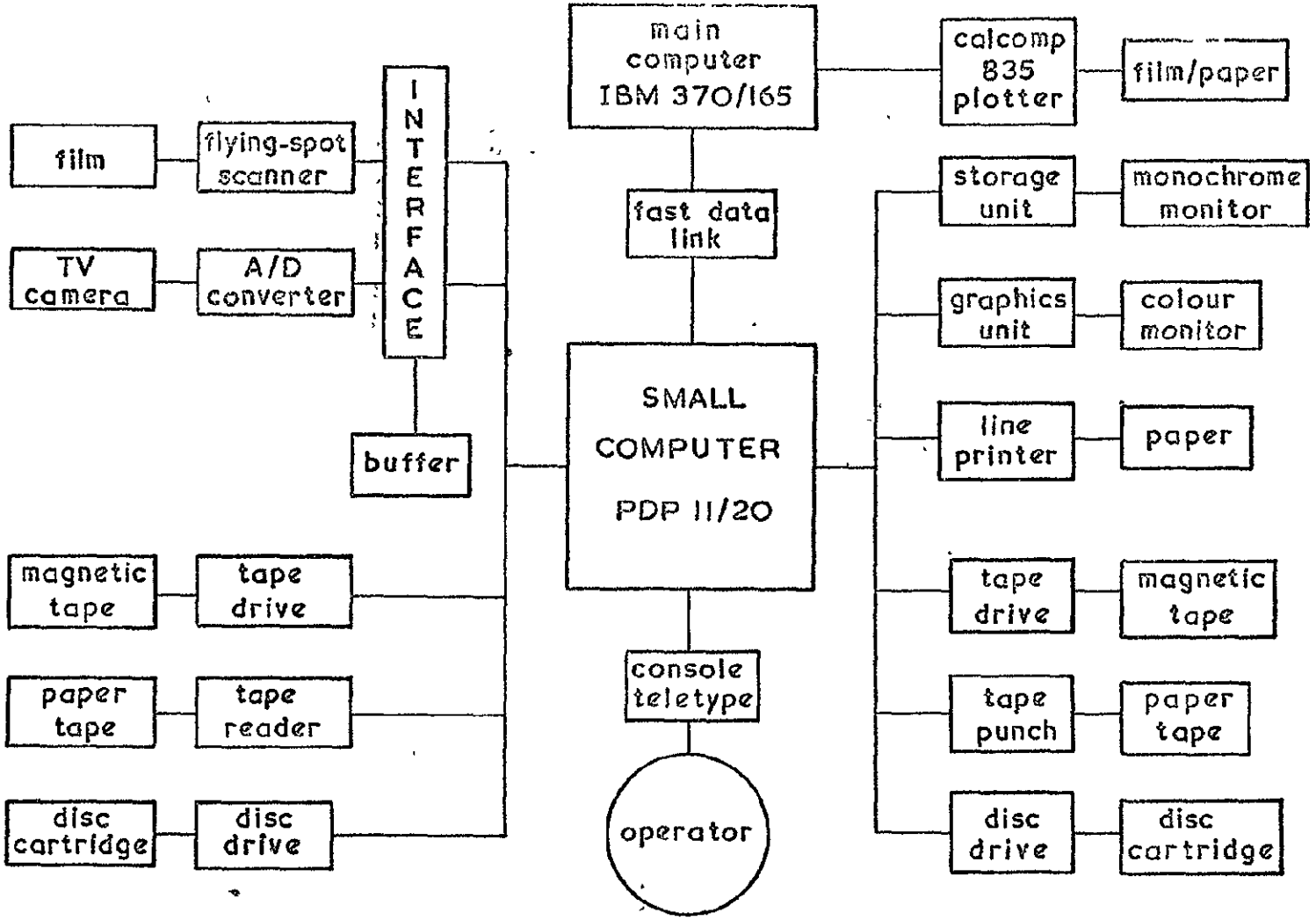

Fig. 5: Harwell image processing system

(a) The entire image presented was viewed on a colour display monitor with 8 colour levels (DEC VT-31 Colour Display Controller with colour T.V. monitor);

(b) By comparison with a monochrome image copy, approximate threshold levels were established for cloud, cloud shadow, and land on the image displayed on the colour monitor;

(c) Areas of the image were identified (if any) where marked disparities were evident in the appropriate threshold levels, necessitating different threshold values in those areas;

(d) Areas of each image were selected for analysis, with regard to features such as lakes, rivers, or the sea. Areas were sought which contained no dark features which might be interpreted objectively as cloud shadow;

(e) Each area for cloud/cloud shadow assessment was then treated in the following ways:

(i) Feature thresholds were accurately determined and checked by reference to displayed histograms of brightness frequency;

(ii) Coordinates of the analysis area(s) were determined;

(iii) The number of picture points within the analysis area(s) were determined within each threshold boundary;

(iv) Percentage values were calculated for the areas covered by cloud, cloud shadow, and land, in relation to the total area viewed.

(f) "Hard copies" of histograms and analysis area threshold "slices" were generated using the IBM 370/168 computer and a Calcomp plotter (see Figs. 6 & 7).

Fig. 6(a) shows a typical hard copy output of a histogram from the IBM 370/168 and Calcomp 835 plotter combination. It refers to analysis area 2 of image 1 (see Section III.3). The ordinate gives the number of picture points, while the abscissa indicates brightness values. A boundary interval of 5 was chosen for the plot. The threshold values for this particular image and analysis area were Cloud, 0-75; Land, 76-116; and Shadow 117-255. The result of applying these thresholds to this particular analysis area is shown in Fig. 6(b). In this plot, the white areas are cloud, the grey, stippled areas are land, and the black areas are shadow. Some slight loss of resolution has occurred because only 61,566 points of a total possible 98,350 were plotted; but the general association of shadow with the cloud cells is readily apparent.

Figs. 7(a) and 7(b) show similar plots for a smaller analysis area in image 2. The thresholds in this area were Cloud, 0-100; Land, 101-137; and Shadow, 138-255. Again a good correspondence is seen, most shadows being intimately related to their associated cumulus cells.

The results are summarised in Section III.3.

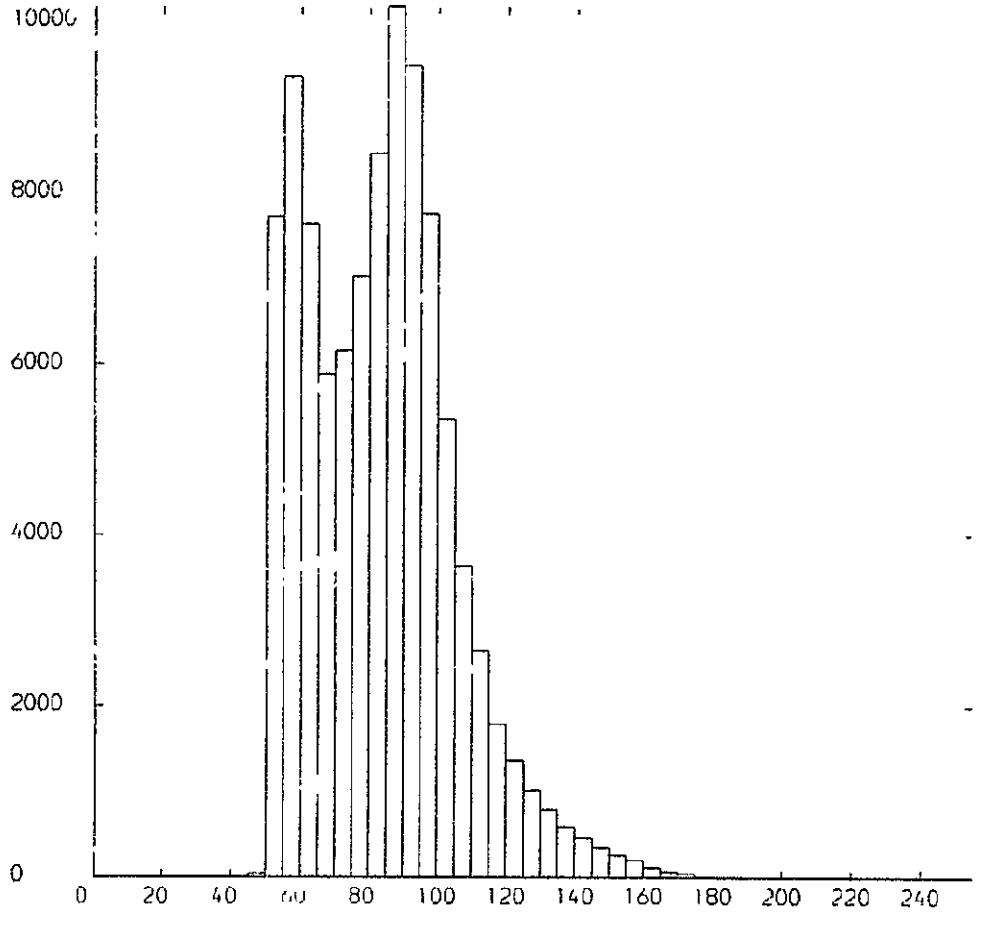

ORIGINAL DISTRIBUTION OF LEVELS
RANGE FROM 0 TO 255 NUMBER OF STEPS= 51
INTERVAL WAS 5
BOUNDARY VALUES ARE
5 10 15 20 25 30 35 40 45 50
55 60 65 70 75 80 85 90 95 100
105 110 115 120 125 130 135 140 145 150
155 160 165 170 175 180 185 190 195 200
205 210 215 220 225 230 235 240 245 250
255

(a)

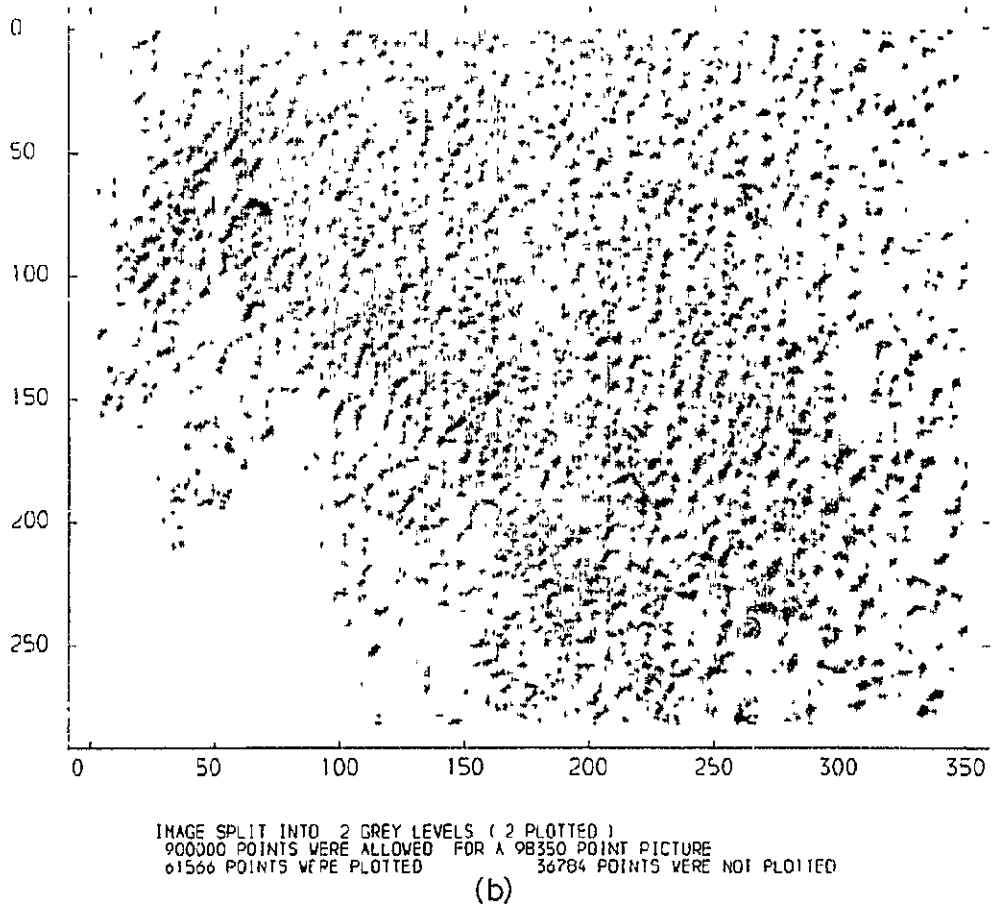

(b)

Fig. 6(a): Histogram of density values from analysis area 2, image 1

Fig. 6(b): Density slice of analysis area 2, image 1

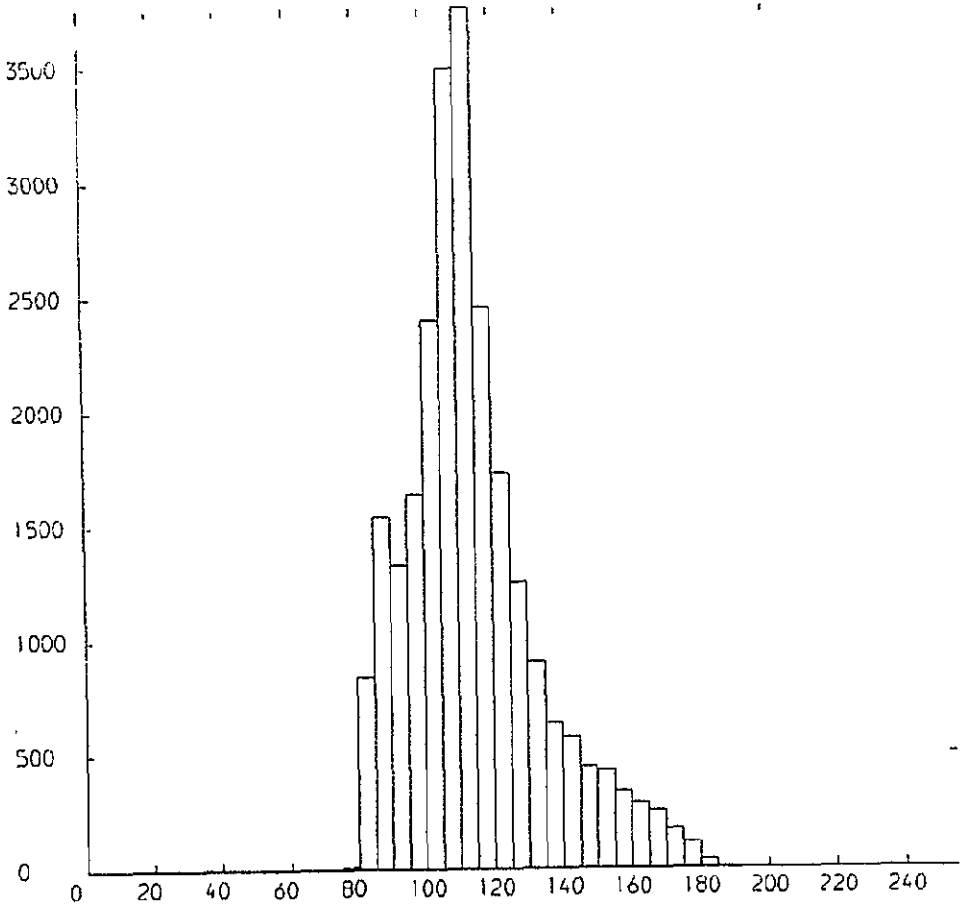

ORIGINAL DISTRIBUTION OF LEVELS
RANGE FROM 0 TO 255 NUMBER OF STEPS= 51
INTERVAL WAS 5
BOUNDARY VALUES ARE

5	10	15	20	25	30	35	40	45	50
55	60	65	70	75	80	85	90	95	100
105	110	115	120	125	130	135	140	145	150
155	160	165	170	175	180	185	190	195	200
205	210	215	220	225	230	235	240	245	250
255									

(a)

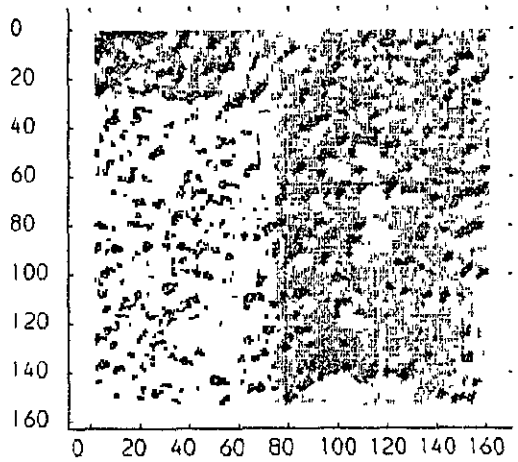

IMAGE SPLIT INTO 2 GREY LEVELS (2 PLOTTED)
900000 POINTS WERE ALLOWED FOR A 24633 POINT PICTURE
19281 POINTS WERE PLOTTED 5352 POINTS WERE NOT PLOTTED

(b)

Fig. 7(a): Histogram of density values from analysis area 3, image 2
(b): Density slice of analysis area 3, image 2

4. Studies of the multispectral characteristics of clouds observed by Landsat 2

One of the most attractive features of the first two Landsat satellites as meteorological observatories has been their multispectral capability in the visible and near-infrared regions of the electromagnetic spectrum. Earlier meteorological satellites, notably of the Nimbus family, have flown multispectral sensing systems for cloud studies, but the best resolutions of the data derived from such systems have been 2-3 orders of magnitude more than the nominal 80m achieved by Landsat. Consequently it was thought that a study of the multispectral characteristics of the clouds imaged over the British Isles by Landsat 2 would comprise a very important part of the cloud and rainfall project as a whole.

Many studies have considered the multispectral responses of Earth surface features portrayed by Landsat imagery, and have used the multispectral data to differentiate both within and between classes of a wide variety of such phenomena (see, e.g., NASA 1975). However, we are unaware of any detailed studies of the multispectral characteristics of clouds observed by Landsat satellites, though Danko (1974) addressed himself in part to such a question. Many recent studies of surface features have been based on analyses of Landsat Computer Compatible Tapes (CCTs). Although we have had to depend on image data instead, which stimulate more uncertainties and imprecision in interpretation, it appears that the principal families of clouds do possess largely distinctive spectral signatures, and yield different histograms of picture brightness from mesoscale areas of cloud fields. Our initial methodology may be summarised as follows:

Selection of imagery

It was established earlier that major cloud types can be differentiated and identified with confidence in Landsat imagery. The cloud families recognised thus were cumulonimbiform, cumuliform, stratiform, stratocumuliform and cirriform. Certain Landsat images were selected to represent "classic" forms of these cloud families and their chief members or cloud types. (see Plates 1-5). For our multispectral study we chose one example of each cloud family, plus an example of the cumulocongestus cloud type, the latter on the grounds that cumulus humilis or mediocris, and cumulocongestus, have substantially different appearances in the Landsat images. Since all four spectral bands were to be investigated, this gave a set of 24 cloud images to be analysed.

All 24 images depicted sea areas around the British Isles. Background brightness constitutes a serious problem for any programme of automatic analysis of cloud imagery. Methods have been devised to reduce the attendant difficulties (see, e.g. Miller, 1971), but none have been (or could be?) entirely satisfactory. We elected to reduce, rather than solve, this problem by analysing clouds viewed over surfaces with relatively even and constant brightness responses and to consider that the background tones were as important as the tones of the cloud surfaces themselves in generating different brightness patterns for clouds of different types. Sea surfaces met such conditions much better than land surfaces, especially in the British region, where convergences of major currents do not occur. The examples chosen were all from the months of June - August.

In view of the added problems that would have been associated with the copying and enlarging of the 70mm transparencies provided routinely by NASA we decided to analyse these transparencies themselves. At their scale 1mm represents approximately 3.37 km on the ground.

Selection of processing system

The system we used for image-analysis was a System P-1000 Photoscan, manufactured by Optronics International Inc. One such unit is located in the Molecular Enzymology Laboratory of the Department of Biochemistry, University of Bristol. The Photoscan P-1000 is a high-speed digital microdensitometer, incorporating an electro-optical rotating drum which converts photometric data on film negatives and positives to digital form for computer processing. In order that an image may be scanned it is placed over an opening in the drum, and clamped to it so that the film adheres exactly to its machined cylindrical surface. For our purposes a sampling area of $10mm^2$ was chosen, representing an area of some 33.7 km^2 on the ground. We wished to sample a sufficiently large area to establish whether the brightness characteristics of fields of different categories of cloud are indeed as clear as eyeball investigations seem to suggest. It seemed likely that cloud fields should be distinguishable from one another if viewed sufficiently broadly to account for their textural characteristics; whether cloud families could be differentiated on the basis of their reflectance characteristics per unit area seemed to be more doubtful. Our hope was that, by compiling sufficiently large populations of summary statistics for quite large areas, both issues might be elucidated simultaneously, the first through areal brightness/frequency distributions, the second through the spectral reflectance graphs constructed for each cloud category from the results for the modal classes in each brightness/frequency histogram.

Accurate registration was attempted for each set of imagery using a clean perspex mask on which were placed the locations of the four registration marks of each frame. In this way the four images of each cloud scene could be registered and a common sampling area identified.

Selection of sampling area

This was defined on the mask by straight-edged, machine-cut, metal foil strips which overlapped to provide a precisely measured imaging area. In operation each image was orientated correctly on the mask provided for its cloud category, and the image, with its mask, was then located on the imaging drum.

The Koehler illumination system of the Photoscan ensures uniform illumination and focussing on the film surface via turret mounted apertures. The light transmitted through each image is measured by a photodetector, and converted to 256 grey-levels.

The choice of scanning aperture is important, as this determines the sampling size for the imagery. There are 3 aperture sizes available for imaging on the Bristol University machine, namely 25, 50 or 100 μm square. In the NASA Landsat Data Users Handbook (1971) (see H 1.4, "Photographic Micro-Image Quality") the following statement is found:

"Because of MTF, granularity, and sensor and recording systems considerations, scans using apertures smaller than 20 μm diameter will be essentially meaningless. Evan scans with aperture sizes of 40 μm will probably not correlate well with macro-density readings evnn when assuming that the investigator has made necessary corrections from specular to diffuse density".

With such considerations in mind, the largest imaging aperture size available (100 μm) was selected in order to minimise such effects. An aperture of 100 μm square corresponds on the image to an area of approximately 337 metres square on the ground. Thus approximately 16 pixels were analysed in each of our microdensitometer spot readings, and something less than 10,000 spot readings were generated for each image area scanned.

Operating practices

The illuminating and imaging optics of the Photoscan are mounted on opposite sides of a "C" carriage through which the cylinder drum rotates. The optical density of each image is measured every 100 μm along the circumference of the drum (Y direction) within the pre-determined area. After each revolution the "C" carriage is stepped in the axial (X) direction by 100 μm. In practice these processes were repeated until the whole 10 mm^2 area of each image had been scanned. Once per revolution, through an opening in the drum opposite the film position, the densitometer photo-detector system is reset to a given known value which represents an optical density of zero as defined by the air path through the slot. Since the drum speed is high (8 revs. per second) the drift of the instrument is far less significant than the least significant bit of density data.

The detector voltage resulting from light transmitted through each image is amplified logarithmically, digitized, displayed, and recorded by interfacing the scanner with a magnetic tape recorder. Each number is representative of a grey-level in the selected density range. In our case the density range was 0 to 2D. Within this range density bears a linear relationship with the output grey levels.

Optical density (D) is defined as:

$$D = \log \frac{Ii}{It}$$

where

Ii is the light intensity impinging on the detector through an air path and

It is the light intensity of the transmitted light.

In addition to the 10 mm^2 sampling area on each image, the 15 step grey-scale tablet was scanned. This scale has undergone the same copying and processing as the image to which it is attached (NASA, 1971, pages 3-5).

Data output

Output from the microdensitometer was recorded on a magnetic tape unit for subsequent processing on a PDP 11/45 mini-computer.

Initial processing was concerned with the recording brightness values of the 15-step grey-scale tablet of each image. A number of data records were examined for each image and the upper boundary value of each of the 15 steps was determined by inspection of the computer print-out. Preferably some type of edge-detection logic (e.g. Rosenfeld, 1970) should have been employed, but this time did not permit. Once the upper boundaries of each step had been determined these values were fed back into the computer in order that the frequency distribution of brightness values for each image could be determined. This procedure was adopted so that we might be able to relate different frequency classes to actual tones on each Landsat image, rather than some arbitrarily chosen density value which might be inappropriate in view of the apparent variations in image processing.

Besides the frequency distributions of the brightness values, other summary statistics were computed also, including means, standard deviations, skewness and kurtosis.

The mean brightness value for each image was determined in the following manner. The store size of the computer is limited (24 k) and was not large enough to hold all the values of each image (8000-9000). Thus the mean brightness value of each record (Y-axis scan) was calculated and the final mean was taken as the mean of the record means. The standard deviation was calculated using the final mean derived as outline above. Skewness and kurtosis values were not found directly on the PDP 11/45 because of problems with the computer program. These were calculated from the frequency distributions using a Hewlett Packard 9801A calculator and an appropriate library program (Prog. 1-3).

The results from this approach are set out in Section III.4. Subsequent to the completion of the Fourth Quarterly Report (Barrett, Grant & Harris, 1976), in which this methodology and its results were first reported, an additional exercise of a complementary nature was undertaken by an undergraduate member of this Department as a Final Honours Year Project. This was designed to indicate whether the multispectral characteristics of clouds varied greatly from season to season: the examples chosen for analysis in this study were drawn (subject to availability) from the summer and winter solstices, and the two equinoxes. A further purpose was to assess whether such seasonal changes as were apparent in cloud brightness and spectral signatures could be explained simply by changes in the angle of solar illumination, or whether other factors also were involved. (Higgitt, 1977)

Method for comparison of seasonal signatures of clouds

Once suitable examples of the five major cloud families (cirriform, cumuliform, stratiform, cumulonimbiform, stratocumuliform) had been identified over sea surfaces near the solstices and equinoxes brightness values for each family for each season were tabulated using a Photolog Cub transmission densitometer to generate the data. Since the smallest available

aperture on this instrument was 1mm the unit areas on the ground were approximately 10.9 sq. km.. The densitometer was first zeroed and its calibration checked as prescribed in the manufacturer's instruction leaflet. Each transparency was placed over the light surface of the densitometer, and a mask carefully positioned to outline exactly the required sample area of cloud. By reference to grid marks on the border of the mask the densitometer probe was moved systematically over the sample area to yield 100 brightness values. The step wedge was then scanned to record brightness values for each of its 15 divisions. The densitometer was re-zeroed between each image analysis. The optical density scale ranged from OD (100% transmission) to 4D (0.01% transmission), whilst most sampled values fell within the range 0.2 - 2.2D. Optical density (D) and transmission (T) are related by the simple equation:

$$\text{Log}_{10} T = 2 - D$$

Once sets of 100 optical density (brightness) values had been obtained from all the images they were punched onto computer data cards, a simple program was written in WATFOR language, and the University ICL 4/50 computer was used to calculate summary statistics: means, standard deviations, skewness, and kurtosis. The cloud brightness values were also standardised separately by allocating each of these to the nearest brightness value on the related grey scale so that frequency distributions could be constructed. The results of these investigations are summarised in Section III.4.

5. A comparative study of clouds investigated simultaneously by aircraft and Landsat 2

In view of the advance knowledge that NASA would endeavour to provide a full coverage of the British test area during the 23rd Landsat Cycle it was possible to arrange with the Meteorological Research Flight (MRF), Royal Aircraft Establishment, Farnborough, Hants., for a maximum of 2 possible sorties to be flown by its Lockheed Hercules XV 208 along anticipated Landsat orbital tracks. The two dates identified for this purpose were 19 March 1976 (when Landsat 2 was expected to pass over East Anglia and south-east England, and 22 March 1976 (when Landsat 2 was expected to pass over the Irish Sea). In the event, as a result of operational difficulties, only the first date was flown. Details of the MRF and the instrumentation on its aircraft, may be found in a recent article by James & Nicholls (1976). Since we had to take "pot luck" with the weather and its attendant clouds for the dates indicated it was decided in advance that the experiment would entail sample investigations of relationships between Landsat-imaged cloud and radiometric data obtained by the Barnes PRT 4 radiometer on the Hercules flying above cloud-top level. For more detailed and sophisticated programmes a "go/no go" choice would have been required, dependent on the suitability of the actual weather conditions, and a promise of Landsat imagery irrespective of the synoptic weather conditions on the dates earmarked as available for such operations.

On 19 March 1976 the Hercules took off from Farnborough at 0912Z in order to begin its run beneath Landsat 2 at approximately 1005Z and peel off at approximately 1030Z. The position of the aircraft was determined throughout by a Decca Navigator.

The portion of the flight path which coincided with the Landsat 2 pass is shown in Plates 8 & 9. The aircraft generally maintained an altitude of 10,058m (33,000'). Since the aircraft flew at a much slower speed than the satellite (the Hercules taking some 23 minutes to follow a course completed by Landsat in about 20 seconds) there was only one point in time when the two sensing systems were viewing the same location instantaneously. This was approximately 1013Z. Consequently there is a greater disparity between the times of aircraft and satellite observations at the southern rather than the northern end of the flight paths, the actual differences being 5 and 16 minutes respectively, rounded to the nearest minute.

The scientific data received from the flight included qualititative cloud descriptions made by the observer (S.Nicholls) at frequent intervals, and (largely cloud-top) temperature data derived from the Barnes PRT 4 radiometer. The following data for this instrument were extracted from the manufacturer's specification, and kindly provided by D.B.Hatton (personal communication).

Table 4

Specifications of the Barnes PRT 4 radiometer

Detector	- thermistor bolometer 1 x 1 mm
Lens	- Irtran 2
Filter	- Indium antimonide *1
Speed	- f/2.4
Focal length	- 30.5 mm
Effective aperture dia	- 12.7 mm
Field of view at ½ energy points	- 2^{o} ($0.96\ 10^{-3}$ st) *2
Spectral bandpass	- 8 to 14 µm
Object distance	- 30 cm to infinity

*1 MRF have permanently installed a bloomed germanium flat window

*2 Represents 5.33 m diameter at 500 ft altitude which is traversed in about 70m S at 150 kt.

The data we received was comprised of one value per second. Since the field of view of the instrument is 2^{o} a ground cover of 350m might be expected in the absence of clouds from 10,050m. A temperature graph along the flight path was constructed from the data received by sampling every tenth value recorded: this yielded a graph more commensurate with the detail available in the Landsat imagery. In order that this might be compared objectively with the related Landsat cloud transect a Joyce-Loebl 3CS scanning microdensitometer was used to provide a graphical representation of Landsat cloud brightness variations along the transect. Using a 5X magnification objective lens, together with a slit size of $1.1mm^2$, a light beam of $100mm^2$ was passed through the Landsat film for both band 4 and band 7 imagery. The aircraft track was marked on a clear plastic overlay. This was used to guide the densitometer beam as the image was moved very slowly beneath it using the automatic X-direction scan, along with the specimen table angular control to rotate the image as required to follow the aircraft track. Since this

traversed 2 Landsat frames a small gap was left in the graphical output to indicate the progression from the one frame to the other. Step wedges for either image were also scanned with identical machine settings, to allow comparisons with the aircraft flightpath brightness transects.

The results are presented and discussed in Section III.5.

6. Landsat 2 image brightness and observed rainfall intensities at selected stations across the British Isles

A study was planned to compare brightness (picture density) values extracted from Landsat 2 imagery and associated ground observations of rainfall intensity to elucidate the relationships between these two significant and related variables. In the search for operational schemes to improve rainfall maps through objective comparisons between gauge data and satellite imagery, rather than through the largely subjective techniques at present in use (see, e.g. Barrett, 1977; Follansbee, 1976; and Martin & Scherer, 1973) relations between image brightness and rainfall intensity might be of primary significance.

Rainfall intensity data

Rainfall is recorded continuously at many locations in the British Isles, but the data therefrom tends to disperse and requires gathering from a number of sources, including:

(a) Metform 3257B (Return of Hourly Observations). This is a sheet completed each day by many stations in the British Isles, listing many meteorological parameters, including the duration and amount of rainfall in each hour. From such data mean rainfall intensity during rainfall events can be evaluated;

(b) Metform 3440. This lists for each hour the duration and amount of observed rainfall. This sheet is completed by those hourly reporting stations not completing a Metform 3257B;

(c) Data from a number of autographic raingauges in the British Isles are held on computer magnetic tape at the Meteorological Office, Bracknell. A copy of this tape was available in the Civil Engineering Department of the University of Bristol, and permission was received from the Meteorological Office and the Civil Engineering Department to extract data relevant to our study. Especially useful for our purposes were two sets of stations more closely clustered than most. One of these clusters is in the English Lake District, the other in South Gloucestershire (near Bristol).

(d) Data from a number of autographic gauges operated by the Civil Engineering Department in South Gloucestershire, but not available under (c). These data were similarly recorded on magnetic tape and abstracted by kind permission.

In order to establish which dates and times would be relevant for our purposes, a "quick look" search of the whole of our

Landsat file was undertaken, comparing each image with the nearest hourly observations of weather depicted by the charts supplied by the Meteorological Office. If any image was found which contained a ground station reporting rainfall either at the time of observation, or within the past hour, then that image was set aside for further analysis. A group of images was thus obtained with the reasonable likelihood of some rainfall occurring at or near the time of the Landsat overpass.

All the stations for which intensity data were available were then plotted accurately onto a map drawn at the same scale as the Landsat imagery (1:3.369M). For each image a clear plastic overlay was prepared showing all the stations within the image area. Small dots were inserted over the registration marks on the image, to provide accurate relocation of the overlay.

A list of stations and dates was therefore established for which rainfall intensity data were to be collected. As all the images selected fell between 1000 and 1100Z, this hourly observation period was chosen for extraction of data from the sources (a) - (d) above. From sources (a) and (b) the intensity value was based on the whole one hour period. However, from sources (c) & (d) it was possible to select a smaller time interval for the intensity evaluation. A period of 6 minutes was chosen (i.e. 1/10 hr.). This shorter period should more accurately reflect the rainfall events at the time of the overpass of Landsat.

Cloud brightness data

These were extracted from the Landsat imagery using a Photolog Cub Transmission Densitometer (Medical & Electrical Instruments Co., Ltd., London) (see also Section II.4). All four wavebands of each image selected were analysed, with the aim of examining band to band differences. As noted above, overlays for each image were used to locate the station positions accurately. On most images there were up to ten stations, but on the images which coincided with the areas of the Lake District and South Gloucestershire there were up to 21 stations for a single image. For the five images in which these higher densities were found, positive prints were made at a scale of 1:0.93M, to allow increased spatial separation of the stations in these particular areas (see Plates 10(a) & (b)).

The spot size selected for the analysis area was of 1.6mm diameter for the normal scale Landsat images, and 2.5mm for the larger scale images. These analysis areas on the image corresponded to circles of 5.4 km. diameter and 2.3 km. diameter respectively.

Some attempt was made next to standardize and normalize the brightness data between different images in order to facilitate comparison between different dates and different images of the same date. Two procedures were applied to the data, the first to try to eliminate as far as possible differences due to processing; the second to reduce differences in brightness due to the change in solar elevation angle over the analysis period.

The first procedure consisted of taking the density values of the 15 step grey scale wedges of each frame of each image. One image was selected as a standard, and its four sets of grey scale values were used as a base set. The appropriate values of the grey scales of a number of other images were plotted against

this base set. In all cases the relationship was linear or slightly sub-linear, the main variation between the different images being slope angle.

Therefore for each of the four wavebands of a particular image, it was possible to fit a simple linear regression, so that the values of any particular image could be transformed to those of the base set. The significance levels for these regressions is shown in the table below:

Table 5

Significance levels for regressions of step wedges on standard step wedges

r^2	Normal Score images	Large Scale images
1.00	57	4
0.99	28	9
0.98	12	2
0.97	1	1
0.96	1	
	99*	16

*Not 100 because one band 6 frame missing from image

As can be seen, the significances fell no lower than 0.96.

Because of the study period used (April 1975 - March 1976) large variations occurred in solar elevation angle, from a maximum of 53° on 13 July 1975 to only 10° on 10 January 1976. Large change in cloud albedo would be due simply to this factor. Therefore it was decided to adjust all the density values to a common solar elevation of 26° (the mean value of elevation from the imagery used). Thus winter (Oct. - Feb.) values of density were decreased numerically (brighter) and summer values (Mar. - Sept.) were increased (darker).

The relationship used was :-

$$\text{normalized density} = \frac{\sin \gamma (x)}{\sin 26^\circ}$$

where x = image density adjusted for standard wedge values

γ = solar angle of image elevation

Measurement Procedure

The densitometer was switched on and allowed to warm up for a short period before the commencement of each working session. A voltage regulator was used to ensure a stable power supply. Each image was selected in turn and the scale was set to zero when viewing through a clear portion at the edge of the image. The calibration of the densitometer was then checked and, if necessary, an adjustment made.

Density values were obtained for each of the 15 steps of the grey scale wedge. A clear plastic overlay with the station positions marked was then used to position the correct area of the image over the measurement aperture for each station in turn. This overlay was removed, and a density value was obtained for each station on the image.

This procedure was repeated for each waveband of each scene, and then for all the images selected for the study. The only alteration to the procedure for the small number of large format images involved the introduction of the larger measurement aperture (2.5mm) into the densitometer before following the method outlined above.

The density values for each station were then adjusted to the standard grey scales, and, finally, these adjusted densities were standardised for solar elevation angle using the formula above.

The final, standardised density values were then compared with related rainfall intensity data by plotting graphs of these two variables, a separate graph being drawn for each waveband. The results are presented in Section III.6.

7. Landsat 2 cloud imagery and radar rain echoes

In the planning stages of this Landsat 2 study, and in the early days of the project once begun, it was hoped that considerable attention might be paid to relations between Landsat-imaged cloudiness and radar-observed rain-echoes. Unfortunately, because of the scattered nature of the Landsat image received from NASA, and our inability to be confident in advance that imagery would be received for a particular area on a particular date led to a large curtailment of this aspect of our work. In the event we were able to undertake only one comparison, using the method outlined below. Even during Cycle 23, for which full coverage had been promised if possible, we were unfortunate in that radar imagery obtained in support of our study by the Royal Signals & Radar Establishment & Edgbaston Observatory (University of Birmingham: courtesy Dr. M.G.Hamilton) covered areas in the west Midlands of England and North Wales for which Landsat imagery were not in fact forthcoming (see Fig. 1(t)). A further limit on our work was the fact that on several occasions for which both Landsat and radar imagery were available no rain fell in the areas covered by the radar systems.

Data from 3 weather radar installations were potentially available for our study, all operated by the Royal Signals & Radar Establishment, Malvern, Worcs. These are located at Castlemartin (S.Wales), Defford (Worcs.), and Llandegla (N.Wales).

The complete Landsat file was examined, and images for dates coinciding with coverage available from the radar stations were noted. Of the 32 in this category only 1 was suitable for further use: for the remainder either no rain was indicated or the radar coverage did not coincide with the time of the Landsat imagery.

The one good image, for 28 January 1976, covered a large area monitored by Castlemartin, whose radar operates on a wave-

length of 3cm, with a 3^{o} vertical beamwidth. The available data came in the form of computer print-outs of a grid with 84^{2} cells based on the National Grid, each grid square having sides of 5 km length. The total coverage area was some 420 km^{2}. The rainfall for each square was recorded on an 8-point scale (see Plate 11). The radar grid was adjusted to fit the latitude and longitude marks of the Landsat imagery, and the grid overlain on the Landsat image. The time of the radar observation was 1045Z, compared with a Landsat image time of 1032Z. Little movement of the rainfall cells was apparent during the 13 minute gap, though the rainfall intensity was probably decreasing.

Results of the data comparisons will be found in Section III.7.

III ACCOMPLISHMENTS

1. A Landsat Cloud Photointerpretation Key

In many studies of satellite imagery the first requirement is the recognition of the types of clouds present over a given area in particular scenes. The complex Landsat Cloud Photointerpretation Key which follows was designed for use by any scientist concerned with cloud identification, whether a professional meteorologist or not. Id does not presume that other data are available to assist or confirm the Landsat indications, being presented in terms of Landsat image characteristics alone.

The Landsat Cloud Photointerpretation Key is structured for maximum flexibility in its application and use. Following American Society of Photogrammetry (1975) it is clear that the suggested scheme may be described in several ways. In terms of its scope, it may be described as a joint Subject/Analagous Area Key, dealing as it does with specified categories of clouds in a mid-latitudinal zone including oceanic and island or fringe-continental areas; in terms of its treatment, it is a Semi-technical and Direct key involving a necessary minimum of technical meteorological terms to characterise features immediately obvious in much of the Landsat imagery; in terms of its organisation, it may be described as a Selective Key, arranged as it is so that the interpreter simply selects that example corresponding to the feature he is attempting to identify, with both Essay Key and Photo-index Key components.

The Key is comprised of three separate, yet inter-related parts, namely:-

(a) The Short Description Key;

(b) The Detailed Description Key; and

(c) The Photo-index Key.

The Short Description Key, for general use, is comprised of brief notes concerning the five basic cloud families and their more important members (most frequent/most widespread/most readily recognized on Landsat imagery in mid-latitude continental fringe regions). The notes are basically descriptive, but brief comments on cloud genesis and synoptic context are also included.

The Detailed Description Key, for more specialized use, is structured on the recognition that there are two basically different ways in which satellite-viewed cloudiness may be described. Although visible imagery from meteorological satellites might, with profit, be approached similarly, the following scheme has been developed to exploit the special characteristics of the Landsat cloud representation, especially its unsurpassed detail. The scheme differentiates between primary and secondary cloud features, namely:

(a) Broadscale features of masses and/or aggregates of clouds, i.e. cloud fields; and

(b) Smaller scale features of masses and/or aggregates of clouds, i.e. structural elements of cloud fields.

Although it has been widely recognised that some clouds

(notably those of the cumulonimbus and cumuliform families) can be described in terms of their individual clouds (or "cells"), problems have arisen in other cases (notably stratiform types) where the search for individual cloud elements is inappropriate. We feel that our differentiation between cloud fields and the structural elements apparent within them is an advance over earlier thinking since it permits all cloud families to be treated alike. In cumuliform cloud fields, for example, the structural elements may be individual cloud cells and/or clusters thereof, and/or organizations of the same; in stratiform cloud fields the identifiable structural elements might be streaks, mottlings or bandings which are evidences of the meso- and/or sub-synoptic scale factors which sculpture the outlines and surfaces of those cloud types which own a dominantly sheet-like appearance in plan.

The Photo-index key illustrates classic examples of the identified cloud families and their significant members or sub-groups.(see Plates 1-5).

Plate 1: Cumulonimbiform

(a) Cumulonimbus

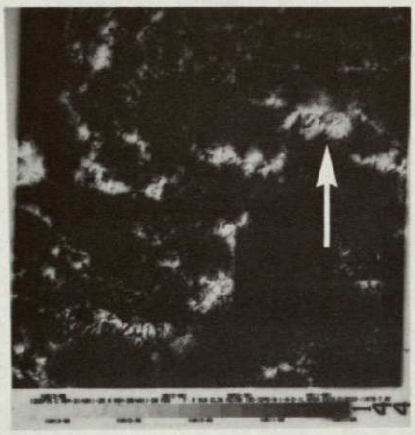

(b) Cumulonimbus

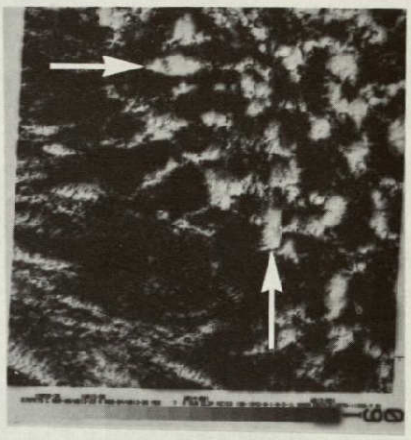

(c) Cumulonimbus with Cirrus

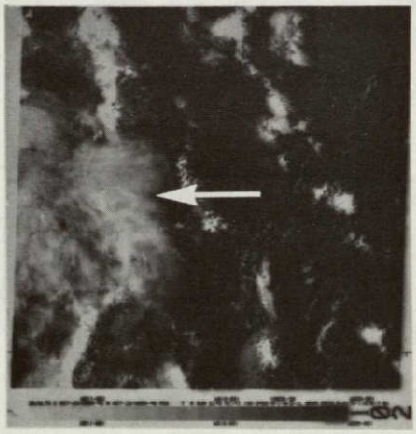

(d) Cumulonimbus with Cirrus

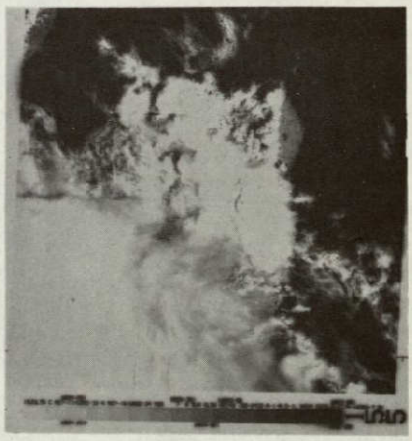

Plate 2: Cumuliform

(a) Cumulus humilis (band 4)

(b) Cumulus humilis (band 7)

(c) Cumulus mediocris

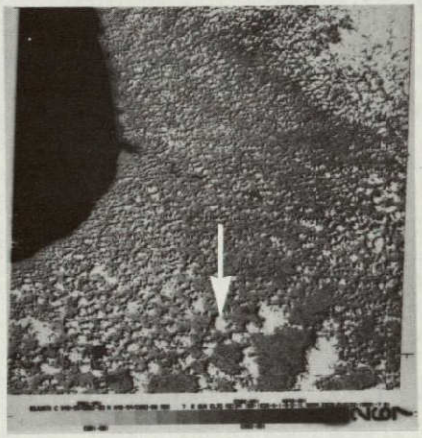

(d) Cumulus congestus

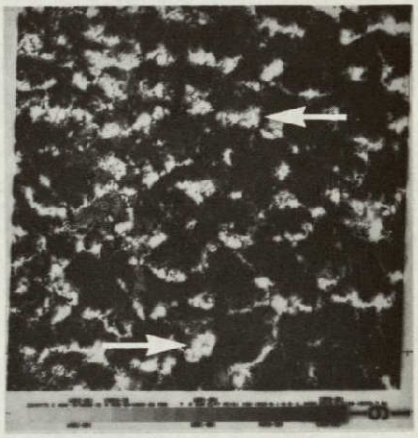

(e) Altocumulus

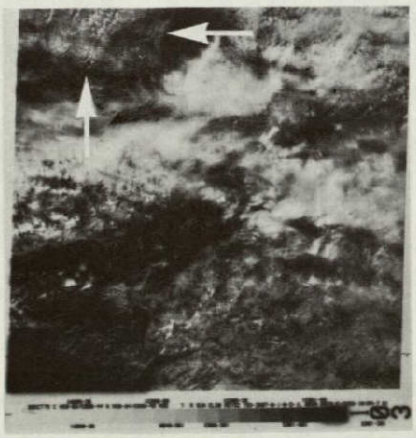

(f) Altocumulus waves

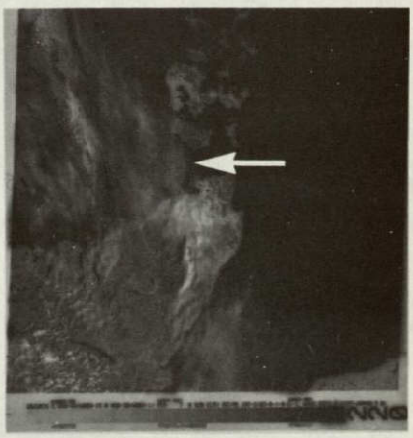

Plate 3: Stratiform

(a) Stratus

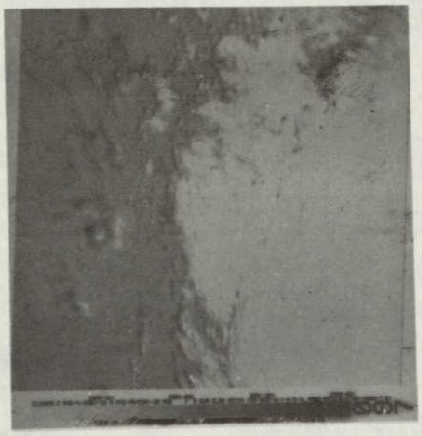

(b) Stratus

(c) Layered Stratiform

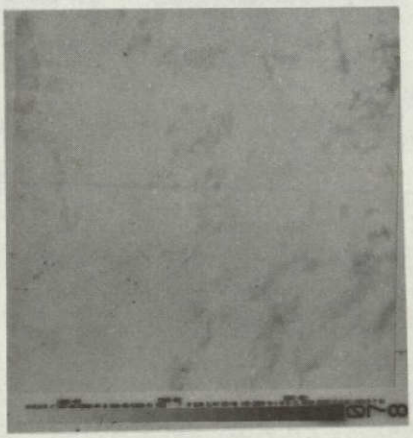

(d) Altostratus

Plate 4: Stratocumuliform

(a) Cells

(b) Ripples

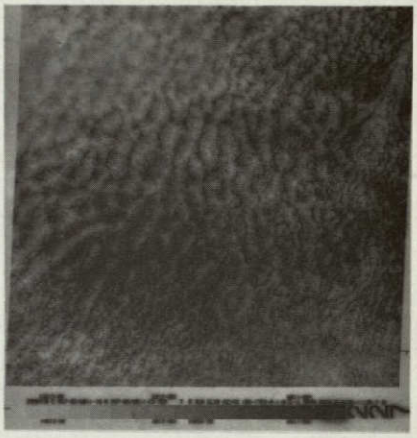

(c) Bands

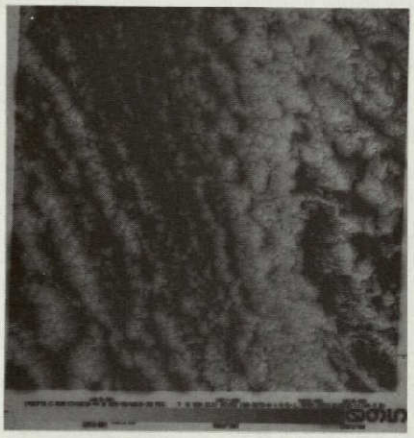

(d) Scallops

(e) Waves

(f) Scallops and waves

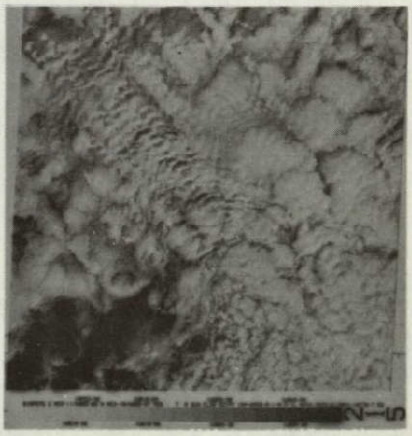

Plate 5: Cirriform

(a) Cirrus fibratus

(b) Cirrus spissatus

(c) Cirrostratus

(d) Cirrocumulus

(e) Condensation trails (band 4)

(f) Condensation trails (band 7)

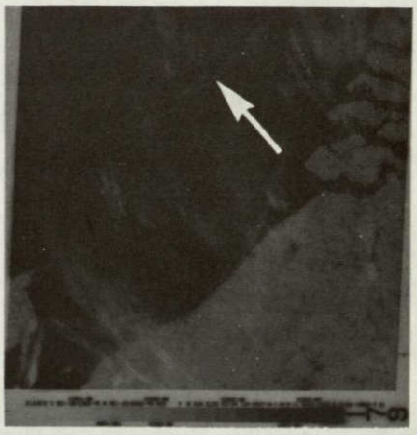

4. Stratocumuliform

5. Cirriform.

Four members of this five-fold primary division of clouds are further divided into a number of members or sub-groups. Some of these sub-groups, for example altostratus and altocumulus, are generally regarded as cloud genera in their own right. However, for most purposes, it is more convenient to regard them as sub-groups of the 5 cloud families. Sub-groupings are shown below, together with the appropriate illustration numbers.

Family	Sub-Groups		Illustration Numbers
1.	(i)	Cumulonimbus	Plates 1 (a) & (b)
	(ii)	Cumulonimbus with Cirrus	Plates 1 (c) & (d)
2.	(i)	Cumulus humilis and Cumulus mediocris	Plates 2(a),(b) & (c)
	(ii)	Cumulus congestus	Plate 2 (d)
	(iii)	Altocumulus	Plates 2 (e) & (f)
3.	(i)	Stratus	Plates 3 (a) & (b)
	(ii)	Layered stratiform (incl. Nimbostratus)	Plate 3 (c)
	(iii)	Altostratus	Plate 3 (d)
4.	(i)	Stratocumulus	Plates 4 (a) to (f)
5.	(i)	Cirrus fibratus	Plate 5 (a)
	(ii)	Cirrus spissatus	Plate 5 (b)
	(iii)	Cirrostratus	Plate 5 (c)
	(iv)	Cirrocumulus	Plate 5 (d)
	(v)	Condensation trails	Plates 5 (e) & (f)

Band Differences:-

As has been noted above, the MSS observes and records Earth radiation in 4 different wavebands. Two of these bands (4 and 5) image in the visible portion of the electromagnetic spectrum, while the others (6 and 7) image in

the short-wave portion, or just into the infra-red. However, all four bands are imaging reflected solar radiation only.

The main differences between the appearances of clouds in the four wavebands are related to the background brightnesses of land and sea surfaces. In bands 4 and 5 both land and sea appear dark grey. Often, there is no clear distinction between land and sea where both occur in a particular image, and the coastline is difficult to distinguish. In bands 6 and 7, the sea appears black, whereas land surfaces appear much lighter (mid-grey to pale-grey tones).

Such differences are significant for the distinguishing of cloud types over land and sea surfaces. As a general rule, bands 6 and 7 seem to be the more useful for identifying clouds over the sea, and bands 4 and 5 for clouds over land. However, where extensive cloud fields occur over land (which is consequently hidden) band 7 is usually the best as textural characteristics tend to be enhanced herein.

In the "band differences" section of the detailed description key below, the use of the term "LAND/SEA" indicates that these considerations apply.

THE SHORT DESCRIPTION KEY

1. Cumulonimbiform

(i) Cumulonimbus

These appear as large, very bright cloud elements whose shape varies from subcircular to irregular. Cloud edges are usually sharply defined, often emphasized by shadows cast by these tall, towering clouds or cloud masses. Fields of cumulonimbus,and the included open spaces, may extend over broad areas with individual clouds organised into lines, closed clusters and more or less regularly patterned open convective cells or honeycombs. Sometimes the cloud masses are chaotically distributed. They form preferentially over relatively warm surfaces and/or where the air is markedly unstable.

(ii) Cumulonimbus with Cirrus

Very bright cumulonimbus clouds are here covered wholly or in part by cirrus which appears greyer and often has a fibrous texture. Where cirrus is present (indicating upper level conditions not conducive to a continuation of vertical cloud growth) the summits are indistinct and margins are ill-defined e.g. where vertical wind-shear causes cirrus plumes to extend beyond the cumulonimbus towers. Fields of cumulonimbus with cirrus are often extensive especially where merging of cirrus anvils occurs, with little cloud-free space between. Strong instability is indicated, often on exposed slopes where orographic and meteorologic factors enhance each other, or along powerful cold fronts or squall lines.

2. Cumuliform

(i) Cumulus humilis and Cumulus mediocris

These involve small cloud elements, generally bright to very bright in tone. These may be circular, sub-circular or irregular in shape. They often occur in fields of irregularly spaced elements, but may be organized, characteristically into open convective cells or streets. The edges of the fields often indicate distributions of surface heating patterns, e.g. in summer, when these are fair weather clouds over land.

(ii) Cumulus congestus

These somewhat larger cumulus clouds are frequently found in conjunction with cumulus humilis and cumulus mediocris, where tower cloud growth is locally more advanced. They are very bright, due to their greater depth. The edges of the elements are sharply defined and shadows from these clouds are often visible over land surfaces where the background is of light to medium tone.

(iii) Altocumulus

Being somewhat higher clouds than those of types (i) or (ii), the small grey elements which are characteristic of this generally shallow cloud type are often seen overlying lower cloud masses. They occur either in irregular fields or organized into narrow, parallel bands transverse to the wind flow. The latter organisation produces "waves" when viewed on the Landsat imagery - these are often orographically induced lee wave clouds.

3. Stratiform

(i) Stratus

This forms generally extensive cloud sheets possessing little or no internal organization visible on the Landsat imagery. The fields are usually bright, though edges of sheets may show tonal variations. They indicate moist layers of air at or near the Earth's surface and may conform more or less closely with topography or coastlines (lowland, valley and coastal fog).

(ii) Layered Stratiform

A generally bright or very bright cloud field, consisting of a number of layers which usually form continuous sheets when viewed on Landsat imagery. Usually frontal in origin and often extending over wide areas. Some texture is visible as a result of changes in thickness and/or shadows cast by higher structural elements. The latter may include stratus, nimbo-stratus and altostratus.

(iii) Altostratus

This occurs characteristically as extensive bands or sheets. Bright appearances prevail but small tonal variations are common, related to changes in thickness of the cloud field which is more usually translucent than transparent. The texture may be smooth or fibrous. Altostratus indicates widespread uplift of moist air, e.g. along warm fronts.

4. Stratocumuliform

These form extensive sheets or bands with characteristic cellular and/or sub-linear sub-structures, although a wide variety of etchings occur related to turbulent processes. Brightness is variable, from medium to bright. These clouds are anticyclonic, forming when low-level convection is overruled by widespread subsidence.

5. Cirriform

Usually a "thin" dull cloud, this often overlies lower cloud formations which are visible when the overlying cirrus is translucent. There are several distinct varieties.

(i) Cirrus fibratus

This is a thin, grey cloud, typically showing a fibrous texture; it is often found in association with Cumulonimbus towers, and along the leading edges of warm and occluding frontal bands of cloud.

(ii) Cirrus spissatus

This may form extensive sheets or bands. Often opaque and white in appearance, its texture is comparatively smooth. It may be found at or near the leading edge of a warm or occluding frontal band of cloud.

(iii) Cirrostratus

Typically forming bright sheets or bands of clouds, with a fibrous texture, this is often associated with advancing warm or occluded fronts.

(iv) Cirrocumulus

Rarely seen; cirrocumulus is composed of tiny, dull, translucent cloud elements which give the cloud field a finely mottled appearance.

(v) Condensation Trails

These appear as thin, dull grey, straight lines or bands, usually of considerable length. They often form criss-cross patterns when numerous trails are present, indicating considerable moisture through depth in the middle and/or upper troposphere.

DETAILED DESCRIPTION KEY

1. CUMULONIMBIFORM

(i) Cumulonimbus

Structural Elements

Nature : Individual cumulonimbus cells

Size : 10 - 20km. across longest dimension.

Form : Subcircular generally, some elongated into oval shapes. Well defined margins.

Brightness : Generally very bright. Occasionally the structure of individual elements causes shadows to be cast down onto lower portions of these tall towering clouds. In these instances the shading of portions of individual elements helps to enhance their towering appearance.

Texture of Each Element : Uniformly smooth; some texture seen when shadows cast - as noted above.

Organisation of Elements : Individual elements may be organised into closed clusters, with overlapping margins (which may cover extensive areas), or open, cellular patterns. These patterns may be honeycombs or lines (where the cells are more regularly spaced), or chaotic distributions (where the cells are less regularly spaced).

Band Differences : 4,5,6 very similar; 7 shows more shadow which enhances cloud structures.

Cloud Fields

Size : May be 150 km. or more across.

Form : Fields of cumulonimbus are often related to relatively warm surfaces, these prompting convective instability under appropriate vertical profile conditions; in such cases the fields may be dominantly over land (summer) or

sea (winter). When related to the state of the atmosphere alone they are characteristically elongated (fronts and/or squall lines) or irregularly-shaped (e.g. trailing cold sectors of depressions).

Brightness : Field brightness depends on the organisation of the individual elements. Generally, the closer the spacing of the cells, the brighter the field, as a whole, appears.

Texture : Similarly depends on organisation; and may vary from a smooth, extensive cloud mass to a mottled, open texture.

Band Differences : LAND/SEA

(ii) Cumulonimbus with Cirrus

Structural Elements

Nature : Individual cumulonimbus cells, with cirrus plumes.

Size : 10 - 30 km. across longest dimension.

Form : Subcircular generally; margins ill defined, especially where the cirrus is dense and blown out from the top of the cumulonimbus tower. This leaves an indistinct, diffuse edge.

Brightness : Very bright. Cirrus, where extending beyond the individual cumulonimbus towers, may appear duller. Individual towers are often seen as brighter elements through the duller, translucent cirrus.

Texture : Little structure is seen in individual elements, which appear smooth. Cirrus plumes may have a fibrous texture.

Organisation of Elements : Often organised into closed clusters, which may cover extensive areas especially where cirrus plumes from individual towers merge to form one cirrus sheet.

Band Differences : Band 7 shows greater texture and structure in the cirrus elements.

Cloud Fields

Size : Very extensive, may be 150 km. or more across.

Form : Cumulonimbus with cirrus anvils normally evolve out of cumulonimbus clouds by a continuous process of transformation. Conditions under which these clouds occur are therefore similar to those which are favourable for the development of Cumulonimbus.

Brightness : Very bright.

Texture : Smooth. Cirrus plumes, where merging, may be diffuse and show a fibrous texture.

Band Differences : Band 7 shows greater texture and structure in the cirrus elements.

2. CUMULIFORM

(1) Cumulus humilis and Cumulus mediocris

Structural Elements

Nature : Individual cumulus cells.

Size : Generally 1 to 5 km. across the longest dimension, some humilis cells may be smaller, down to the limits of the Landsat resolution.

Form : Varied; may be circular, sub-circular or irregular. Edges are generally sharply defined. There may be some small shadows cast onto the ground if vertical development is locally accentuated.

Brightness : Bright to very bright; the cloud edge on the side away from the sun is often marked by ground shadow (if over land), which contrasts strongly with the cloud itself.

Texture : Generally no texture is seen in individual elements, which appear smooth. If vertical development is marked, as in some larger clouds, then shadows caused by higher portions of a cloud are seen on lower portions. This gives a faintly mottled appearance to these clouds.

Organisation of Elements : Commonly occur in irregularly organised fields, individual or parallel lines, or uniform, open cellular patterns.

Lines consist of individual Cumulus humilis and mediocris elements. (They may also contain Cumulus congestus). A field may contain 50 to 100 lines, with the spacing between the lines varying, but generally it is similar in magnitude to the width of the cloud lines, or slightly larger. The lines may be straight, or gently curved, and may occur over either land or sea surfaces.

Open, cellular patterns are formed from various Cumulus subgroups which cluster together to form honeycomb patterns often covering extensive areas.

Band Differences : LAND/SEA - very marked.

Cloud Fields.

Size : Lines may be 100 km. or more in length, and one field may consist of numerous (50+) lines. Open cellular patterns and chaotic distributions may cover wide areas, often the whole of a single image.

Form : Convection processes are responsible for their formation, individual cells forming in the thermals associated with instability in the lower troposphere. This instability may be due to surface receipt of solar radiation, and/or warming of the base of a cold air mass by passage over a relatively warm surface. Therefore, the margins of cumulus fields are closely related to surface heating patterns.

Brightness : Varies, depending on the spacing of the cloud lines or cellular patterns and also the background (land or sea). Generally, the closer the elements, the brighter the field.

Texture : Non-uniform, an alternating pattern of white and black or dark-grey; regularly repeated in the case of lines, irregular mottling in the case of open cells.

Band Differences : LAND/SEA - marked.

(ii) Cumulus congestus

Structural Elements.

Nature : Individual congestus cells.

Size : 10-20 km. across longest dimension.

Form : Varied:may be circular, sub-circular or irregular. Edges are sharply defined and shadows cast on side away from the sun.

Brightness : Usually very bright, may be some shadows cast on lower portions of an element if vertical development is marked, hence darker tones occur.

Texture : Little on individual elements which appear uniformly smooth except where shadows are cast.

Organisation of Elements : Commonly found in association with other cumulus subgroups. May occur in lines or open cells, marking locations of locally enhanced vertical development.

Band Differences : LAND/SEA. Bands 6 and 7 show more marked shadows on individual clouds than bands 4 and 5. Shadows cast over land by individual clouds are more marked in bands 6 and 7 than bands 4 and 5.

Cloud Fields.

Size : Variable, usually congestus elements are constituents of large cumuliform fields (containing humilis, mediocris and sometimes cumulonimbus clouds) which may cover extensive areas.

Form : Normally found in association with other cumuliform and cumulonimbiform varieties, being an intermediate form between the less well developed cumulus varieties, and the more advanced development of cumulonimbus. They are, therefore, similarly associated with surface heating patterns.

Brightness : Very bright to bright, depending on the spacing of elements in the cloud field.

Texture : Irregular mottling prevails; when elements are arranged linearly, bands or stripes occur.

Band Differences : LAND/SEA.

(iii) Altocumulus

Structural Elements.

Size : Individual elements difficult to distinguish; generally small - 1km. or less.

Form : Generally irregular, edges may be diffuse with cirrus smudging common.

Brightness : Generally grey; may be white where thin cirrus is above.

Texture : Not distinguishable.

Organisation of Elements : Either irregularly spaced, or found in narrow parallel bands which are often sinuous, and generally perpendicular to the direction of wind flow at the cloud level. There may be 10 or 15 bands in a space of 30 km., with uniform spacing.

Band Differences : LAND/SEA. Band 7 tends to show organisations of elements better than bands 4 and 5, especially where thin cirrus overlies the altocumulus.

Cloud Fields

Size : Irregularly spaced elements may form fairly extensive fields, covering an area with the longest dimension approx. 50km. Parallel bands may be 100 km. or more in length (in the

direction parallel to the bands) and the distance across the bands may be 30km.

Form : Fields of altocumulus indicate unstable air in the middle troposphere. Often the fields are closely related to topography, being visible evidence of orographic waves. These are triggered by local orographic lifting. The cloud waves generally lie transverse to the wind direction, and may extend considerable distances downwind, forming extensive fields.

Brightness : Generally grey-white where overlain by cirrus.

Texture : Where elements are irregularly spaced they give a "lumpy" appearance. When in bands, they appear as smooth waves or ripples.

Band Differences : LAND/SEA.

3. STRATIFORM

(i) Stratus

Structural Elements

Nature : Streaks, mottles, bands.

Size : Variable, from small, irregular mottled areas, to extensive streaks or bands which may be 100 km. or more in length, and bands may be 50km. or more wide.

Form : Variable; mottles may be subcircular or irregular in shape, streaks are normally long and thin and bands are often long and broad.

Brightness : Bright, usually white. Occasionally grey if the elements are thin.

Texture : Only slight tonal variations are visible and usually the elements are rather indistinct.

Organisation of Elements : Stratus fields are generally amorphous sheets with little or no internal organisation. They may be comprised of very few elements, or a great number, e.g. a large sheet may contain a few bands or many streaks.

Band Differences : Individual elements are seen more easily in band 7 than the other bands.

Cloud Fields.

Size : May cover a whole frame or more.

Form : The development of stratus fields is a result of cooling in the lower troposphere, and the shape of the fields may be more or less strongly influenced by topography, coast-lines and wind direction, for example, valley or lowland fog, or fog formed over the sea and advected over the coast by an onshore wind.

Brightness : Usually bright; edges of a sheet may show varied tones where the elements become thinner.

Texture : Usually relatively smooth.

Band Differences : Difference of tones enhanced in band 7.

(ii) Layered Stratiform

Structural Elements

Nature : Streaks, mottles, bands.

Size : Variable, from small mottles to long streaks and wide bands.

Form : Mottles may be subcircular or irregular; bands are generally wide and straight with streaks being long and thin, gently curved or straight.

Brightness : Very bright.

Texture : Irregular texture may occur due to the casting of shadows by some elements at higher altitudes.

Organisation of Elements : A variety of elements at different altitudes are characteristic of this cloud type. The elements may include bands and/or mottles of stratus and nimbostratus (where rain is falling) with streaks of altostratus above.

Band Differences : Band 7 provides greater detail of individual elements.

Cloud Fields.

Size : Generally extensive - 100km. or more across, even 1000 km. in length.

Form : Usually frontal in origin; therefore the shapes of the cloud fields are related to synoptic-scale weather development rather than more localised factors, and are characteristically broad, more or less curvilinear bands where fronts are active; broken, discontinuous and/or amorphous patterns where fronts are dissipating.

Brightness : Bright to very bright.

Texture : Irregular, due to changes in thickness and casting of shadows.

Band Differences : Band 7 reveals textural differences more clearly.

(iii) Altostratus

Structural Elements

Nature : Streaks and/or bands.

Size : Generally extensive.

Form : Streaks or bands may be in straight lines or gently curved.

Brightness : Bright.

Texture : Smooth, or fibrous.

Organisation of Elements : Generally form extensive sheets or bands.

Band Differences : Band 7 shows slightly more texture (if present).

Cloud Fields

Size : Very Extensive - may cover a complete frame.

Form : Usually related to synoptic-scale weather factors; a major causation is the slow ascent of extensive layers of air to sufficiently high levels for condensation to occur. This frequently happens along warm and/or occluding frontal planes.

Brightness : Bright, though may show tonal variations due to changes in thickness.

Texture : Fibrous generally.

Band Differences : Emphasis of texture in band 7.

4. STRATOCUMULIFORM

(i) Stratocumulus

Structural Elements

Nature : Mottles, streaks.

Size : Generally small. Mottles are usually 3-5km. across, though they are occasionally outside these limits. Streaks are usually narrow, less than 1 km. across, and may be a few kilometres in length.

Form : Mottles take a wide variety of shapes; they may be irregular, subcircular or circular. Streaks are straight or gently curved.

Brightness : Varies - from dull grey to bright, depending on the depth of the cloud and the sun elevation angle. As the latter increases, the brightness generally increases.

Texture : Streaks are usually smooth. Mottles may show some fine, irregular texture due to tonal variations caused by their uneven upper surfaces.

Organisation of Elements : Groupings of structural elements may be identified at two levels of aggregation. At the first level of aggregation, the formation of more or less closed clusters (consisting of perhaps 10 to 20 mottles or streaks) is common. These primary groupings are then further aggregated to form bands, sheets or scallop shapes, which may extend over large areas.

Band Differences : LAND/SEA; band 7 enables the texture and organisation of the elements to be seen more easily.

Cloud Fields

Size : Extensive - may cover a complete frame, or a number of consecutive frames.

Form : Fields of stratocumulus are associated with large scale subsidence to the level of the tops of the cloud fields under anticyclonic conditions. The cloud elements are formed by lower level convection and etched by turbulent processes. The different spatial organizations and textures so characteristic of this cloud family are not wholly understood at the present time, but are probably due to the interaction of particular synoptic and sub-synoptic scale factors.

Brightness : Medium to bright, depending on cloud thickness, organisation and sun elevation angle. Generally, thicker, more closely spaced fields appear brighter.

Texture : Cloud field textures are numerous - a result of the wide variety of element organisations at two levels of aggregation. They include more or less fine mottlings, scallops, "cauliflower"-like textures of certain closed cellular organisations and ripple-like textures when bands are arranged in rows.

Band Differences : Band 7 is again most useful in discerning textural and organisational characteristics within cloud fields.

5. CIRRIFORM

(i) Cirrus fibratus

Structural Elements

Nature : Streaks or fibres.

Size : Variable in length, from a few kilometres to 50 or 100 kms. Generally narrow in width, being a few kms. at most.

Form : Usually straight or gently curved.

Brightness : Dull grey and translucent; may be brighter, white tones if thicker and opaque.

Texture : Smooth.

Organisation of Elements : Numerous streaks or fibres may be organised into narrow or wide bands, and occasionally enough elements may be present to form an amorphous sheet. Thin streaks or filaments may sometimes be seen lying transverse to the major cloud axes.

Band Differences : LAND/SEA.

Cloud Fields

Size : May be extensive, occurring in diffuse sheets.

Form : Where blown from cumulonimbus towers, fields of cirrus fibratus will be related to the organisation of the towers and the direction of wind flow in the upper troposphere. If related to an advancing frontal system, the cloud field shape will be dependent on synoptic factors.

Brightness : Usually dull and translucent, revealing lower cloud formations, which appear as brighter patches in the cirrus field.

Texture : Commonly fibrous or banded.

Band Differences : LAND/SEA; in band 4, cirrus appears slightly brighter, especially where the cloud field is thicker.

(ii) Cirrus Spissatus

Note:

It is not possible on LANDSAT imagery to identify seperate structural elements and therefore the structural Element-Cloud Fields subdivision is not used.

Nature : Amorphous sheets or bands.

Size : Variable from small patches, to extensive sheets extending over a complete frame or a number of consecutive frames.

Form : In general, the comments applied to cirrus fibratus apply here also. If found chaotically distributed, this may be related to cumulonimbus towers which have now dissipated; here the field will bear some relation to previous cumulonimbus fields.

Brightness : Bright, usually white in appearance.

Texture : Smooth.

Band Differences : Band 7 shows slightly more texture in the cloud field, especially where the cloud may be thinner, and lower cloud layers may become visible.

(iii) Cirrostratus

Structural Elements

Nature : Streaks or bands.

Size : Variable - may be a few or many kilometres in length, but are usually narrow, being only a few kilometres wide.

Form : Straight or gently curged.

Brightness : Medium grey to white;usually opaque.

Texture : Rather smooth.

Organisation of Elements : The streaks or bands are usually closely arranged to form wide sheets or bands, with little or no space between the elements.

Band Differences : Somewhat brighter in band 4 than band 7.

Cloud Fields

Size : Variable, usually extensive.

Form : Usually frontal in origin, forming bands ahead of the surface positions of the frontal planes (behind cirrus fibratus, ahead of altostratus).

Brightness : Usually bright, pale grey to white tones. If thin, may be translucent revealing lower cloud as brighter patches.

Texture : Commonly fibrous, with thin bands or streaks.

Band Differences : Band 4 is generally brighter; band 7 reveals greater textural detail.

(iv) Cirrocumulus

Structural Elements

Nature : Small cells.

Size : 300 metres to 1 kilometre across.

Form : Each cell is circular or oval shaped.

Brightness : Dull grey, translucent.

Texture : Smooth.

Organisation of Elements : Closely spaced cells in an irregularly shaped field. May form bands with diffuse edges.

Band Differences : LAND/SEA; elements appear slightly brighter in band 4 than band 7.

Cloud Fields

Size : Field may be 50 km. or more across.

Form : Generally patches of restricted extent. Sometimes ahead of surface frontal positions in the cirriform zone. A rare cloud type.

Brightness : Dull grey and translucent. Lower cloud forms may be seen as brighter patches through the overlying cirrocumulus.

Texture : The field presents a dappled or rippled texture.

Band Differences : LAND/SEA - band 4 is brighter than band 7.

(v) Condensation Trails

Structural Elements

Nature : Streaks or bands

Size : Individual streaks may be 100 km. or more in length. They are usually very narrow, perhaps 1 or 2 km. wide at most. Bands may be of similar length, but are usually broader, perhaps 5-20 km.. wide.

Form : Streaks are usually straight lines with sharp edges, this straightness being their most readily identifiable characteristic. Bands are usually streaks which have been drawn out by wind shear, and their margins are therefore not so sharply defined.

Brightness : Pale to medium grey tones.

Texture : Streaks are smooth; bands may show fibrous or feathery texture.

Organisation of Elements : When numerous trails are present, criss-cross patterns form which appear like irregularly spaced grids.

Band Differences : LAND/SEA; band 4 is slightly brighter.

Cloud Fields

Size	:	Fields of condensation trails may extend over considerable areas, but there are often extensive gaps between individual elements.
Form	:	Related to patterns of aircraft movement and wind patterns aloft when conditions are suitable for their formation.
Brightness	:	Usually dull grey, due to large spaces between individual elements.
Texture	:	Feathery or wispy appearance if bands are present; if streaks dominate then an irregular grid pattern occurs.
Band Differences	:	LAND/SEA - band 4 is usually slightly brighter.

2. Comparisons between cloud cover evaluated from Landsat 2 imagery and conventional meteorological stations across the British Isles

Plates 6 & 7 illustrate the Quantimet 720 Image Analysing Computer used after the manner described in Section II.2 for the evaluation of total cloud amount within selected areas on Landsat 2 images.

Some partial, preliminary, results from this programme were reported earlier by Barrett & Grant (1976). Full results for the entire period covered by our Landsat 2 study are presented here. They are summarised in contingency tables (Figs. 8 to 13) and frequency graphs (Fig. 14). The first contingency table (Fig. 8) sums the results of all three observational methods compared for all the dominant cloud categories used in this study. Perhaps the most striking feature of Figure 8 is the similarity of tables (a) and (b). It can be seen that, with respect to both the satellite image observer and the Quantimet, the surface observer consistently overestimates the cloud amount. This is especially apparent in the middle of the okta scale. At the upper end of the scale (7 to 8 oktas) the satellite image observer and the Quantimet tend to overestimate with respect to the ground observer. When table (c) of Figure 8 is examined, it can be seen that the results obtained by the satellite image observer and estimations based on the Quantimet are similar with respect to the whole okta scale. Some notable erratics remain, but these are isolated, individual instances, for which there are usually obvious reasons.

The findings above are interesting when compared to the findings of previous studies. The majority of studies of this type (including those by Clapp (1964), Barnes et al. (1967), Cooley et al. (1967) and Malberg (1973) have found that the ground observer usually overestimates the cloud amount with respect to satellite observations. A number of reasons have been advanced for this discrepancy. These can be divided into 2 groups, the first concerned with surface estimations, the second with satellite imagery estimations of cloud amount.

(a) Surface estimations:

The surface observers view of the sky is complicated by the fact that his perspective changes continuously from the zenith to the horizon. A number of different proposals have been made in the literature (summarised by Neuberger, 1951) as to the apparent shape of the sky, but all agree that the perspective is flattened to a greater, or lesser, extent. The amount of apparent flattening cannot be accounted for simply, as it is not only related to physical conditions in the atmosphere, but also to psychological factors which vary among observers. It certainly varies with both cloud type and cloud height (Miller and Neuberger, 1945). Because of this apparent flattening, approximately half the sky is below an elevation angle of 30°. Therefore, the instruction to the surface observer to "give equal weight to the areas around the zenith and those at a lower elevation angle" (HMSO, 1969) seems somewhat inappropriate.

Because of the flattening of perspective, in scattered cloud situations, the observer will see the sides, as well

(a)

(b)

PLATE 6 : The Quantimet 720 image analysis system at ADAS, Cambridge:

(a) The main module (right) displaying Landsat 2 image input from epidiascope (left); and

(b) the operator engaged in a man-machine interaction process.

(Courtesy, Ministry of Agriculture).

(a)

(b)

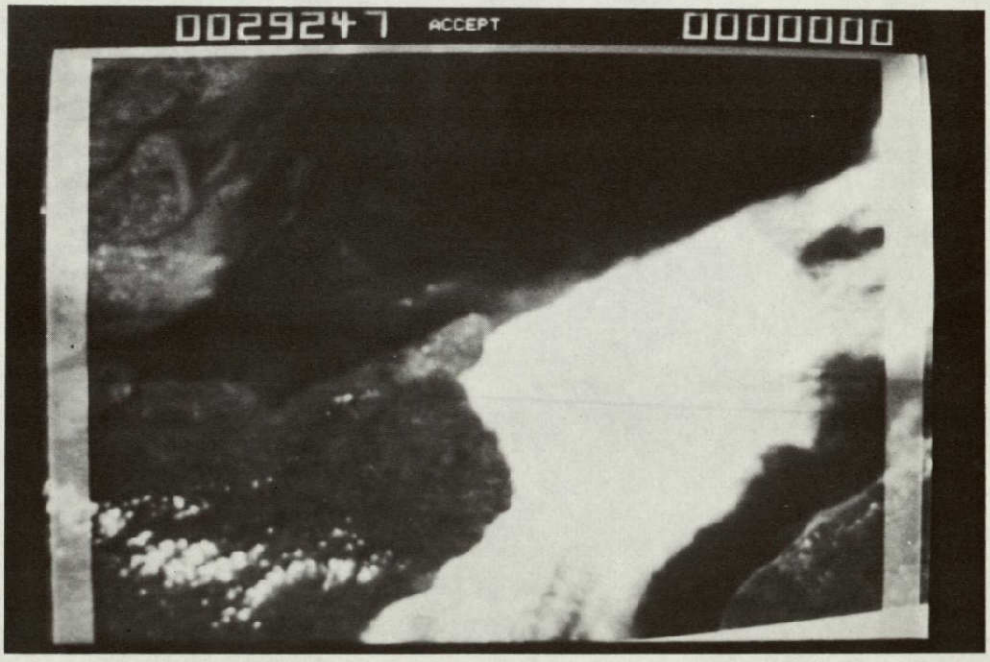

PLATE 7: Stages in the process of estimating cloud area on a Landsat 2 image: (a) The detection area (grey disc) is positioned for Manston (Kent); the number of picture points is indicated on the menu at top left. (b) The area within the detection circle above the cloud brightness threshold has been summed in terms of picture points. The result is indicated at top left.

(Courtesy, Ministry of Agriculture).

(a)

Surface observer

v

Satellite image observer

Satellite image observer

Surface observer	0	1	2	3	4	5	6	7	8	Σ_r
0		1		1						2
1	4	5	1							10
2			2	1						3
3		3	2	1		1				7
4		1	1	1	1					4
5		3	2	2	2	2		1	1	13
6		1	1	1	4	4	5	7		23
7			1	1	3	3	4	32	16	60
8						3		4	77	84
Σ_c	4	14	10	8	10	13	9	44	94	206

(b)

Surface observer

v

Quantimet

Quantimet

Surface observer	0	1	2	3	4	5	6	7	8	Σ_r
0		1			1					2
1	5	3	2							10
2			1	1	1					3
3		2	4				1			7
4			2	1	1					4
5		2	1	1	4	3	1		1	13
6	1			1	3	4	9	3	2	23
7		1		1	4		11	23	20	60
8						1	2	10	71	84
Σ_c	6	9	10	5	14	8	24	36	94	206

(c)

Satellite image observer

v

Quantimet

Quantimet

Satellite image observer	0	1	2	3	4	5	6	7	8	Σ_r
0	4									4
1	2	8	4							14
2		1	5	2	2					10
3			1	3	4					8
4					5	4	1			10
5					3	4	6			13
6							9			9
7							8	29	7	44
8								7	87	94
Σ_c	6	9	10	5	14	8	24	36	94	206

Fig. 9: Stratocumuliform clouds dominant

(a)

Surface observer

v

Satellite image observer

Satellite image observer

Surface observer	0	1	2	3	4	5	6	7	8	Σ_r
0		1								1
1	3	21	2							26
2	3	5	1							9
3		5	1							6
4		3	1							4
5		2		2		1				5
6			3	1		1	1	2	1	9
7			1		1	2	1	13	7	25
8									10	10
Σ_s	6	37	9	3	1	4	2	15	18	95

(b)

Surface observer

v

Quantimet

Quantimet

Surface observer	0	1	2	3	4	5	6	7	8	Σ_r
0		1								1
1	5	18	3							26
2	4	4	1							9
3		5	1							6
4		1	3							4
5		1	2		1		1			5
6			3		1	1	1	1	2	9
7				1	1	1	5	7	10	25
8								1	9	10
Σ_s	9	30	13	1	3	2	7	9	21	95

(c)

Satellite image observer

v

Quantimet

Quantimet

Satellite image observer	0	1	2	3	4	5	6	7	8	Σ_r
0	6									6
1	3	30	4							37
2			8	1						9
3			1		1	1				3
4					1					1
5					1	1	2			4
6							1	1		2
7							4	7	4	15
8								1	17	18
Σ_c	9	30	13	1	3	2	7	9	21	95

Fig. 10: Cumuliform clouds dominant

(a)

Surface observer

v

Satellite image observer

Satellite image observer

Surface observer	0	1	2	3	4	5	6	7	8	Σ_r
0										
1		1		1						2
2	1									1
3										
4										
5										
6				1						1
7					2	1		5	6	14
8								7	55	62
Σ_c	1	1		2	2	1		12	61	80

(b)

Surface observer

v

Quantimet

Quantimet

Surface observer	0	1	2	3	4	5	6	7	8	Σ_r
0										
1			1	1						2
2	1									1
3										
4										
5										
6		1								1
7					1	1	1	5	6	14
8								8	54	62
Σ_c	1	1	1	1	1	1	1	13	60	80

(c)

Satellite image observer

v

Quantimet

Quantimet

Satellite image observer	0	1	2	3	4	5	6	7	8	Σ_r
0	1									1
1			1							1
2										
3		1		1						2
4					1	1				2
5							1			1
6										
7								10	2	12
8								3	58	61
Σ_c	1	1	1	1	1	1	1	13	60	80

Fig. 11: Stratiform clouds dominant

(a)

Surface observer

v

Satellite image observer

Satellite image observer

Surface observer	0	1	2	3	4	5	6	7	8	Σ_r
0										
1	4	2								6
2		1								1
3		3								3
4										
5										
6				1				1		2
7		1				1	1	4		7
8										
Σ_c	4	7		1		1	1	5		19

(b)

Surface observer

v

Quantimet

Quantimet

Surface observer	0	1	2	3	4	5	6	7	8	Σ_r
0										
1	6									6
2	1									1
3	1	1							1	3
4										
5										
6					1	1				2
7		2		1			1	2	1	7
8										
Σ_c	8	3		1	1	1	1	2	2	19

(c)

Satellite image observer

v

Quantimet

Quantimet

Satellite image observer	0	1	2	3	4	5	6	7	8	Σ_r
0	4									4
1	4	2							1	7
2										
3					1					1
4										
5		1								1
6				1						1
7						1	1	2	1	5
8										
Σ_c	8	3		1	1	1	1	2	2	19

Fig. 12: Cirriform clouds dominant

(a)

Surface observer

v

Satellite image observer

Satellite image observer

Surface observer	0	1	2	3	4	5	6	7	8	Σ_r
0										
1										
2										
3		1								1
4		1		1						2
5										
6			1		2					3
7					1		1	1	1	4
8							1	1	1	3
Σ_c		2	1	1	3		2	2	2	13

(b)

Surface observer

v

Quantimet

Quantimet

Surface observer	0	1	2	3	4	5	6	7	8	Σ_r
0										
1										
2										
3		1								1
4			1	1						2
5										
6				1	1	1				3
7						1	1	1	1	4
8							1	1	1	3
Σ_c		1	1	2	1	2	2	2	2	13

(c)

Satellite image observer

v

Quantimet

Quantimet

Satellite image observer	0	1	2	3	4	5	6	7	8	Σ_r
0										
1		1	1							2
2				1						1
3				1						1
4					1	2				3
5										
6							2			2
7								2		2
8									2	2
Σ_c		1	1	2	1	2	2	2	2	13

Fig. 13: Cumulonimbiform clouds dominant

as the bases of clouds, and he may have difficulty in distinguishing gaps in the cloud, especially when these are at low elevation angles. For these reasons, the surface observer may frequently overestimate the cloud amount.

(b) Satellite image estimations:

In satellite imagery, the perspective problem is generally of minor importance, because of the orbiting altitude of the satellite. In Landsat imagery, for example, the maximum angle of view from the vertical is nearly 6^{o}. A problem frequently encountered in estimating cloud amounts in satellite imagery is that of limited resolution of the sensor. In most previous studies, the imagery used was not of sufficient resolution to allow the detection of small cloud elements. Therefore, the satellite estimates would frequently be too low on occasions when small cumulus cells were present. The same discrepancy, but of different sign occurs when the cloud amount tends towards 8/8. Here small gaps in the clouds may not be resolved and therefore overestimates may occur.

With Landsat imagery, the resolution is sufficiently good to minimise the above problems. However, although small darker, patches in the cloud can be seen, the image analyst must decide whether these are due to shadows or actual gaps. It was found in this study that on numerous occasions, gaps were not identified as such, so causing the overestimation of cloud amount in the satellite imagery at the upper end of 0 to 8 scale.

Despite the good resolution of the MSS, it still proved extremely difficult to identify thin cirrus clouds reported at surface stations. This was especially true on the Quantimet, where the cirrus (if seen) was frequently much darker than many background features.

The remaining contingency tables (Figures 9 to 13) break down the data to facilitate comparisons for individual cloud types:

Stratocumuliform cloud (Fig.9). The overall pattern which emerges in Fig.9 is similar to that for all cloud types (Fig.8). Again the surface observer overestimates, especially in the middle (4 to 5 okta region) of the scale, while at the upper-end of the scale, the estimations from the satellite imagery are the greater.

Cumuliform clouds (Fig.10). The usual pattern emerges. Overestimation by the surface observer is more concentrated at the lower and middle portions of the scale. Again the relationship between the satellite image observer and the Quantimet is fairly consistent.

Stratiform clouds (Fig.11). Here there are few estimates in the middle of the scale. Those we obtained are greater for the surface observer. At the upper end of the scale (7 to 8 oktas) where the majority of estimates occur, good agreement is seen between all 3 methods.

Cirriform clouds (Fig.12). This shows the difficulty of cirrus detection, especially by the Quantimet. Both the surface and satellite image observers overestimate with respect to the machine.

Cumulonimbiform clouds (Fig.13). This cloud type was not frequently encountered. However, the general trend of overestimation at the surface is seen from the tables.

Figure 14 shows frequency graphs for all cloud types (a) and individual families of clouds (b) - (e). Each depicts the frequency (as a % of the total cases) as the ordinate, and the cloud amount as the abscissa. The graphs for all cloud types (Fig.14(a)) reveals maxima at 1 & 8 oktas. This type of cloud frequency distribution has been termed "J" shaped (Barrett, 1976b). Figure 14(b) shows the frequency of stratocumuliform cloud. Here the predominance of large cloud amounts is noteworthy. Such a feature is even more marked with stratiform cloud (Fig.14(d)). For cumuliform cloud (Fig.14(c)) more varied results are obtained by the three methods of analysis. The surface observer produces peaks at 1 & 7 oktas, the satellite image analyst at 1 & 8 oktas, with a minor maximum at 5 oktas also, whilst the Quantimet operator produces peaks at 1 & 8 oktas with a minor peak at 4 oktas. These differences probably result from combinations of psychological, mechanical, and other practical influences. Figures 14(e) & (f) are the most complex, which may be due in large measure to the comparatively low numbers of observations which underlie the graphs.

3. Relations between clouds and their shadows in Landsat 2 imagery

Following the method outlined in Section II.3, results of observed relationships between five different types of clouds and their attendant shadows on the ground were obtained from analyses of 5 selected Landsat 2 images.

For each of the five images in turn two tables were compiled. The first listed co-ordinates of each individual analysis area within that image, together with the numbers of picture points in the analysis areas, and a summation of these values to indicate their total extent. The second gave, for each individual analysis area, observed amounts of cloud, cloud shadow, and land. These amounts were expressed both as numbers of picture points and as percentages of the areas within which they were observed. Relationships were also calculated to relate the areas of cloud shadow to the cloud with which it was associated, and the size of the analysis area itself. Tables 6 & 7 exemplify the detailed findings presented in this form.

From the complete set of results a graph was constructed (Fig.15) to show the changing relationships between % cloud cover and associated cloud shadow as a percentage of that cloud cover for five different cloud situations which included some widely disparate categories of clouds. As might be expected, the associated shadow is relatively small with sheet clouds like stratus, increasing markedly with scattered tower clouds of cumuliform varieties. In the most extreme case (image 2) the cloud cover in the area assessed on the Harwell system was only 19.2%, whereas the area affected by cloud plus cloud shadow was 10.2% higher, at 29.4%. Higher shadow amounts are likely to be

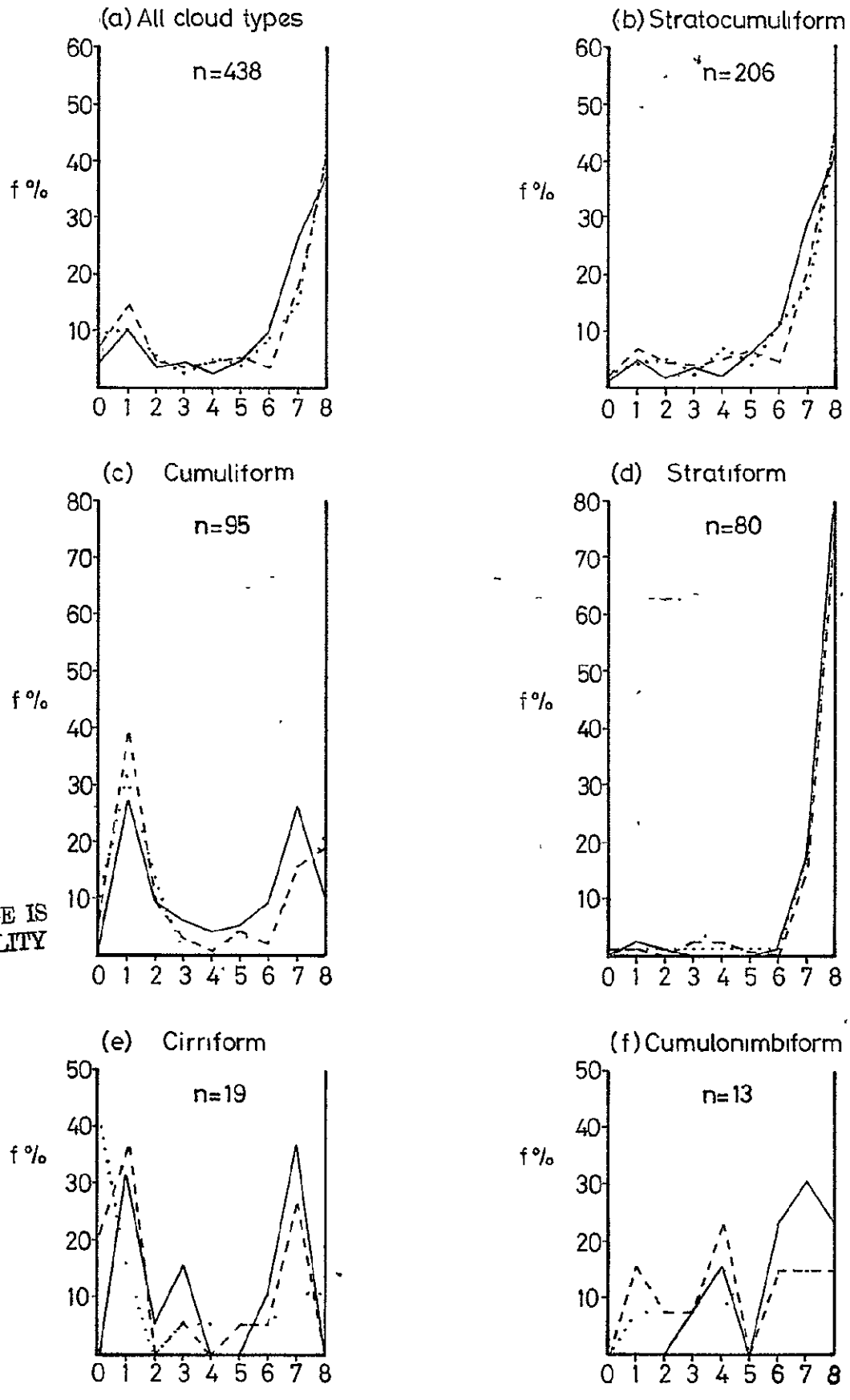

Fig. 14: Frequency distributions from Quantimet study

Table 6

Example from image 1, 3 June 1975 (1006:10 GMT). Cloud Type - Cumulus (mediocris & humilis): Co-ordinates and areas (picture points) of individual analysis areas.

Analysis Area	Co-ordinates Xmax	Xmin	Difference X(max-min)+1	Co-ordinates Ymax	Ymin	Difference Y(max-min)+1	Picture Points Total Area
1	567	391	176 - 177	589	49	540 - 541	95,757
2	390	41	349 - 350	605	325	280 - 281	98,350
3	223	43	180 - 181	324	220	104 - 105	19,005
4	390	245	145 - 146	233	197	36 - 37	5,402
5	390	345	45 - 46	195	137	58 - 59	2,714
6	390	223	167 - 168	324	234	90 - 91	15,288
						Total	236,516

Note: The lengths of the sides of the rectangular analysis areas are shown in the difference columns. To enable the determination of the number of picture points in each analysis area, one must be added to each side length before multiplying the X and Y lengths together.

Table 7

Cloud, Land & Shadow amounts (picture points, with percentages in brackets) in each analysis area specified in Table 6

Area	Cloud	Land	Shadow	Shadow as a % of Cloud
1	32,370(33.8)	57,551(60.1)	5,836(6.1)	18.0
2	36,784(37.4)	54,931(55.9)	6,635(6.7)	18.0
3	6,237(32.8)	11,542(60.7)	1,226(6.5)	19.7
4	2,086(38.6)	3,000(55.5)	316(5.9)	15.2
5	1,232(45.4)	1,283(47.3)	199(7.3)	16.2
6	4,982(32.6)	9,314(60.9)	992(6.5)	19.9
Totals:	83,691(35.4)	137,621(58.2)	15,204(6.4)	Mean = 18.2

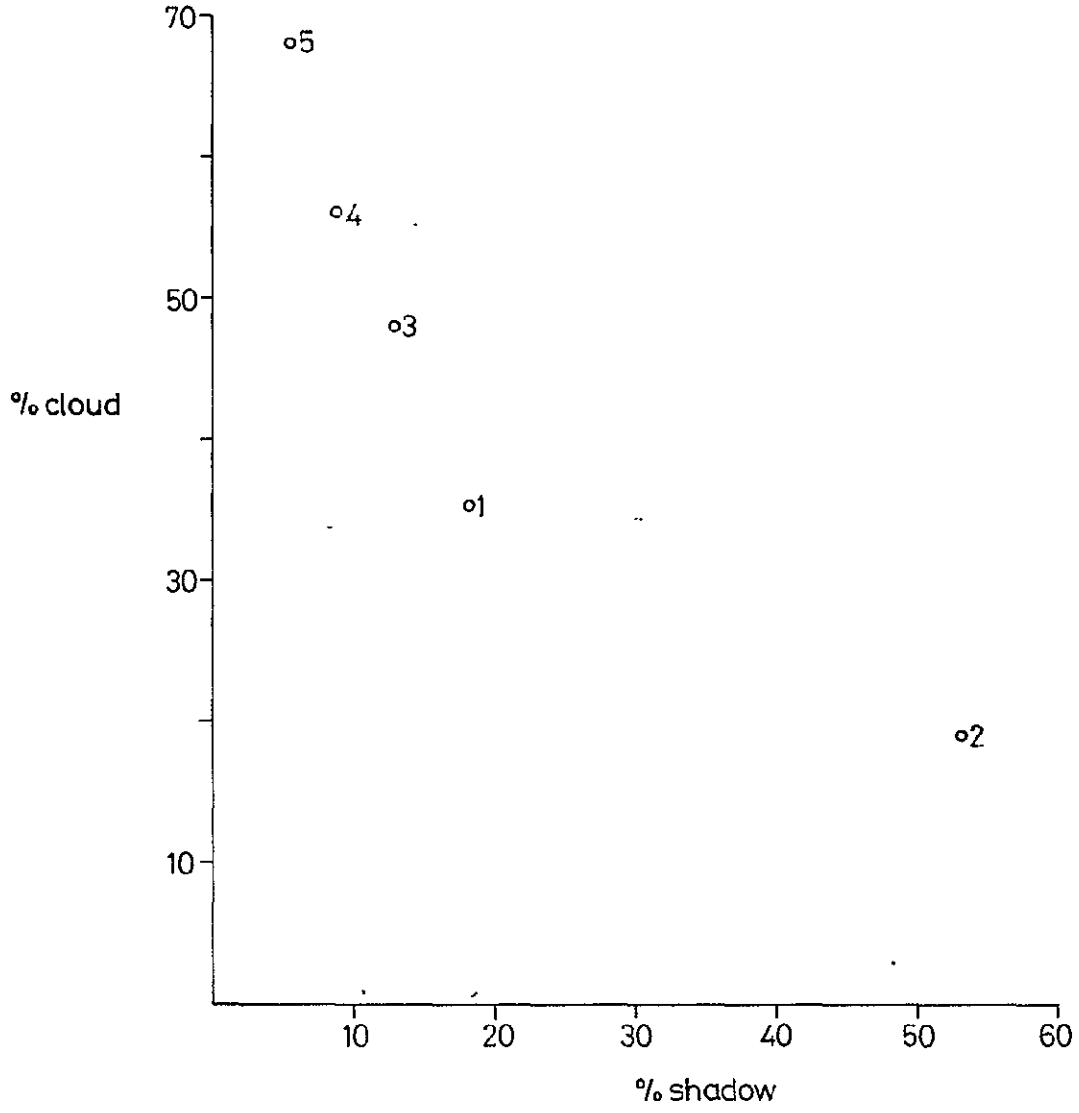

Key.

1 Cu humilis + Cu mediocris
2 " " " " "
3 Ac
4 St + As
5: Sc + As

Fig. 15: Cloud shadow study, relationship between % cloud and % shadow

associated with small, cellular, clouds because the total cloud perimeters within a cloud field will be much higher in comparison with the total area cloud covered than which f'atten clouds which merge into sheets.

It should be noted that the examples studied in this pilot project were all drawn from the months of June and July, when the sun elevation was between 49° - 56°. The shadow effects in other seasons of the year will be substantially greater than those reported here. It would be useful to extend this type of study to ascertain how closely empirical results conform to a theoretical model designed to account for the shadow effects which might be expected in Landsat frames affected by different categories - and mixtures - of clouds in different latitudinal zones at different times of the year. Such a model might involve the clouds themselves (height of cloud base, cloud depth, element size and spacing, etc.), illumination variables (solar elevation and azimuth), and the morphology of the local land surface (slope angle and orientation).

4. Multispectral characteristics of clouds observed by Landsat 2

For analytical purposes, all the brightness [illegible] produced by the Photoscan P-1000microdensitometer in terms of 256 grey-levels were converted to optical density values in the range 0 to 2D. This was a straight-forward procedure as the density bears a linear relationship with the grey-levels, as noted previously.

Fig.16 shows the 15-step grey-scale tablets, plotted as a function of density and waveband. The divisions correspond to the upper limit of each step, the procedure for determining which was outlined above. Step 8 of each wedge is shaded to act as a reference. Step 1 (white) is at the left-hand side, and step 15 (black) is at the right-hand side.

Perhaps the most important fact emerging from this diagram is the wide variation of step width. Generally, the brighter steps, with densities less than 1D, are narrower than the darker steps with densities greater than 1D. The first step is somewhat anomalous in that it has no lower limit. Another notable feature is the variation from image to image in position of similar steps. This variation occurs both between wavebands for a particular frame, and also between one frame and another. Thus, for example, in the illustration of cumulus humilis, corresponding steps of band 7 are generally brighter than those of band 6. Such differences are due in part to variations in the processing of Landsat images.

A serious problem of interpretation therefore arises. Are the differences in brightness in a particular scene in different wavebands due principally to differences in target reflectance, or differences in processing? It is clear from our results that the influences of image processing must be borne in mind constantly as we move towards drawing conclusions from these data. Ideally, the two components of variation should be determined and separated; this we could not achieve in our study.

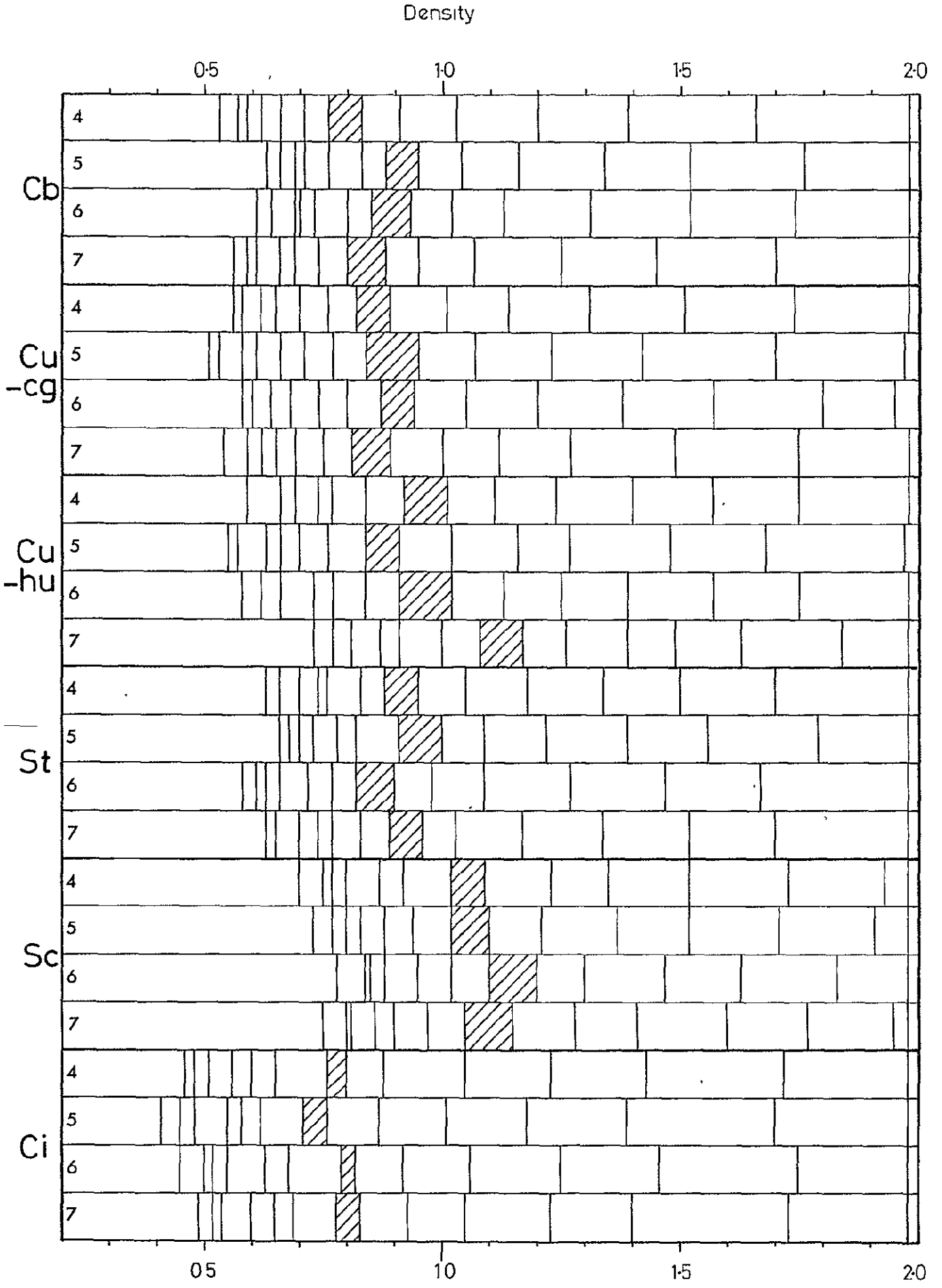

Fig. 16: Grey-scale tablets

Brightness characteristics of Landsat-imaged clouds in summer graphical results

Figures 17a to f show frequency distributions of individual cloud types in each waveband in relation to the 15 step grey-scale. Frequencies have been converted from number counts to percentages to facilitate comparison between different cloud types. Notwithstanding our earlier comments on variations in picture processing, some important differences do occur.

(a) Cumulonimbiform (Fig.17(a)): Bands 4 and 7 show apparently similar distributions, with band 7 being displaced slightly towards the darker end of the scale. Bands 5 and 6, however, possess a strong modal category, well displaced towards the brighter end of the scale.

(b) Cumulus congestus (Fig.17(b)): The frequency distributions of all four wavebands range across the whole step-wedge scale. All the distributions are essentially similar, some minor differences, occurring at the dark end of the scale in steps 14 and 15.

(c) Cumulus humilis (Fig.17(c)): Unlike the cumulus congestus graphs of Fig.17(b), these distributions are restricted in range to the darker end of the scale. This reflects the lower brightness responses of these small cloud cells and the larger areas of dark sea background between them.

(d) Stratiform (Fig.17(d)): Each waveband shows a marked clustering of values at the bright end of the scale, indeed in band 5 almost 100% of the data points are contained within the brightest step. This is undoubtedly due to extensive saturation of the image by this cloud type. The distributions of bands 6 and 7 show tails extending well into the darker portion of the scale.

(e) Stratocumuliform (Fig.17(e)): Bands 4 and 5 have similar distributions, extending across a wide range of values, peaking gently in the centre of the scale. In band 6 there is a slight displacement towards the dark end of the scale. In band 7 there is a significant displacement towards the darker end of the scale, and the range of values is more restricted.

(f) Cirriform (Fig.17(f)): Bands 4, 5 and 6 are similar to one another, with distributions located in the darker portion of the scale and a fairly wide range of values (over 8/9 steps). Band 7 possesses a marked displacement towards the dark end of the scale and the range of values is limited to the darkest 6 steps.

Figures 17(a)-(f) reveal, therefore, that differences in brightness occur both between the wavebands for individual cloud types as well as, more strikingly, between similar wavebands for different cloud sypes. To facilitate the examination of these differences, cumulative frequency distributions were plotted (see Figs.18(a)-(d)).

These graphs consist of plots of percentage cumulative frequency on an arithmetic probability scale, against image density on an arithmetic scale. First, the average density of each step was found. In the case of step 1 the average density was found by determining the average density range of steps 2 to

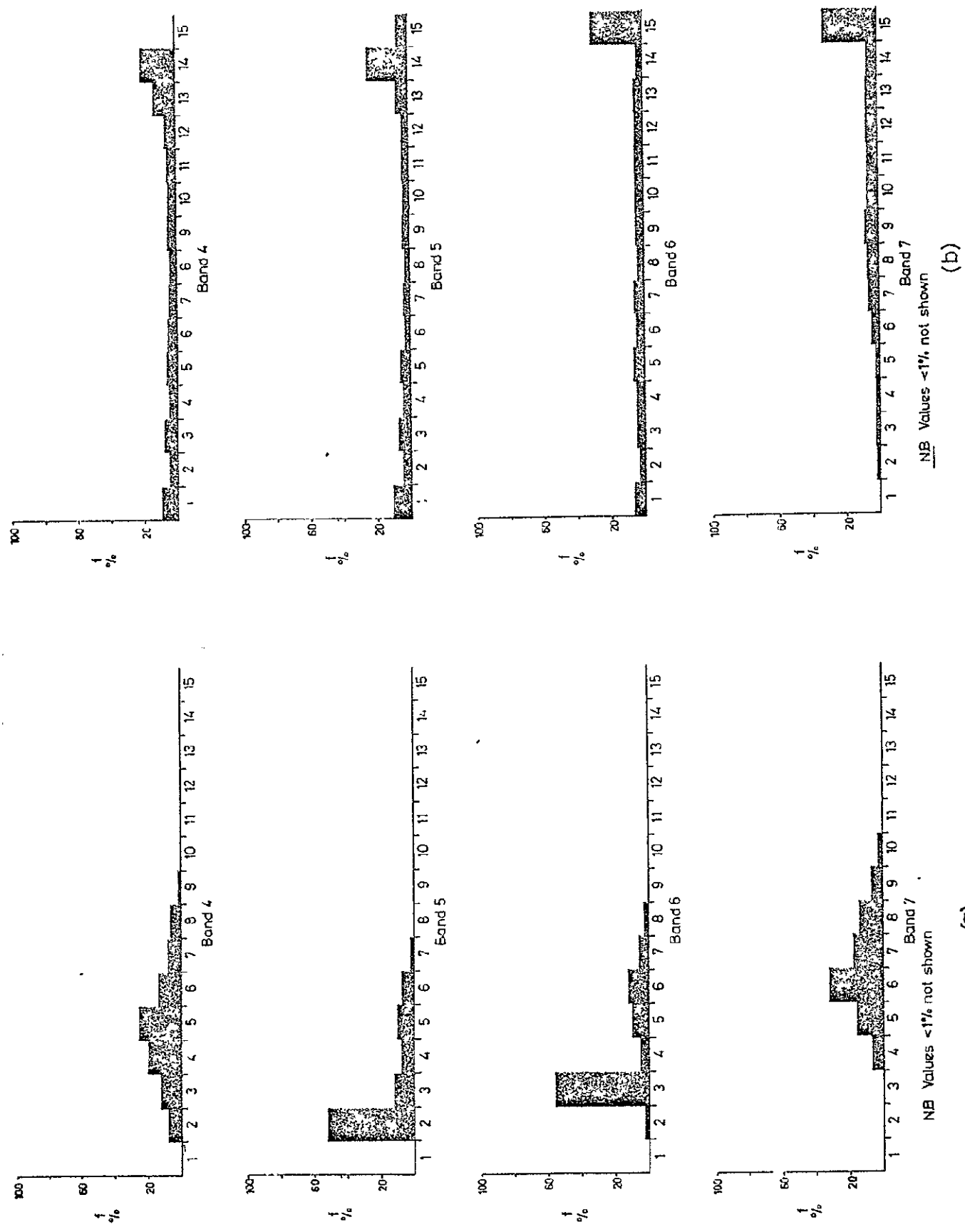

Frequency distributions of clouds from multispectral analyses

Fig. 17(a): Cumulonimbiform

Fig. 17(b): Cumulus congestus

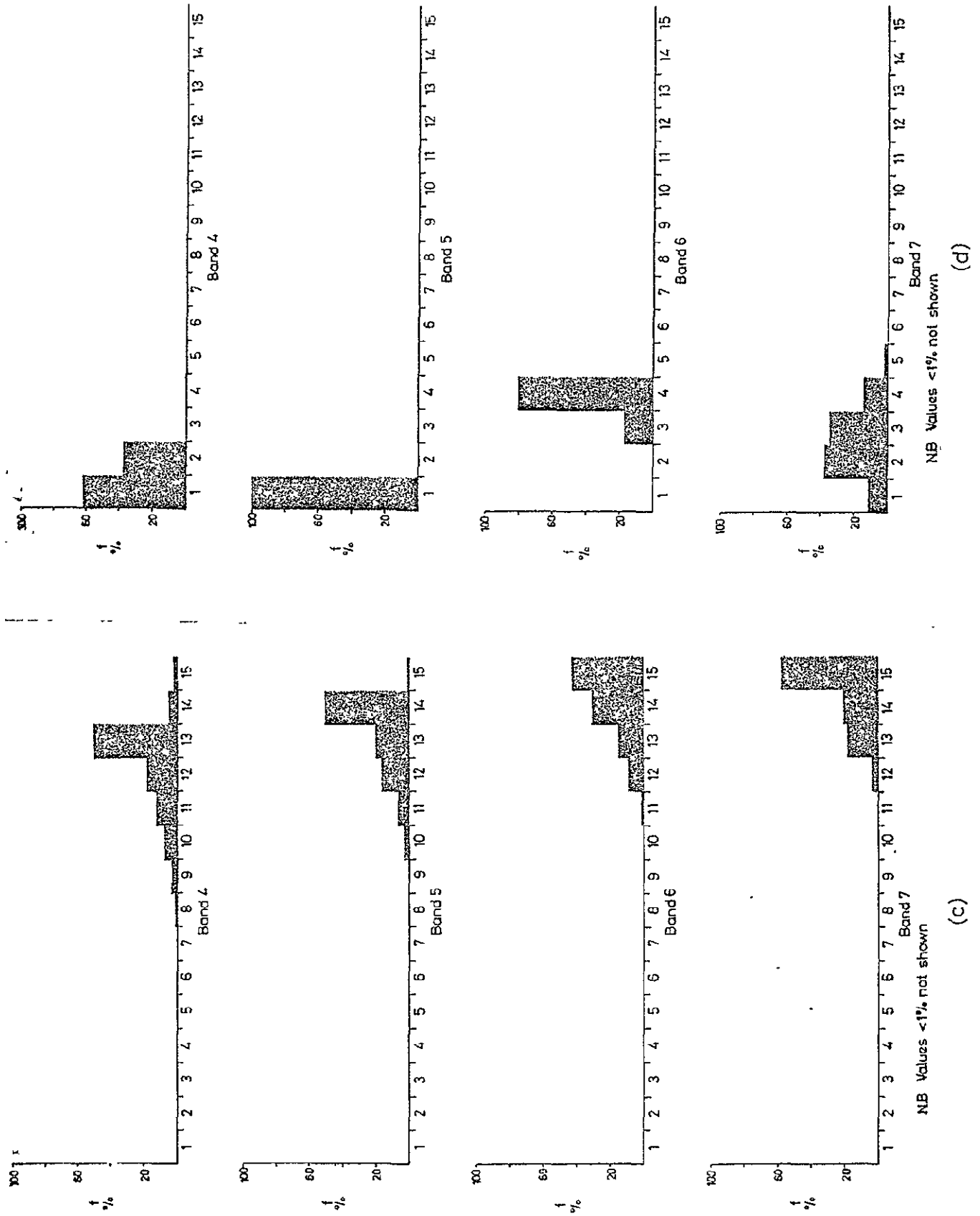

Frequency distributions of clouds from multispectral analyses

Fig. 17(c): Cumulus humilis

Fig. 17 (d): Stratiform

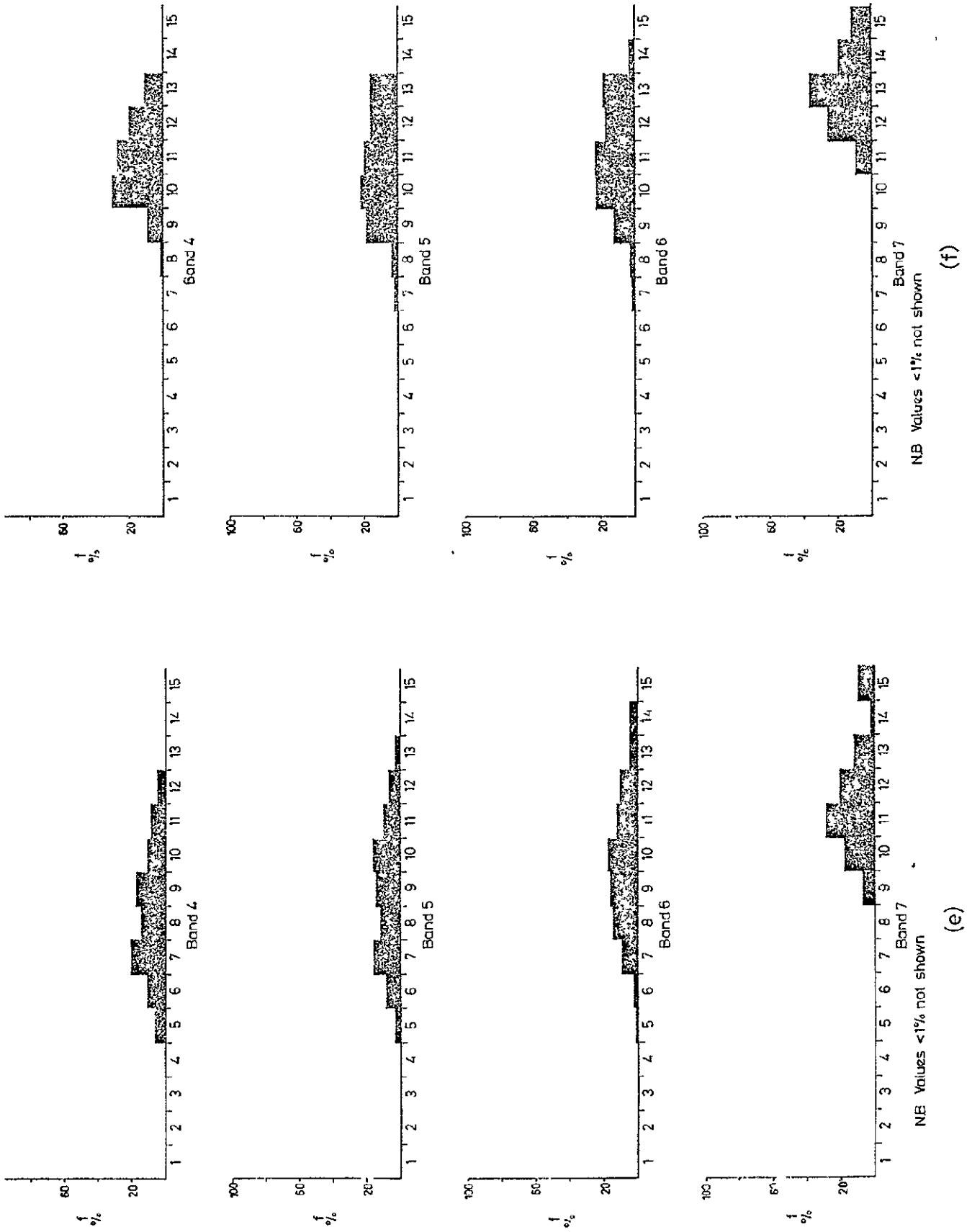

Frequency distributions of clouds from multispectral analyses

Fig. 17 (e) Stratocumuliform

Fig. 17 (f) Cirriform

5 inclusive. This value was then halved, and subtracted from the upper limit value of step 1 to provide an average value for the brightness of that step. The advantage of using arithmetic probability paper in this analysis is that if the distributions plotted are normal, then a straight line will occur on the graph. A brief examination of these diagrams shows that the distributions were not normal. The chief points that emerged from this analysis were as follows:

(a) Band 4 cumulative frequency distributions (Fig.18(a)): Here stratiform and cumulonimbiform clouds appear to give similar results, both having the majority of their values at the bright end of the scale. Similarly cirriform and stratocumuliform clouds are similar to each other, their curves lying close together across much of the graph. At first sight this may appear strange as the graphs of their respective frequency distributions (Figs.17(e) and 17(f)) apparently revealed considerable differences. However, when one examines Figure 16, it can be seen that stratocumuliform grey-scale values are considerably brighter than corresponding cirriform values. This is taken into account more fully in Figure 18(a) where actual density values are employed on the abscissa, not grey-scale step numbers as in Figure 17. Generally, most cloud types follow paths which are roughly parallel over much of the scale in Figure 18. The most notable exception to this is cumulocongestus. The plot for this cloud category starts well to the left of the graph and generally rises less steeply than those for the other cloud types except at the dark end of the scale. The tendency for this cloud type then, is for its plot to cut across the plots for cirriform, stratocumuliform and cumulus humilis.

(b) Band 5 cumulative frequency distributions (Fig.18(b)): These are essentially similar to the band 4 plots in Figure 18(a). However, the stratiform curve is shorter due to the clustering of its values at the bright end of the scale. The cumulus congestus curve again lies across those for the other types.

(c) Band 6 cumulative frequency distributions (Fig.18(c)): For the first time stratiform extends into darker portions of the scale than does cumulonimbiform. Stratocumuliform is now markedly displaced towards the dark end of the scale in comparison to cirrus. Cumulus humilis is similarly displaced towards darker levels, although it retains its approximately parallel position with respect to cirriform and stratocumuliform. Cumulocongestus intersects the other distributions at quite large angles, as in bands 4 and 5. At the dark end of the scale, the final 30% of its distribution follows a similar path to that of cumulus humilis.

(d) Band 7 cumulative frequency distributions (Fig.18(d)): In this waveband, cumulonimbiform has been displaced quite markedly towards the dark portion of the scale. The whole of its curve is on the darker side of the stratiform curve. Cirriform and stratocumuliform distributions now follow very similar paths, both having been displaced markedly towards the darker portion of the scale than in band 6. Cumulus humilis is darker than in band 6. This is probably due to the darkening of the sea background

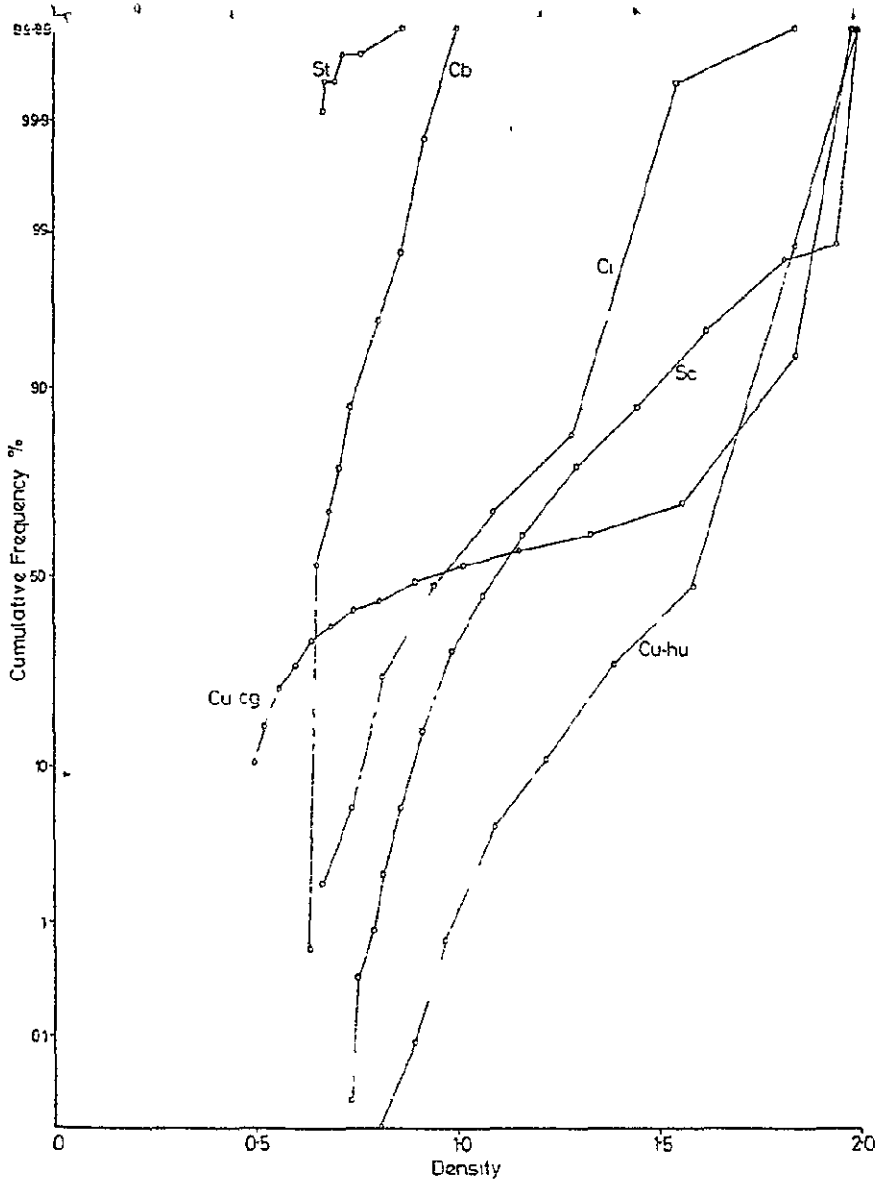

(a)

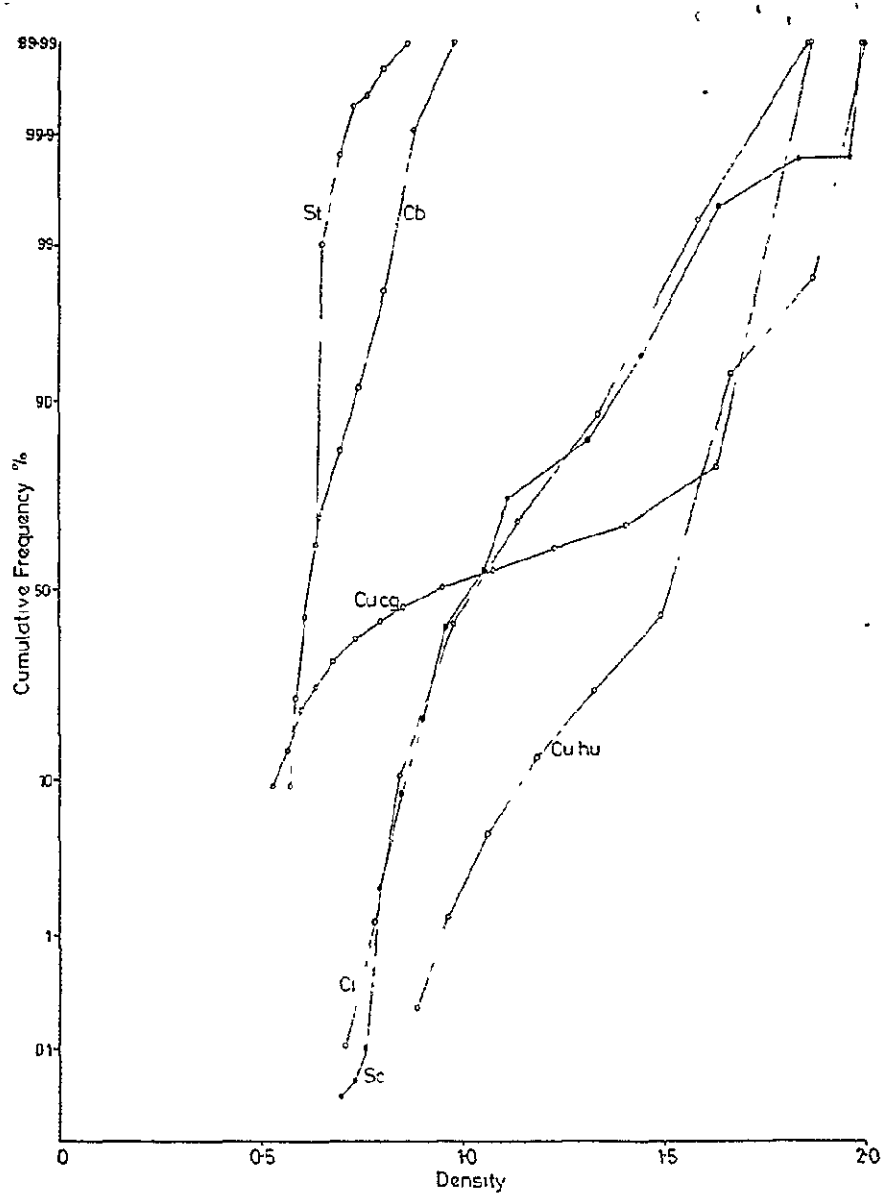

(b)

Fig. 18(a): Band 4 Cumulative Frequency Distributions.

Fig. 18(b): Band 5 Cumulative Frequency Distributions.

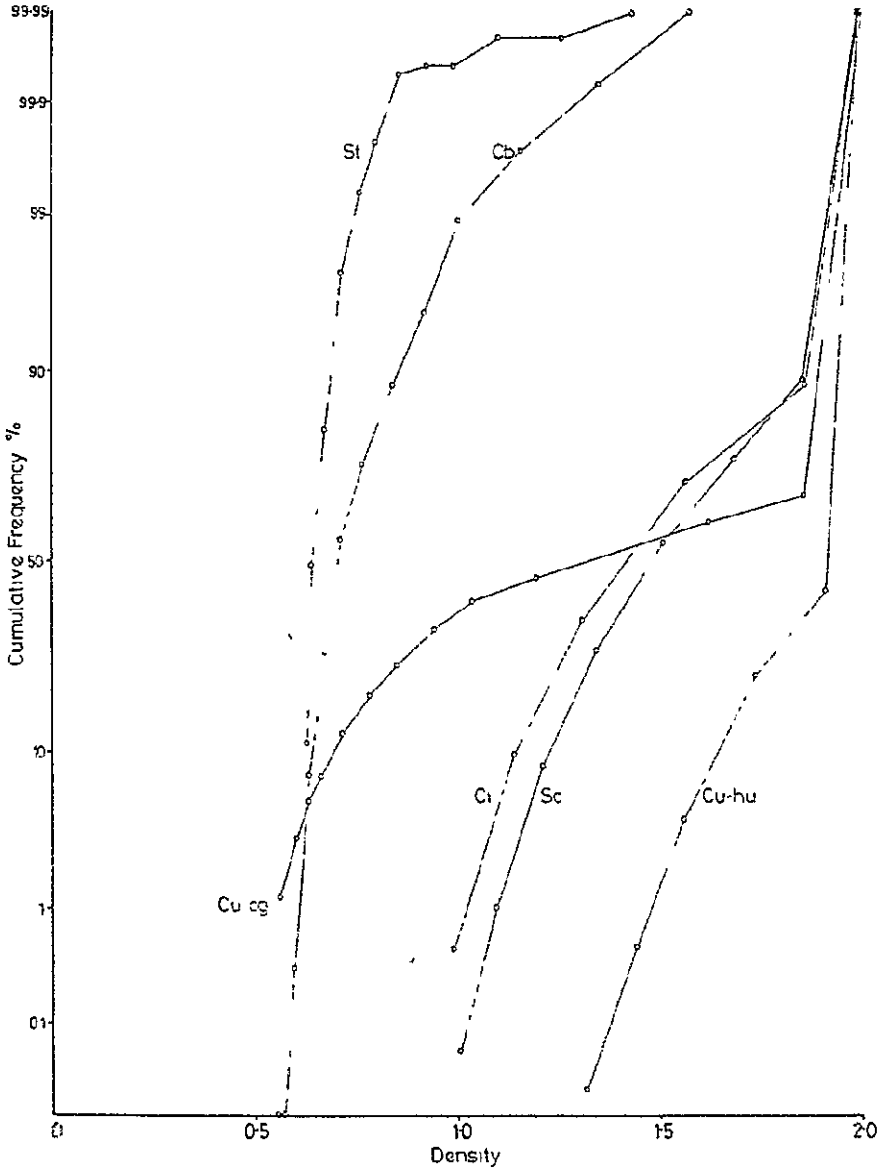

(c)

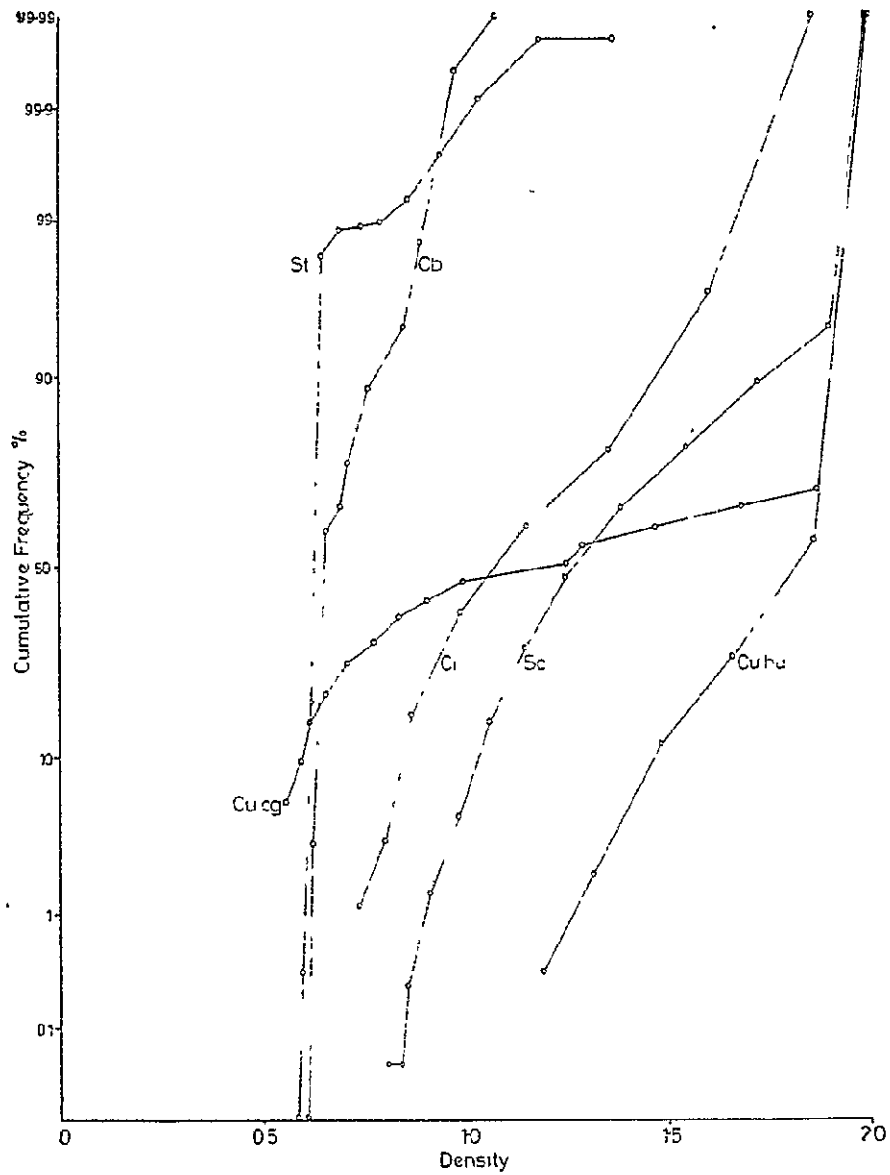

(d)

Fig. 18 (c) Band 6 Cumulative Frequency Distributions.

Fig. 18 (d) Band 7 Cumulative Frequency Distributions

which comprises a larger proportion of this image between the small cumulus cells. This effect is also seen in the case of cirriform and stratocumuliform, both of which contain some areas of sea in the imaging area.

These diagrams, Figures 18(a)-(d), show that marked differences in reflectance characteristics do occur between cloud types and that these differences change from one waveband to another. It is thought that such differences are indeed due principally to target characteristics, not processing practices, for more account is taken of the grey-scale differences in these diagrams through the use of the actual density values of the steps rather than their numbers in the grey-scale.

Brightness characteristics of six categories of clouds in summer: summary statistical results

In addition to such graphical descriptions of the brightness frequency distributions, it is possible to gain further insight into the nature of cloud differences by deriving summary statistics via the method of moments. This is a computational method; the analysis of the mean and standard deviation was carried out on the PDP 11/45 mini-computer. Skewness and kurtosis coefficients were determined on a Hewlett-Packard calculator from the frequency distributions derived by the PDP 11/45. The results of the computations are presented in Table 8.

There are some interesting differences between the summary statistics and the impressions gained of the distributions presented in Figures 17(a)-(f). For example, the cumulonimbiform statistics show that the kurtosis ("peakedness") of the distributions increases steadily from band 4 through to band 7. An examination of Figure 17(a) alone would probably have led one to conclude that bands 5 and 6 were more "peaked" than either bands 4 or 7. Cumulocongestus clouds show relatively large standard deviations, a fact less unexpected when Figure 17(b) is examined. A small negative skewness value is noted in band 7 which corresponds to the increased frequency of values at the dark end of the scale (step 15). The cumulus humilis distributions (Fig.17(c)) are asymmetrical in nature and this produces negative skewness values for all wavebands. Mean brightness values show a similar trend in all the cloud types. Generally, the mean brightness of each successive waveband is slightly darker than the preceding waveband. There are two exceptions to this general rule. Both occur in waveband 5 in the cirriform and stratiform cloud types. Such a decrease in brightness with waveband is probably explained by the decreasing brightness of the background area (the sea) with successive wavebands.

Besides this slight anomaly in the general trend of mean brightness values, stratiform clouds also present some other noteworthy summary statistics. The skewness values recorded are very large, indicating extreme asymmetry of the distribution. This is perhaps not surprising when Figure 17(d) is examined, especially with respect to band 5. However, the kurtosis values seem excessively high when one considers that in sediment analysis values of kurtosis greater than 3.00 indicate extreme leptokurticity (peakedness) and are uncommon.

TABLE 8

Summary statistics for six categories of clouds in summer

Cloud Type	Waveband Number	No. of Data Points	Mean	S.D.	Skewness	Kurtosis
Cumulonimbiform	4	9215	0.65	0.07	1.09	4.13
	5	9215	0.69	0.06	1.75	5.94
	6	9215	0.71	0.07	1.78	6.02
	7	9215	0.76	0.10	1.90	10.05
Cumulus congestus	4	8084	1.13	0.49	0.27	1.46
	5	8084	1.17	0.58	0.22	1.35
	6	8084	1.23	0.57	0.09	1.31
	7	8084	1.40	0.52	-0.09	1.39
Cumulus humilis	4	9025	1.55	0.22	-0.70	3.07
	5	9025	1.63	0.23	-0.82	2.54
	6	9025	1.85	0.18	-1.17	3.44
	7	9025	1.92	0.12	-1.53	4.52
Stratiform	4	8272	0.63	0.01	1.62	13.44
	5	8272	0.57	0.01	50.95	2789.26
	6	8366	0.64	0.04	10.87	168.44
	7	8366	0.66	0.04	3.03	45.02
Stratocumuliform	4	9100	1.12	0.22	0.79	3.21
	5	9100	1.20	0.26	0.87	3.29
	6	9100	1.40	0.28	0.55	2.35
	7	9100	1.59	0.23	0.17	2.08
Cirriform	4	7896	1.14	1.14	0.63	2.71
	5	7896	1.09	1.09	0.49	2.09
	6	7896	1.21	1.21	0.49	2.26
	7	7896	1.57	1.57	0.10	1.96

Spectral reflectance graphs for six categories of clouds

The results summarised in the 3 sections above are all related to characteristics of cloud as viewed over areas of about 33.7 km^2 on the ground. It would be interesting to investigate the degrees of similarity between those results and others for a range of smaller areas. Whilst we must be cautious not to read too much into the results obtained, it seems legitimate to attempt to interpret them in terms of what they may indicate concerning the characteristics of cloud elements viewed by the microdensitometer over areas of about 337m^2 on the ground. Taking the modal classes in Figures 17(a)-(f) to indicate the most representative brightness values for each cloud category in each waveband we have compiled a set of spectral reflectance graphs for the six cloud examples (see Figs.19(a)-(f)). It appears therefrom that the spectral reflectance signatures for different categories of clouds possess some marked differences both in form and position on the axes. Not surprisingly the cumuliform and cumulocongestus curves are generally similar, whilst the stratiform and cumulonimbiform curves are disappointingly alike.

It would seem well worthwhile investigating the multispectral differences of Landsat-imaged clouds more carefully, perhaps through the use of digital data from the CCTs so that the full resolution of the imagery might be employed and picture processing problems thereby eliminated.

Discussion of the Photoscan P-1000 results

It is in the field of sedimentary petrology and geology that these types of statistical analysis have reached their greatest sophistication. The technique of moment analysis has been used to identify and differentiate sediments (e.g. Folk and Ward, 1957) and in the interpretation of the depositional histories of different sediments (e.g. Greenwood, 1972). Generally, bivariate plots have been employed, with each of the four summary statistics being plotted in turn against each of the others. However, Folk and Ward (1957, p.23) managed to produce a four-variate graph to represent the relationships between the four summary statistics in one diagram. Often, the analysis of such data has been extended by using clustering and discriminant analyses as classification procedures to allow new data values to be assigned correctly to previously determined groupings.

It is felt that this latter type of analysis may prove most useful in attempts to assign new cloud information in Landsat data to previously determined cloud types, defined in terms of their moment statistics. However, some problems would have to be solved before this were to be possible. For example, our results for stratiform clouds indicate that the application of such techniques to non-normally distributed data without some prior transformation can lead to misleading, possibly erroneous, results and conclusions. One solution might be to transform the data after initial statistics had been calculated. For example, Folk and Ward (1957) produced a transformed kurtosis statistic (K') derived from the ordinary kurtosis value, (K). The relationship is as follows:

$$K' = \frac{K}{(K + 1)}$$

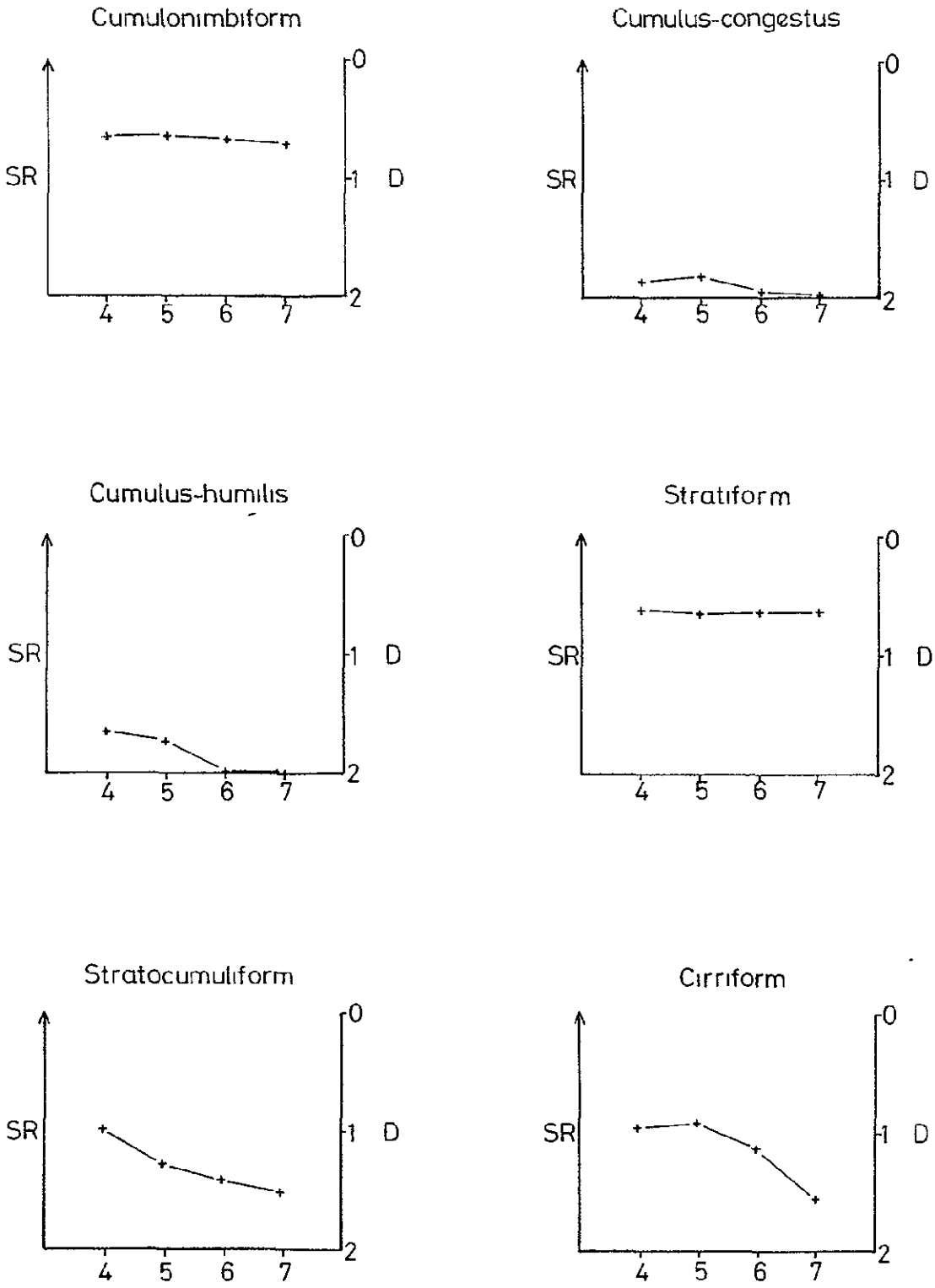

Fig. 19: Spectral reflectance graphs

If this transformation had been applied in our study, the range of kurtosis values would have ranged from about 0.5 to 1.0, much less than the range we found. This transformation produces an approximately normal kurtosis distribution (Folk and Ward, 1957, p.15).

A further problem with our distributions is that at the brightest end of the scale they are "open-ended": no lower limit was defined. Folk (1965), in discussing grain size analyses of sediments, felt that the application of the method of moments to such open-ended distributions might not be justified. This may be pertinent to our extreme results for stratiform clouds, where likely saturation of the image caused many values to be located in the unbounded step 1 of the grey-scale step-wedge.

It is apparent, therefore, that considerable work remains to be done if a worthy aim is to produce an operational cloud identification scheme for Landsat-type imagery based on cloud brightness statistics. However, the difficulties should not prove insurmountable if careful thought is given to experimental design and operation.

Seasonal variations in brightness characteristics of Landsat-imaged clouds

In Section II.4 it was explained that, subsequent to the initial multispectral cloud study based on data obtained from a Photoscan P-1000 rotating drum microdensitometer some consideration was given by an undergraduate student to data obtained using a much simpler Photolog Cub spot densitomer. Although these results were obtained in a less sophisticated manner for unit areas of a different size they are worth reporting for the conclusions they support concerning the degrees of seasonal variations in cloud brightness and the factors involved in producing them. Table 9 sets out the numerical results in terms of accumulated brightness values for each Landsat MSS waveband. In some cases it was not possible to identify in our image file a suitable image or images to illustrate a particular category of cloud at or near a given solstice or equinox. This explains, for example, why no results are given for any cloud category in Spring.

(i) Cirriform (Table 9): No suitable example of cirriform cloud could be found for the period around the autumn equinox, but the summer distributions of brightness obtained are very similar to those obtained by Barrett, Grant & Harris (1976). The main difference from the earlier study is that the step values for cloud brightness are more closely grouped, a feature which is found in many of the other cloud families' distributions, and this reflects the larger sampling area, which takes the average value of a much larger number of pixels on the image. Bands 4, 5 and 6 are fairly similar to one another, with distributions located towards the darker portion of the scale. This would be expected for a cloud which is thin, and probably largely composed of ice crystals, so having a low albedo. Band 7 is markedly displaced towards the darker end of the scale, and this is found also with all the other cloud types. In the winter example there is a much closer grouping of values, they being found only in steps 13 and 14.

C-2

A. CIRRIFORM (June 23rd 1975 Solar Alt. 56°)

4)	-	-	-	-	-	-	-	-	16	61	23	-	-	-	-
5)	-	-	-	-	-	-	-	1	37	38	21	3	-	-	-
6)	-	-	-	-	-	-	-	1	21	46	27	4	-	-	-
7)	-	-	-	-	-	-	-	-	-	4	33	45	18	-	-

(Jan. 12th 1976 Solar Alt: 11°)

4)	-	-	-	-	-	-	-	-	-	-	-	-	73	27	-
5)	-	-	-	-	-	-	-	-	-	-	-	-	50	50	-
6)	*	*	*	*	*	*	*	*	*	*	*	*	*	*	*
7)	-	-	-	-	-	-	-	-	-	-	-	-	1	99	-

B. CUMULIFORM (Jul. 2nd 1975 Solar Alt. 54°)

4)	-	-	-	-	-	-	-	-	1	1	12	60	26	-	-
5)	-	-	-	-	-	-	-	-	-	1	6	34	59	-	-
6)	-	-	-	-	-	-	-	-	-	-	2	12	65	21	-
7)	-	-	-	-	-	-	-	-	-	-	-	-	10	85	5

(Sep. 12th 1975 Solar Alt. 33°)

4)	-	-	-	-	-	-	-	-	-	-	-	5	61	31	3
5)	-	-	-	-	-	-	-	-	-	-	-	2	42	56	-
6)	-	-	-	-	-	-	-	-	-	-	-	1	17	74	8
7)	-	-	-	-	-	-	-	-	-	-	-	-	-	68	32

(Dec. 28th 1975 Solar Alt. 12°)

4)	-	-	-	-	-	-	-	-	-	-	-	-	15	85	-
5)	-	-	-	-	-	-	-	-	-	-	-	-	10	90	-
6)	-	-	-	-	-	-	-	-	-	-	-	-	11	77	12
7)	-	-	-	-	-	-	-	-	-	-	-	-	1	47	52

C. STRATIFORM (June 17th 1975 Solar Alt. 51°)

4)	82	18	-	-	-	-	-	-	-	-	-	-	-	-	-
5)	86	14	-	-	-	-	-	-	-	-	-	-	-	-	-
6)	32	68	-	-	-	-	-	-	-	-	-	-	-	-	-
7)	16	84	-	-	-	-	-	-	-	-	-	-	-	-	-

(Sep. 1st 1975 Solar Alt. 42°)

4)	87	13	-	-	-	-	-	-	-	-	-	-	-	-	-
5)	100	-	-	-	-	-	-	-	-	-	-	-	-	-	-
6)	86	14	-	-	-	-	-	-	-	-	-	-	-	-	-
7)	72	24	4	-	-	-	-	-	-	-	-	-	-	-	-

(Jan. 10th 1976 Solar Alt. 13°)

4)	-	-	-	-	-	-	-	-	-	-	87	13	-	-	-
5)	-	-	-	-	-	-	-	-	-	44	56	-	-	-	-
6)	-	-	-	-	-	-	-	-	-	-	100	-	-	-	-
7)	-	-	-	-	-	-	-	-	-	-	11	89	-	-	-
	1	2	3	4	5	6	7	8	9	10	11	12	13	14	15

GREY SCALE

Table 9

Brightness Frequency Distributions

D. CUMULONIMBIFORM (June 16th 1975 Solar Alt. 52°)

4)	-	1	22	13	6	15	5	12	6	6	4	8	2	-	-
5)	-	2	17	16	5	8	5	12	10	11	3	9	2	-	-
6)	-	4	20	11	6	4	7	8	11	12	5	9	3	-	-
7)	-	-	8	12	7	10	9	9	10	12	9	7	5	2	-

(Sep. 12th 1975 Solar Alt. 36°)

4)	-	4	5	8	14	17	11	10	9	6	6	6	4	-	-
5)	-	10	10	8	12	15	8	14	4	5	6	5	5	1	-
6)	-	3	10	14	7	7	7	13	11	9	9	4	4	2	-
7)	*	*	*	*	*	*	*	*	*	*	*	*	*	*	*

(Dec. 28th 1975 Solar Alt. 11°)

4)	-	-	-	-	-	-	-	-	-	3	17	47	29	4	-
5)	-	-	-	-	-	-	-	-	-	19	34	31	15	1	-
6)	-	-	-	-	-	-	-	-	-	8	38	38	13	3	-
7)	-	-	-	-	-	-	-	-	-	-	17	40	36	7	-

E. STRATOCUMULIFORM (June 26th 1975 Solar Alt. 51°)

4)	48	18	9	10	10	3	2	-	-	-	-	-	-	-	-
5)	51	25	11	5	4	1	3	-	-	-	-	-	-	-	-
6)	47	32	9	4	2	2	3	1	-	-	-	-	-	-	-
7)	9	20	16	13	13	5	11	9	3	1	-	-	-	-	-

(Sep. 14th 1975 Solar Alt. 32°)

4)	-	1	-	8	12	14	20	16	17	6	2	4	-	-	-
5)	-	-	3	14	13	14	11	24	11	6	4	4	-	-	-
6)	-	-	1	7	17	24	15	12	11	6	5	2	-	-	-
7)	-	-	-	-	-	11	20	20	22	15	7	5	-	-	-

(Dec. 25th 1975 Solar Alt. 12°)

4)	-	-	-	-	-	-	-	-	-	-	3	77	20	-	-
5)	-	-	-	-	-	-	-	-	-	-	11	83	6	-	-
6)	-	-	-	-	-	-	-	-	-	-	11	67	22	-	-
7)	-	-	-	-	-	-	-	-	-	-	-	10	74	16	-
	1	2	3	4	5	6	7	8	9	10	11	12	13	14	15

GREY SCALE

Table 9 (cont)

Brightness Frequency Distributions

(ii) Cumuliform (Table 9B): In the summer, there is a steady change between bands 4 and 7, with each successive image darker. They are noticeably negatively skewed distributions, with the few brighter values corresponding to the small scattered bright clouds, but a large number of dark values recorded mainly over the dark sea background. In autumn, and more so in winter, the bright tails on the distribution curves are much more truncated, indicating perhaps less contrast between the sea, though this is darker, and the clouds as a lower solar elevation results in more shadows in and around the individual cloud cells. One might also expect cumulus clouds at these times of the year to be less active in growth and development, hence they may be thinner and have a lower liquid water content.

(iii) Stratiform (Table 9C): Here, both summer and autumn examples have virtually saturated the pictures in bands 4, 5 and 6, and in the autumn example in band 5 all the brightness values lie in step 1 of the grey-scale. This saturation effectively conceals any important differences between summer and autumn, though summer stratiform would probably be brighter on an extended grey-scale. In winter, distributions are very closely clustered around step 11 of the grey-scale, this uniformity suggesting perhaps a fairly even cloud surface. As in summer and autumn, band 5 appears to have the highest number of bright values and band 7 the lowest, though there is not a great deal of difference between any of the bands.

(iv) Cumulonimbiform (Table 9D): This shows the widest distribution of brightness values of any cloud family, especially in summer and autumn. It is the only case where the distributions extend further over the grey-scale than in the Photoscan P-1000 study, and this is probably due to the necessary inclusion of small dark sea areas between the large cloud cells in order to make up the required size of sample area. There is some evidence of double peaking in all wavelengths in the summer, with the larger peak at the brighter end of the distributions representing the bright tops of the larger convective cells and the darker peak the shadows between cells. The autumn distribution is fairly similar, though with a darker modal class, but the winter pattern is quite different. This is a fairly strongly peaked curve much further towards the darker end of the scale, and with little difference between any of the wavebands.

(v) Stratocumuliform (Table 9E): The distribution graphs for the three seasons are very different from one another. In summer, there is a strong modal category in the brightest step, suggesting that the large scallops of the stratocumuliform cloud type are saturating the image. Unlike stratiform cloud, however, there is a long tail extending 7 or 8 steps into the grey-scale in response to much greater surface irregularities. In the autumn there is no such strong modal class, but rather a gently peaked curve, extending across a wide range of values either side of the centre of the scale. The winter curves are very highly peaked in bands 12 and 13 and have very little spread at all.

Over all, Table 9 shows that there are considerable differences in brightness distributions in different wavebands and in different seasons. In general, bands 4, 5 and 6 behave fairly similarly, but band 7 tends to be darker and usually has a more strongly peaked distribution. There is usually much less difference between the brightness values observed in summer and autumn than between those two seasons and winter. The period around the winter solstice tends to have curves displaced well towards the dark end of the scale and noticeably more peaked than the other seasons.

While these simple distribution curves and tables show something of the seasonal and spectral brightness changes, further statistical graphs of various types are required to evaluate the differences more precisely. These were derived from the tables of summary moment statistics calculated by the computer. Though such results should not strictly be applied to non-normally distributed data without some prior transformation, it was felt that the deviations from normality were unlikely to be of enough significance to invalidate the results.

Three separate sets of graphs were constructed based on central measures of cloud brightness for each cloud type, each central value being related to the appropriate grey-scale in order to minimise the effects of variable image processing (Figs. 20 & 21). The first set of graphs (Fig.20) shows the seasonal variations in mean measured brightness and conveys very similar impressions to those of the earlier frequency distributions. Summer is generally brightest as expected, except in the case of the saturated stratiform images, and summer and autumn values are usually closer together than either are to those of the winter. The quite different forms of graphs in the different cloud types could be one of the bases for an automated cloud-type identification system of the future. Broadly similar patterns are apparent in sets of graphs of seasonal variations in modal brightness. One notable exception is for cumulonimbiform cloud, where the modes are considerably brighter than the means, showing a strongly positively skewed distribution probably due to the exceptional brightness in the limited areas of the cell tops compared to the rest of the cloud mass.

In the graphs of central tendency (Fig.21), an attempt has been made, using the method suggested by Winston (1971), to normalize the brightness values by allowing for the differing intensity of sun illumination for varying solar elevation. The first step in their construction was to convert the recorded optical density values (means, determined by computer) of the autumn and winter cloud samples to values of transmission of light through the images: this is related more directly to brightness. The transmission values were divided by the cosine of the solar zenith angle in order to standardise for vertical solar illumination; then the results were multiplied by the cosine of the summer solar zenith angle for that cloud type, and the resultant transmission values had then been standardised with respect to summer sun illumination. The transformed transmission values were converted back into optical density values and the new readings were compared with the grey-scale for each transparency.

If there were isotropic scattering from the clouds, then the transformed brightness values could be related fairly directly to spectral albedo. As has been pointed out earlier, however, (e.g. by Ruff et al. 1968) this is not quite the case, especially

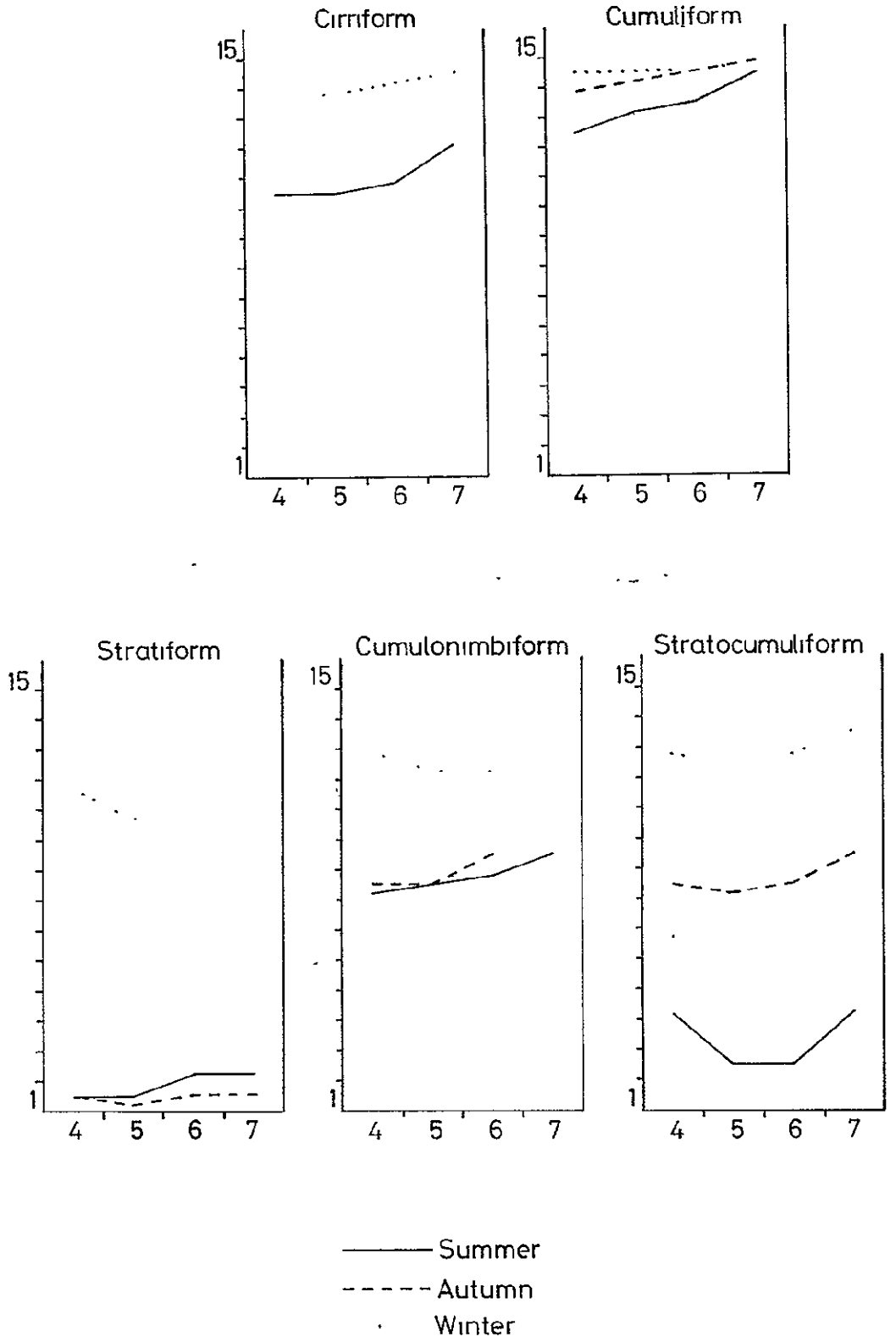

Fig. 20: Seasonal variations in mean brightness measured on grey-scale

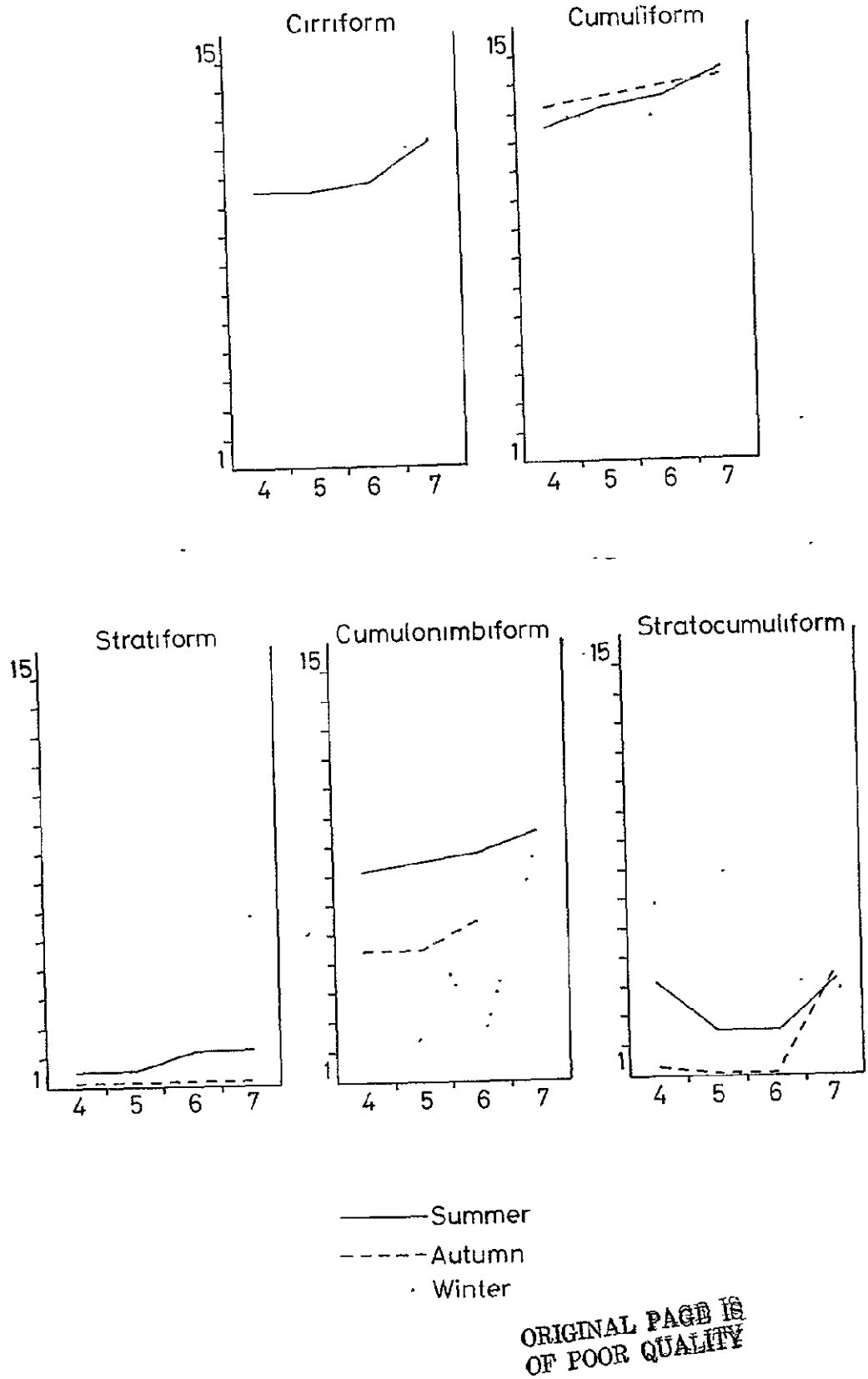

Fig. 21: Seasonal variations in mean brightness, standardised for summer solar elevation, measured on grey-scale

at low solar elevations. Naturally, with the mean brightness values all standardised for summer solar elevation, the graph curves are generally considerably closer to each other. Winter is no longer necessarily the producer of the darkest images and in the longer wavebands in the cumulonimbiform and cumuliform it becomes the brightest of the three. These two cloud families both contain large numbers of clouds with steeply-sloping sides where a near-horizontal solar beam has more chance of being reflected vertically upwards than it would in the case of a sheet cloud. In fact, it is found that with the sheet cloud types, the examples around the winter solstice period are the darkest as relatively little radiation can be reflected steeply upwards even though total albedo may well increase at such low solar elevations. There is not much difference between summer and autumn values, and in the case of stratiform cloud brightness, an already virtually saturated autumn image becomes "super-saturated" after transformation.

A useful statistical measure of spread of a distribution is the coefficient of variation (c.o.v.), which allows one to compare several groups with respect to their relative homogeneity in instances where the groups have very different means; it is simply calculated, being the standard deviation divided by the mean. A high value of c.o.v. is due to large variations in cloud brightness within the sampling area and may indicate atmospheric instability or large-scale turbulence. The highest values (see Fig.22) were obtained in summer and autumn in cumulonimbiform cloud fields, which are very unstable areas. The winter value of c.o.v. in cumulonimbiform is much lower and indeed the lowest c.o.v. values are found in winter in all the cloud families (except in the case of stratiform, where summer and autumn brightness values are artificially close together due to image saturation). Both cumuliform and stratocumuliform c.o.v. values are highest in autumn, perhaps indicating more instability or turbulence then than in the summer.

Two further graphs were constructed (Higgitt, 1977; not included here) to show the seasonal variations in skewness and kurtosis of brightness frequency distributions. In the first, winter values were almost invariably the most negatively skewed, showing a high concentration of dark values along with a lesser number of brighter values. Stratiform and cirriform showed little skewness, while cumuliform was the only cloud type consistently negatively skewed, due to the large area covered by a dark sea background. Cumulonimbiform and, to an even greater extent, stratocumuliform, clouds showed strong positive skewness, the former being greatest in the autumn and the latter in the summer.

For a normal distribution, kurtosis values greater than about three indicate excessive peakedness. Consequently it appeared that the summer and autumn values for stratocumuliform were exceptional. Probably they were caused by strong contrasts between relatively uniform bright scallops and more limited shadow areas surrounding them within the sample area. A similar explanation may account for the high autumn peakedness in cumulonimbiform cloud fields. The clouds (cirriform and stratiform) which reflect in a relatively uniform manner showed near-normal peakedness, while cumuliform, with its dark peak and limited scattered brighter values was also moderately leptokurtic.

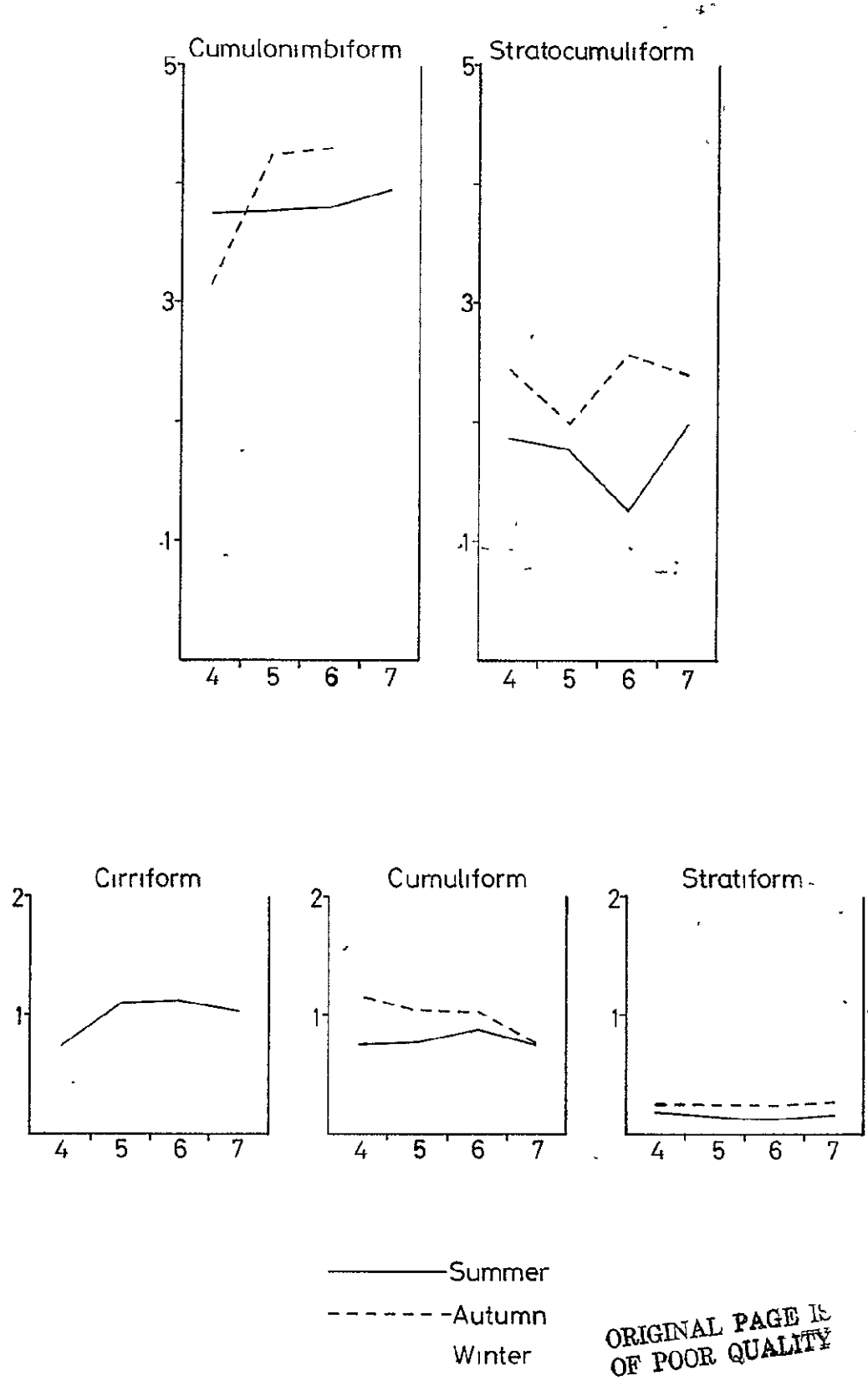

Fig. 22: Seasonal variations in the coefficient of variation of brightness distribution

Conclusions of the seasonal cloud brightness study

It would appear that there are considerable statistical variations in the brightness characteristics of cloud families with changing season, and that these are not related simply to the variations in solar angle. Much of the change in brightness frequency distributions may be due to changes in water content, particle-size distribution and form of the upper cloud surface. Further research is recommended in these directions. As for multispectral cloud signature characteristics, it appeared that the results were reasonable comparable with those obtained earlier using the Photoscan P-1000 despite the much larger sampling area and spot size and consequent loss of resolution.

5. Simultaneous observations of clouds by aircraft and Landsat 2

This sub-section is concerned with comparisons between observations made simultaneously and near-simultaneously over East Anglia by Landsat 2 and the Hercules aircraft of the Meteorological Research Flight (see Section II.5).

Radiometric data obtained from a Barnes PRT 4 on the Hercules are summarised in Figure 23, a temperature transformation based on one-tenth of the data frequency recorded during the flight on 19 March 1977. It is clear from the graph that considerable temperature variations were observed during the flight, which, fortuitously, crossed cloud fields of some variety. The absolute range of observed temperatures was from +1.8°C to -26.2°C. Because of the significance of quite small changes of cloud conditions for such detailed comparisons between the radiation temperatures and reflectance properties of the cloud surfaces we propose, at this stage, to draw only qualitative conclusions from the data to hand. At a later stage we intend to return to these data to consider whether more sophisticated methods of comparison might yield more quantitative results.

Comparisons between the Hercules radiation temperature graph (Fig.23) and the Landsat imagery (Plates 8 & 9)

Initially, between 1008 and 1010, the cloud-top temperature was cold, between -12 to -19°C. At this stage the aircraft was flying over stratocumulus, reported as 6 oktas by the observer, who also noted cirrus ahead of the Hercules. Between 1010 and 1012 a sharp rise in temperature took place, to -2.5°C corresponding with a small break in cloud, before decreasing again over stratocumulus. The cloud between 1012 and 1016 was more broken, with a more textured surface: this is reflected in the temperature curve which oscillates between -8°C and -14°C. The observer at this time recorded 2 oktas cover of cirrus. Some cirrus is visible in the Landsat imagery, especially on the band 4 image, to the west of the flight path. This appears to be an aircraft contrail dispersing.

Between 1016 and 1017 the edge of the stratocumulus field was reached, a fact noted by the observer. Correspondingly, the temperature trace rises sharply for this time and reaches the maximum temperature of the flight (+1.8°C) shortly after 1018. Between 1018 and 1025 the aircraft passed over some isolated cumulus cells and well broken cumulus and stratocumulus. The

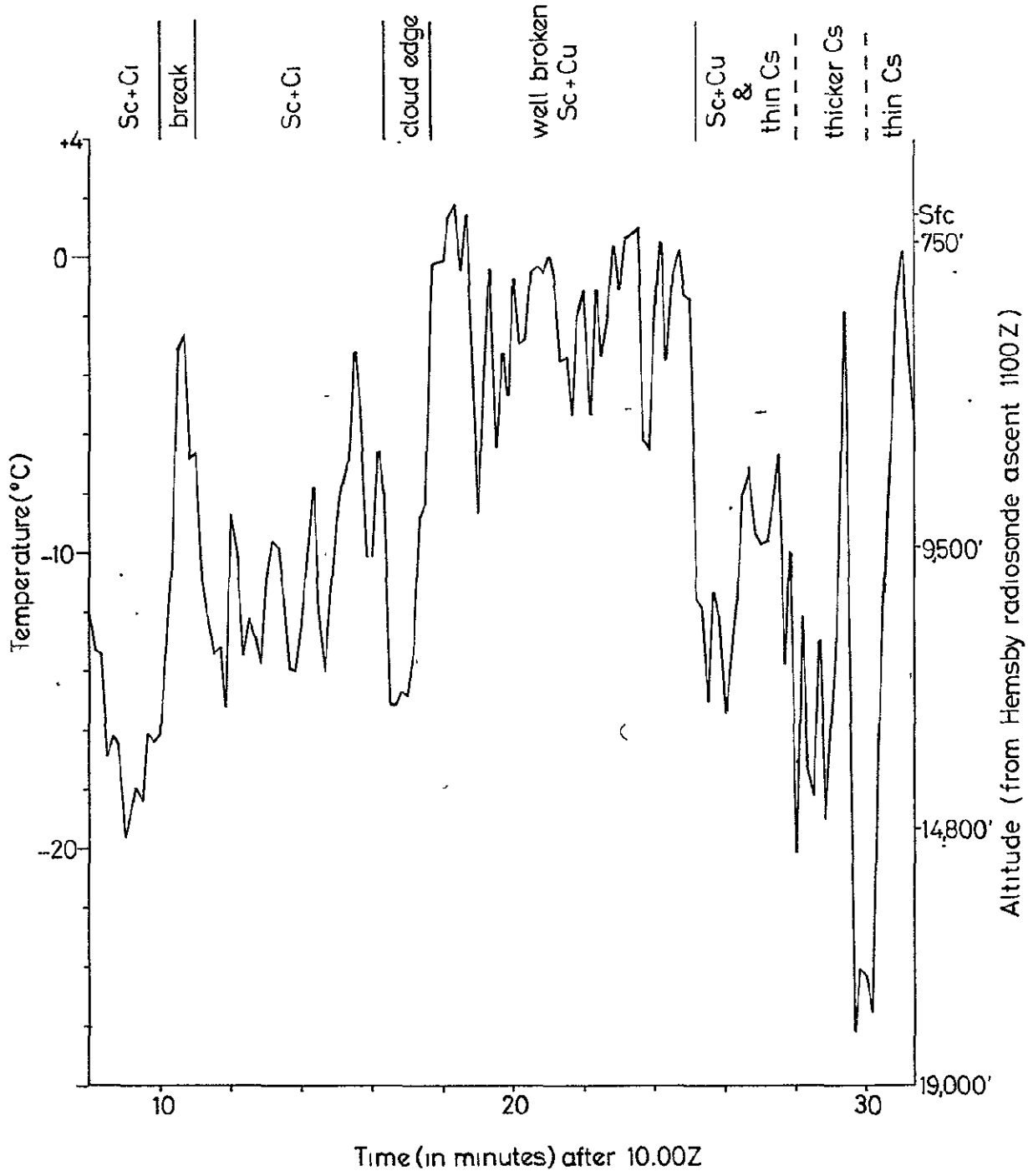

Fig. 23: Barnes PRT-4 radiation temperature trace. Sampling interval = 10 secs.

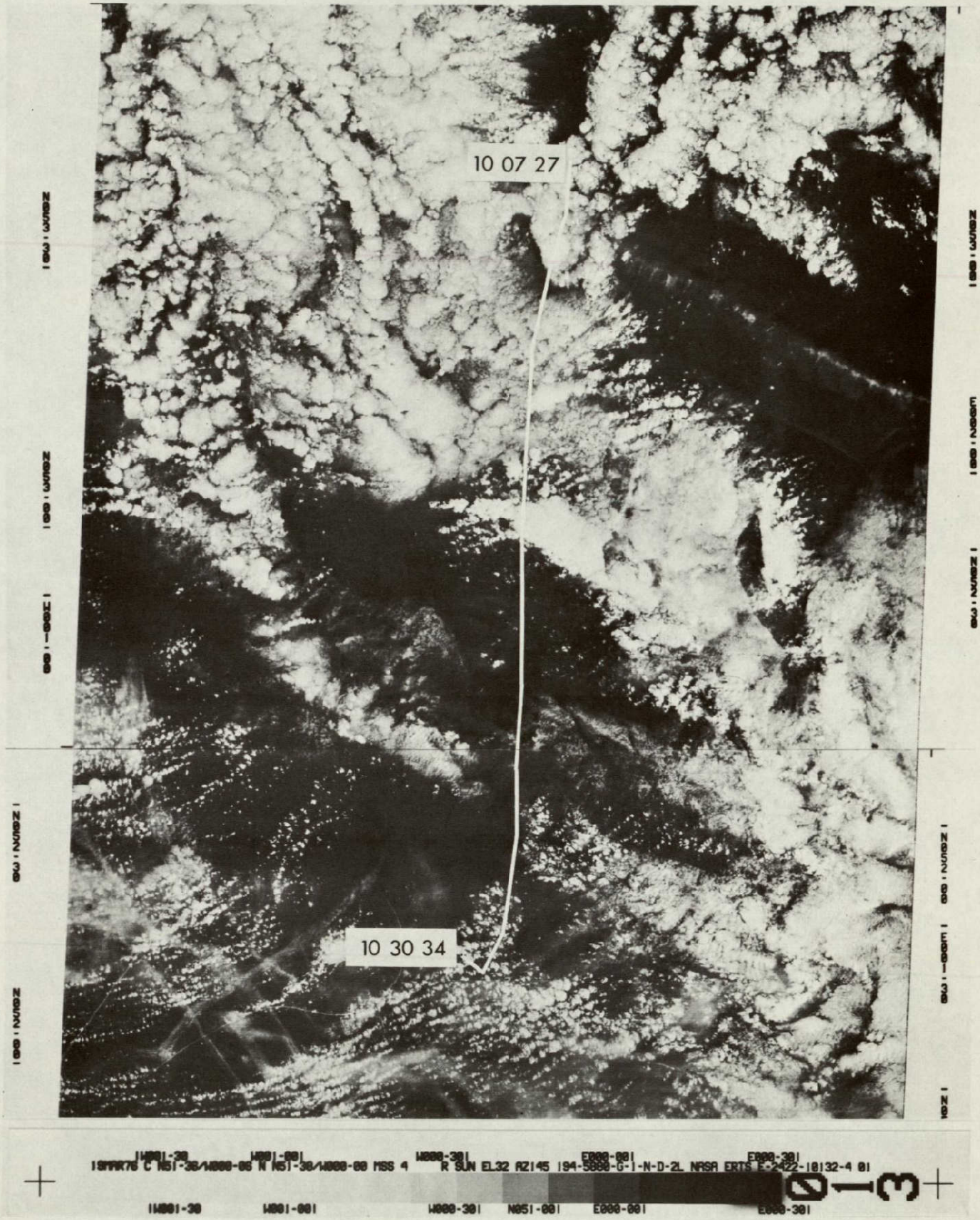

PLATE 8: Landsat 2 imagery of E. Anglia with track of research aircraft taking simultaneous observations of clouds. Band 4.

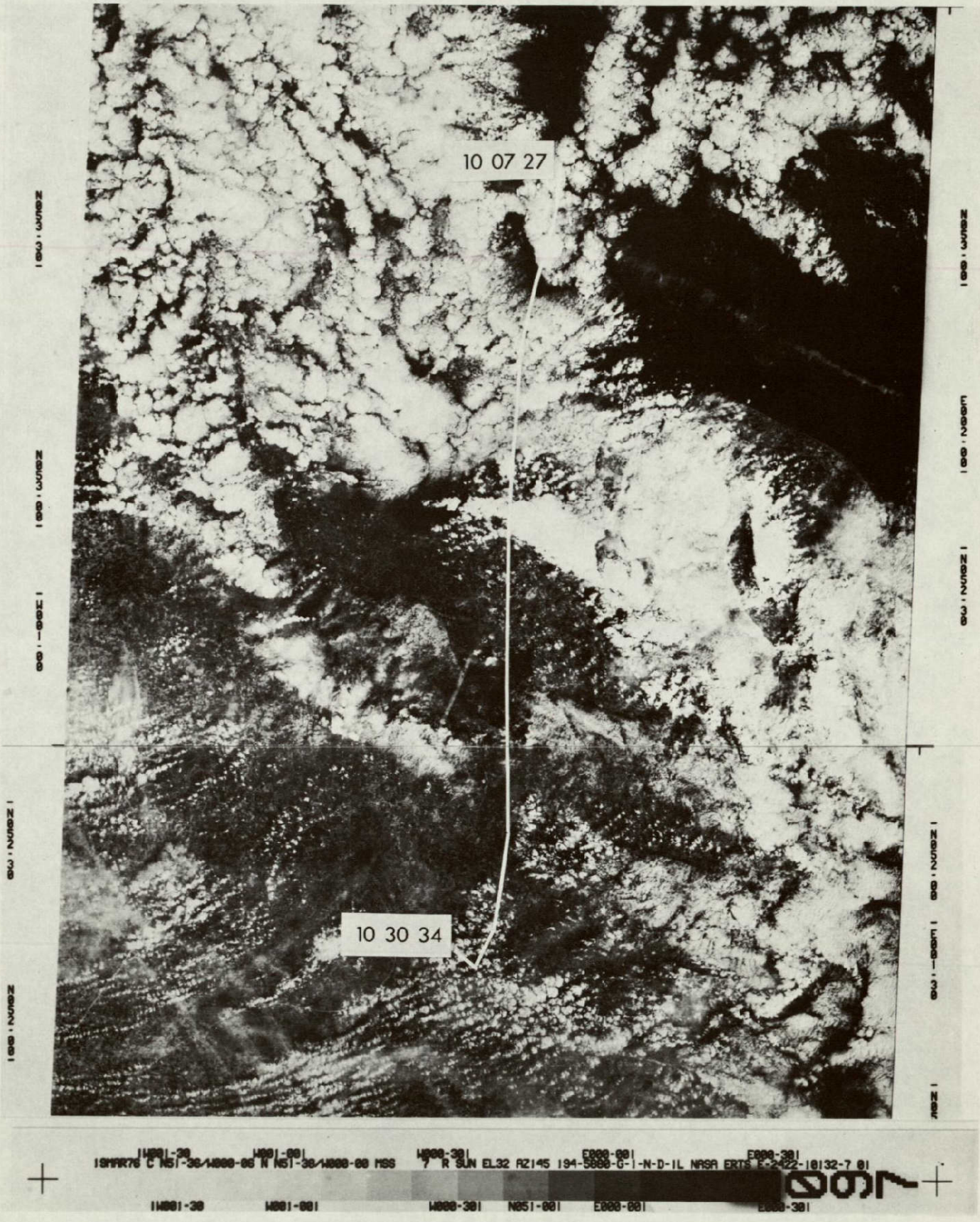

PLATE 9: Landsat 2 imagery of E. Anglia with track of research aircraft taking simultaneous observations of clouds. Band 7.

temperature oscillates around a temperature of about -3°C, occasionally rising above 0°C.

At 1026 the observer noted that the aircraft was at the cloud top, and he reports 8 oktas of cirrostratus. This cirrus is just discernible on the band 4 image, but the lower cumulus and stratocumulus clouds are considerably brighter, and not obscured by the thin cirrus. The temperature dropped now that the aircraft was over a more continuous cloud field. At 1028, the observer noted that the cirrus was thickening, and indeed at this point the upper level cloud begins to obscure the lower level cumulus and stratocumulus. A very low temperature of -26.2°C was recorded just before the end of the flight at 1030. This must have been caused by the surrounding thick cirrus, given as 8 oktas of cirrostratus by the observer. A rapid rise in temperature occurred just afterwards, indicating a break in the cloud canopy.

Comparisons between the Hercules radiation temperature graph (Fig.23) and the Landsat brightness transect graphs (Figs. 24 & 25)

Despite the complications anticipated by the time differences separating some of the aircraft and satellite observations notable similarities are evident between Figure 23 and Figures 24 & 25. Higher radiation temperatures, corresponding to breaks in the cloud are usually reflected in the brightness transects by higher picture densities. For example, between 1010 & 1012 a break in the cloud results in an increase in temperature and a marked decrease in image brightness, particularly in band 7. Certainly the variability of brightness is generally greater in band 7 than band 4, which seems to be caused mainly in this case by spectral reflectance characteristics of thin cirrus, which appears to have a greater influence on image brightness in band 4 than band 7. This conforms to our findings on the multispectral characteristics of clouds, reported in Section III.4.

6. Landsat 2 image brightness and observed rainfall intensities at selected stations across the British Isles

Rainfall intensity data were tabulated along with picture brightness data (in the form of normalised density values) following the procedures outlined in Section II.6. Two examples of the tabulations prepared for different images are presented in Table 10. These data relate to the images portrayed in Plate 10.

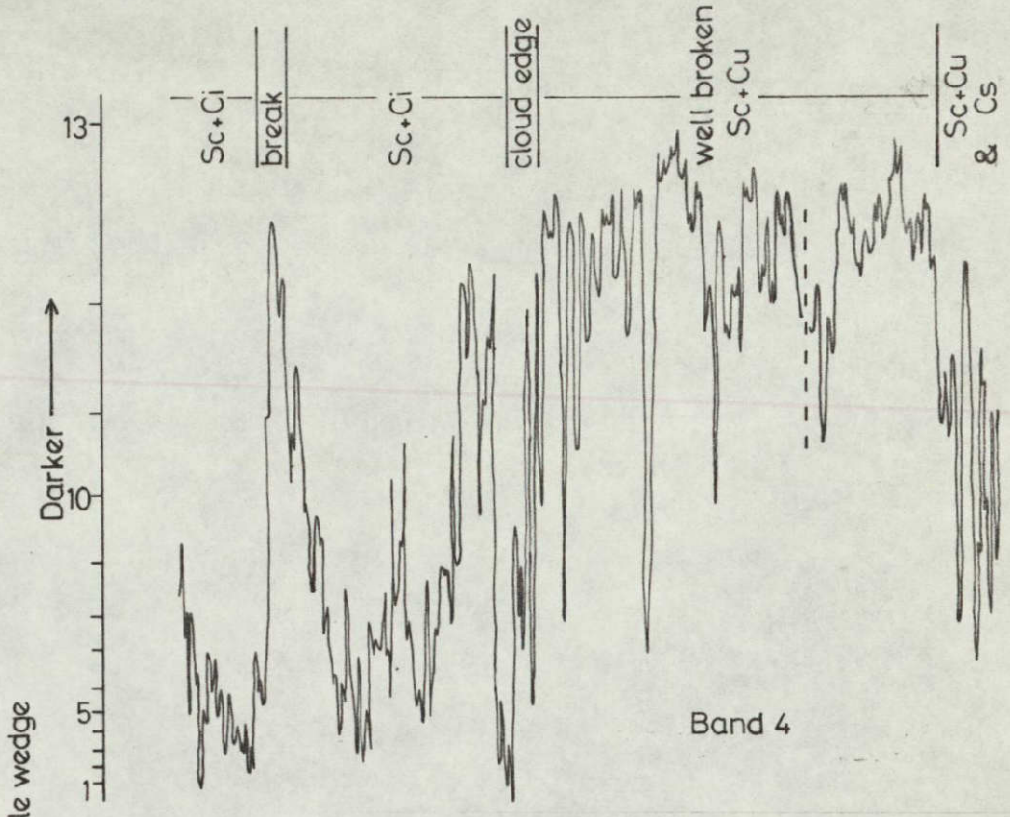

Fig. 24: Band 4 density transect over East Anglia

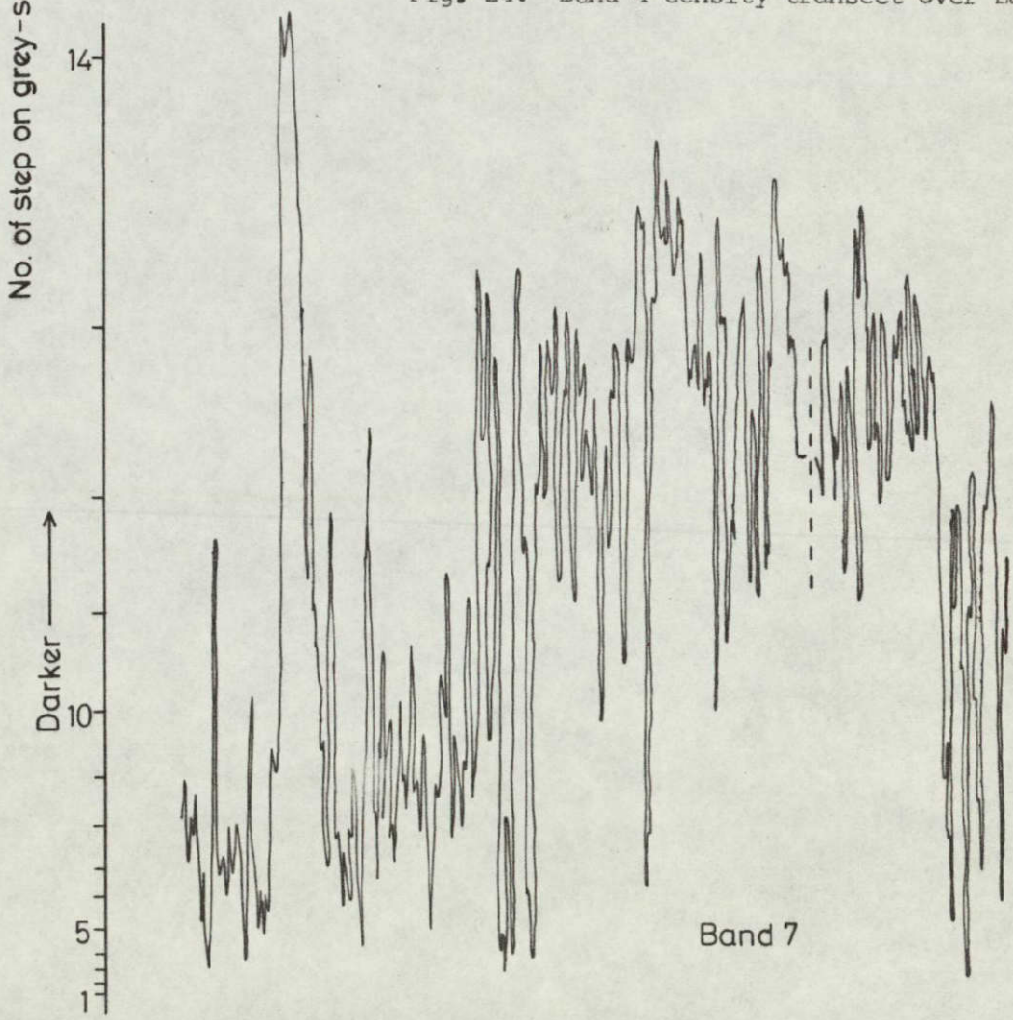

Fig. 25: Band 7 density transect over East Anglia

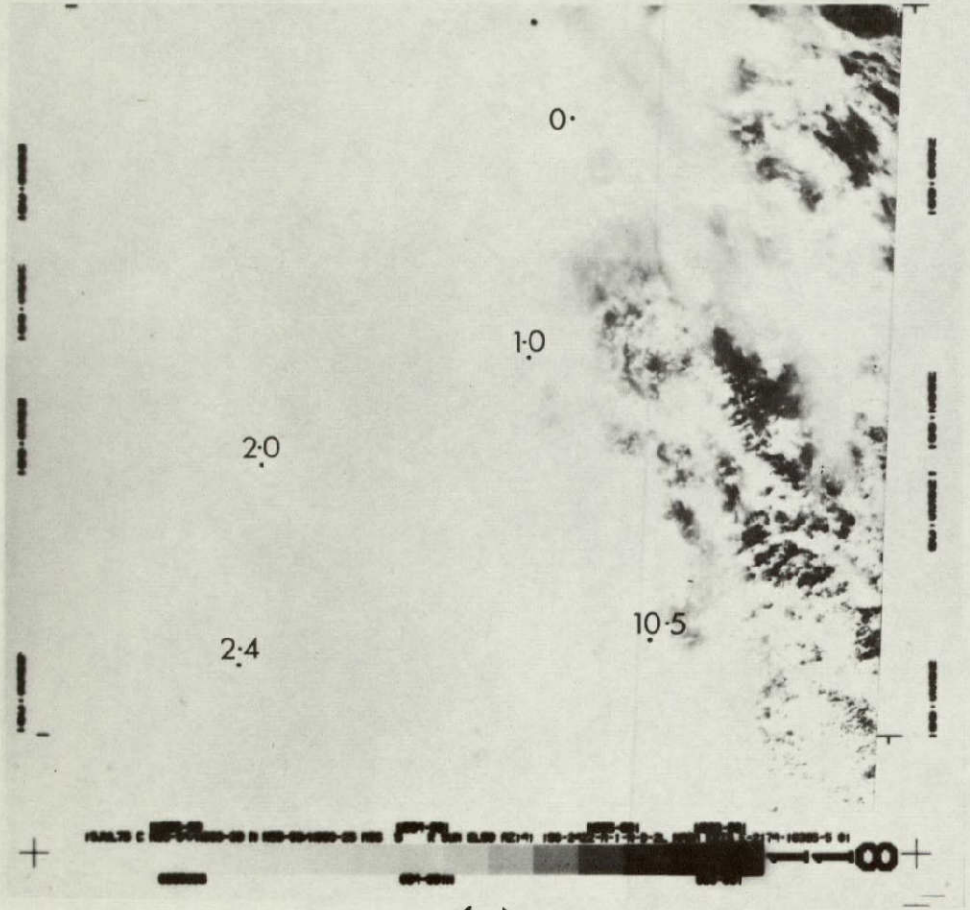

(a)

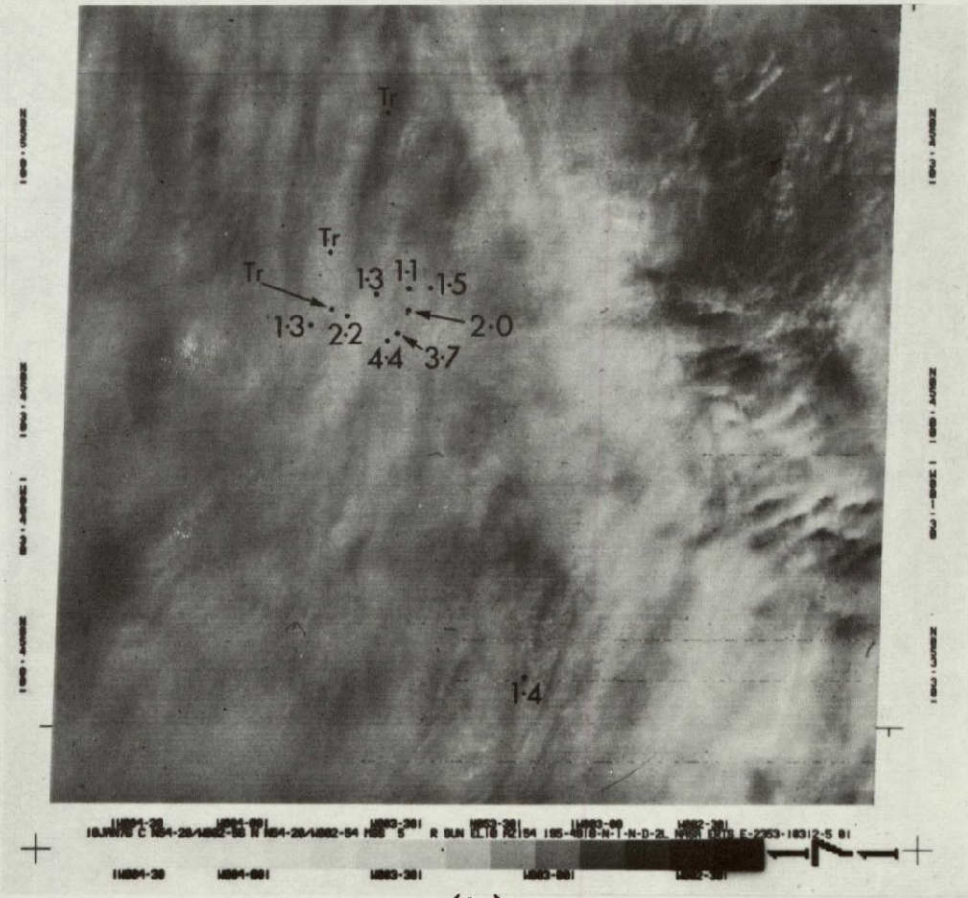

(b)

PLATE 10: Landsat 2 imagery and observed rainfall intensities. (Band 5).
a) 15 July 1975 10:38:50 G.M.T. Sthn.Scotland.
b) 10 January 1976 10:31:20 G.M.T. Lake District.
(Note: Intensities in $mm.hr^{-1}$. Tr = Trace)

Table 10

Sample tabulations of Landsat image brightness and rainfall intensity data

(a) Southern Scotland, 1038:50Z, 15 July 1975

Station	Cloud type	Rainfall Intensity (mm $hr.^{-1}$)	Image brightness per band			
			4	5	6	7
Leuchars	Cu + St cu	0	0.52	0.49	0.37	0.52
Turnhouse	Cu + St cu	1.0	0.35	0.44	0.31	0.33
Eskdalemuir	Cu + Cu Nb	10.5	0.38	0.44	0.31	0.35
Prestwick	Lay^{d} St	2.4	0.37	0.42	0.31	0.31
Glasgow	Lay^{d} St	2.0	0.37	0.44	0.33	0.31

(b) Lake District, 10 January 1976, 1031:20Z

Station	Cloud type	Rainfall Intensity (mm hr^{-1})	Image brightness per band			
			4	5	6	7
Carlisle	Layered St	Tr *	0.47	0.43	0.41	0.48
Squires Gate	"	1.4	0.38	0.35	0.31	0.39
Seathwaite	"	4.4	0.36	0.33	0.29	0.37
Stonethwaite	"	3.7	0.37	0.34	0.31	0.38
Dale Head	"	2.0	0.38	0.35	0.31	0.38
Groove Beck	"	1.5	0.40	0.37	0.34	0.40
Threlkeld	"	1.1	0.39	0.35	0.33	0.39
How Farm	"	1.3	0.38	0.34	0.32	0.37
Linskeldfield	"	Tr	0.38	0.34	0.30	0.37
Bleaberry Tarn	"	2.2	0.38	0.34	0.30	0.37
Cornhow	"	Tr	0.37	0.33	0.30	0.37
Lampligh Hall	"	1.3	0.39	0.35	0.32	0.39

*Note:- Trace (less than 0.05 mm of rain in the past hour)

It is clear from Table 10 that large variations in rainfall occurred in some cases with little or no variation in cloud density. This impression is strengthened by Figures 26(a)-(d), which present the full results for the study. A noteworthy feature of these graphs is their marked similarity to one another, indicating only small band-to-band changes in relations between rainfall intensity and image density. The rainfall intensity values are mostly clustered between 0.2 - 0.5D in all 4 wavebands, there being little or no systematic change in their relations with image density. It is possible that some experimental factors influenced these results. Such factors may have included the following:

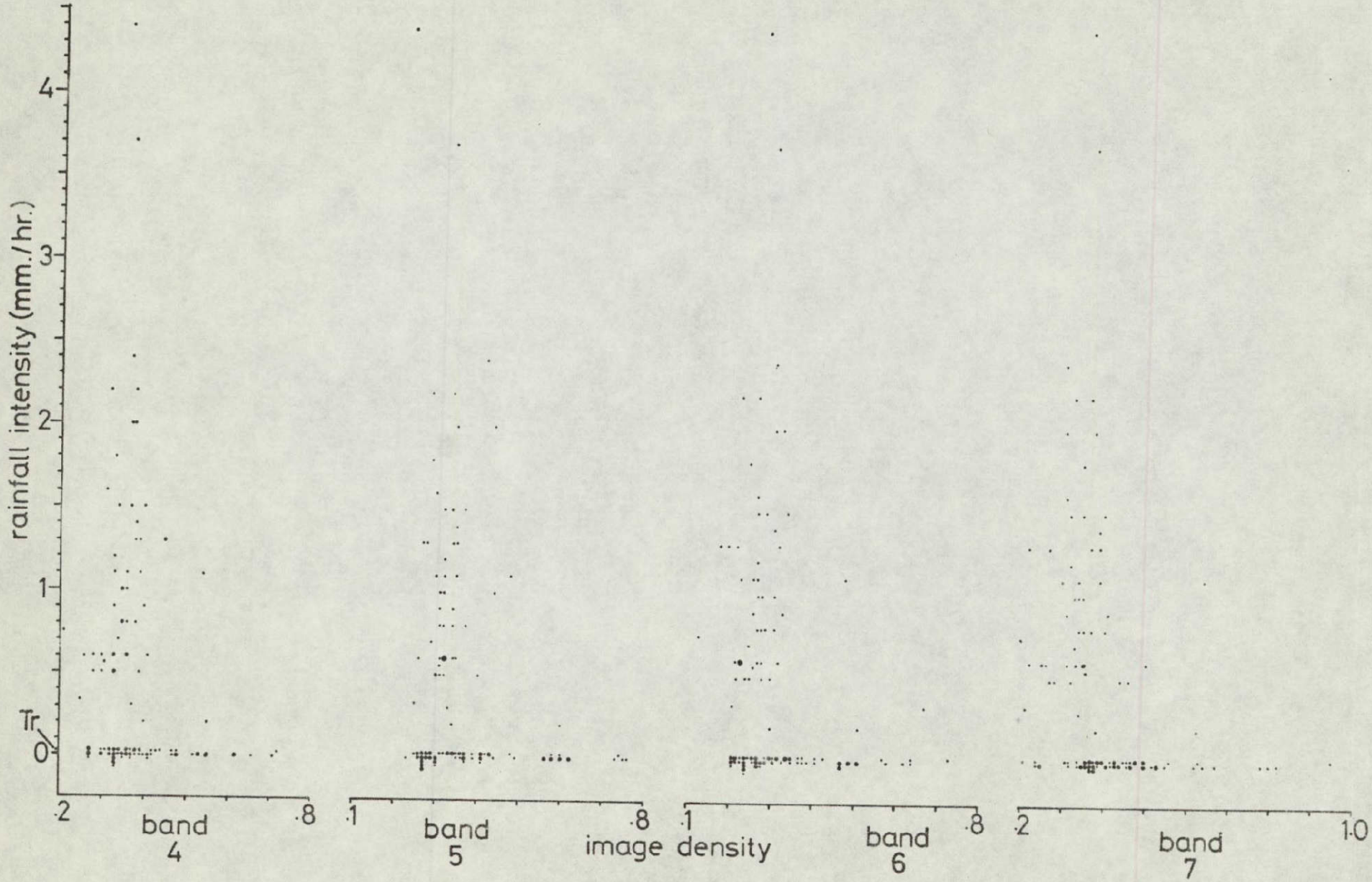

Fig. 26: Image density and rainfall intensity relationships

(a) The rainfall intensity values used in this study were averaged over 1 hour periods (1000-1100Z), whilst the Landsat images portrayed instaneous cloud characteristics. Rainfall intensity at the moment of imaging may not have been represented well by the hourly rainfall data. (Had more time been available for our study some of the data could have been re-processed to yield rainfall intensities for shorter periods of time (e.g. 10 mins. astride the time of the Landsat imagery)).

(b) In assessing image densities, areas around each rainfall station (point locations) were examined. These areas had diameters of 5.4 km on normal-scale imagery, and 2.3 km on the large-scale imagery.

(c) Figures 26(a)-(d) do not reveal the cloud types for which density values were established. The overwhelming majority of the 195 separate cases examined involved stratified cloud of one or more layers, often with low-level stratocumulus. Such situations accounted for 170 cases. The remaining 25 cases mostly involved cumulonimbus (22), with a few instances involving cumulus and stratocumulus (3).

Earlier studies, mainly concerned with tropical or sub-tropical regions have suggested that relationships generally exist between convective cloud brightness (in weather satellite imagery) and rainfall, such that "bright clouds are thicker, and thick clouds are wetter" (Griffith & Woodley, 1973). It would appear from our results that, in middle latitudes at least, a less simple relationship exists between cloud brightness and rainfall intensity, and that additional factors would need to be taken into account were image brightness distributions to be invoked in programmes to map rainfall wholly or in part from satellite data. This matter deserves further attention. Perhaps the most realistic solution for an operational programme would involve a "man/machine mix" method to integrate conventional and/or rainfall radar data with cloud imagery along lines developed by Barrett (see, e.g. 1974, 1977a & 1977b) or Follansbee (1976).

7. Landsat 2 cloud imagery and radar rain-echoes

Section II.7 reported that we were able to undertake only one comparison between a Landsat 2 scene and rainfall radar observations, partly due to the untimeliness of most of our Landsat imagery vis-a-vis the "on-off" pattern of the radar network in the U.K., which is still in relatively early stages of testing and development. Plate 11 reveals that, for the case in hand, the rainfall pattern was centred in a large cell to the north and east of the image centre, with some smaller, scattered, and less intense areas further south. The size of the main cell was approximately 90 km by 30 km, the heaviest rain falling along its north-eastern margin (the leading edge, for the cloud was moving from the south-west). Multilevel cloud is evident along this margin, with stratus or stratocumulus near the surface, altocumulus at middle levels, and a canopy of thick cirrus aloft. The heaviest rainfall seems to lie in the altocumulus zone, perhaps as a result of accentuated lifting processes. These areas of cloud and rain were on the eastern edge of a frontal trough extending from east of Iceland to northern Spain. It is possible that the cloud and rain in the Landsat image were associated with a weak warm frontal feature shown on the synoptic

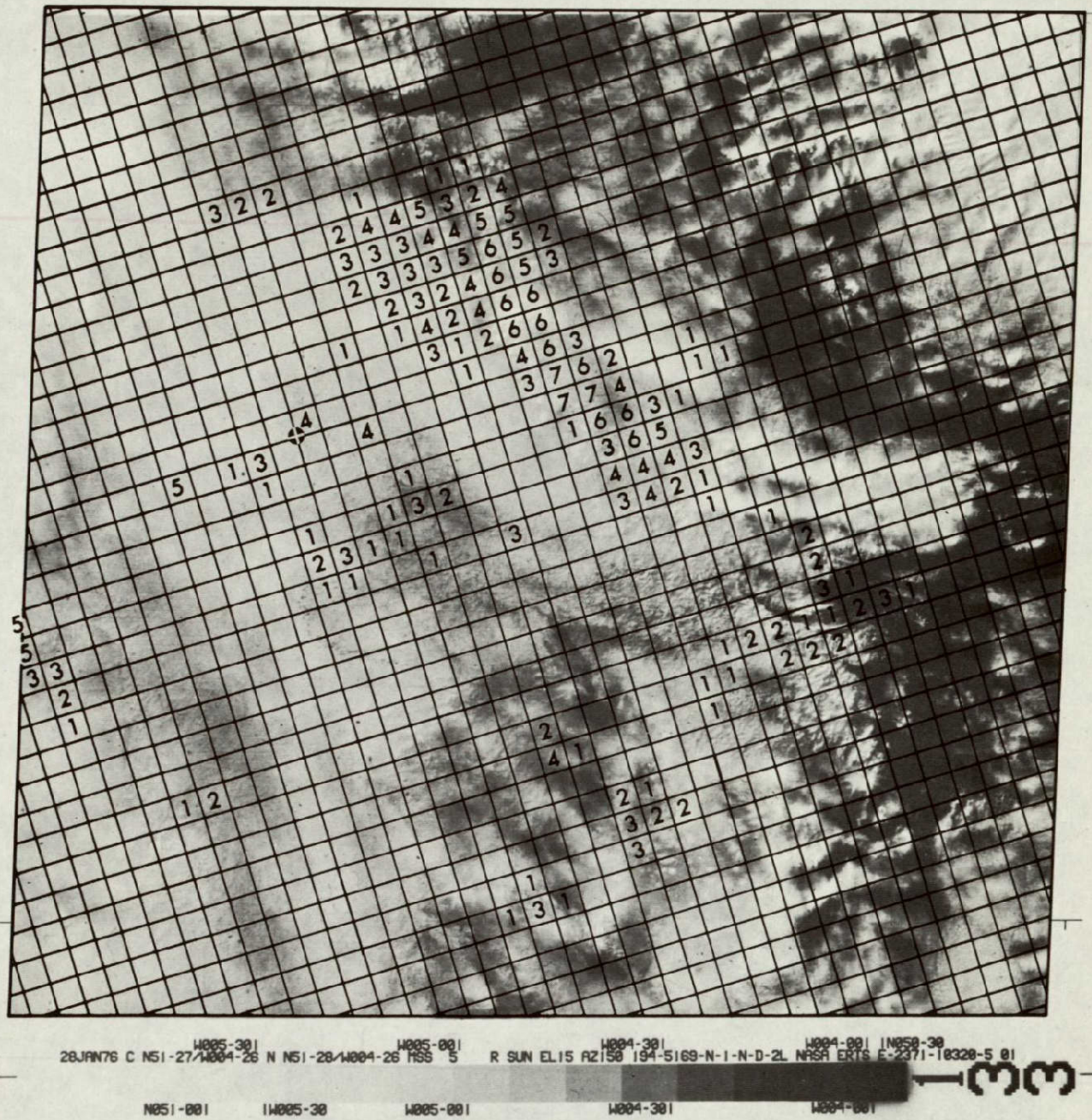

PLATE 11: Landsat 2 imagery over South Wales, with associated rainfall intensities derived by Castlemartin radar.

Note: 0 = less than 0.2 $mm.hr^{-1}$
1 = 0.2 to 0.4 $mm.hr^{-1}$
2 = 0.4 to 0.8 $mm.hr^{-1}$
3 = 0.8 to 1.6 $mm.hr^{-1}$
4 = 1.6 to 3.2 $mm.hr^{-1}$
5 = 3.2 to 6.4 $mm.hr^{-1}$
6 = 6.4 to 12.8 $mm.hr^{-1}$
7 = 12.8 $mm.hr^{-1}$ +

IV SIGNIFICANT RESULTS

1. The Landsat Cloud Photointerpretation Key

The Landsat Cloud Photointerpretation Key presented in this report is thought to be the first based on Landsat cloud imagery, and should be of immediate interest and use to the meteorological community as well as other Landsat investigators. However, it will be of significance also to those concerned with the planning of future satellite projects, most of which will almost certainly provide higher resolution data than their current counterparts or precursors. It seems to be accepted generally that resolutions of 1.0 - 2.5 km are adequate for meteorological satellite operations in the foreseeable future; sensory systems on future polar-orbiting weather satellites like Tiros-N (1.0 km) and on geostationary weather satellites like Meteosat (2.5 km) will have such capabilities.

Our experience with Landsat indicates that a higher resolution has many advantages, not least in cloud recognition.

2. Satellites as platforms for evaluating total cloud amounts

It has been demonstrated that satellites with a sufficiently high resolution capability in the visible region of the electromagnetic spectrum can be used to check the accuracy of estimates of total cloud amount assessed subjectively from the ground, and to reveal areas of performance in which corrections should be made.

Increasing attention is being paid to cloud cover in models of both the heat and hydrological budgets of the Earth (see GARP, 1975). It would seem that satellites imaging once or twice daily with a resolution equal to, or a little less than that of the Landsat 2 system could contribute very significantly to the mapping of cloud cover for both climatological and meteorological purposes. It was remarked above that cloud type recognition can be undertaken with more confidence using Landsat imagery than imagery from current operational meteorological satellites. To this conclusion we can add the complementary belief that the assessment of total cloud cover could be based with benefit upon higher resolution data than current meteorological satellite data and/or ground observing procedures.

3. The significance of cloud shadow for Landsat 2 image utility

It has been demonstrated that, in middle latitudes in summer, cloud shadow may obscure at least half as much again of the land surface covered by an individual Landsat frame as the cloud itself. That proportion would increase with latitude and/or time of year towards the winter solstice. We consider that cloud shadow effects may be of sufficient magnitude in some cases to warrant special mention being made of them in Landsat catalogs for general circulation to the user community.

4. The multispectral characteristics of clouds imaged by Landsat 2

Analyses of sample multispectral images for six different

categories of clouds in summer revealed marked differences between the reflectance characteristics of cloud fields in the visible/near-infrared region of the spectrum. The results hold out hope that, given the additional (thermal infrared) channel on Landsat C, an acceptable multispectral method might be devised for the objective classification of cloud types for unit areas down to individual pixel size. Studies of cloud fields imaged at different times of the year suggest that the reflectance properties and associated spectral signatures of clouds change seasonally for reasons additional to the cyclic changes of solar illumination. These reasons seem to include changes in cloud composition and the height and form of the upper surfaces of clouds.

5. Aircraft as sources of data in support of Landsat cloud image analysis

One study of Landsat 2 imagery and radiation temperature data from a synchronised aircraft flight suggests that observations from aircraft might be very useful in detailed studies of different cloud types in terms of their radiative properties, and their influences on local radiation budgets. The evident relationships observed between cloud types, cloud reflectances, and thermal infrared radiation temperature patterns were generally rather straightforward, and easy to interpret.

6. Landsat 2 image brightness and observed rainfall intensities in the British Isles

Our rather numerous individual observations of Landsat 2 image brightness and recorded rainfall, when aggregated for each MSS waveband, reveal no simple relationship and strongly suggest that image brightness alone could not be used as a reliable indicator of rainfall intensity in the British Isles. It is possible, however, that useful relationships might be established through the utilisation of devices (statistical, empirical, physical) to differentiate between clouds which have similar appearances in the MSS wavebands, yet perform very differently in terms of resulting rain.

7. The value of synchronous studies of Landsat 2 cloud imagery and radar rain echoes

Our single example of synchronised Landsat 2 cloud imagery and simultaneous radar rainfall intensity data revealed that a synoptic weather structure not represented on the nearest synoptic chart to it in time was still significant in terms of both associated cloud and rainfall. Landsat 2 has more to offer than meteorological satellites for synchronous studies of this kind in that the relations between cloud and rain can be examined in greater spatial detail.

V PUBLICATIONS

The following publications arising wholly and directly from this ERTS Follow-on Study have been made during the 21 months allocated to it. Further publications will be made following the approval of the Final Report.

1. Quarterly Reports

E.C.Barrett & C.K.Grant (1975)

Mesoscale assessments of cloud and rainfall over the British Isles. First Quarterly Report, ERTS Follow-on Program Study No. 2962A, NASA-CR-146033, Greenbelt, Md., 28pp.

E.C.Barrett & C.K.Grant (1976)

The identification of cloud types in Landsat MSS images, Second Quarterly Report, ERTS Follow-on Program Study No. 2962A, NASA-CR-146647, Greenbelt, Md., 31pp.

E.C.Barrett & C.K.Grant (1976)

Comparisons of cloud cover evaluated from Landsat imagery and meteorological stations across the British Isles, Third Quarterly Report, ERTS Follow-on Program Study No. 2962A, NASA-CR-148216, Greenbelt, Md., 45pp.

E.C.Barrett, C.K.Grant & R.Harris (1976)

Multispectral characteristics of clouds observed by Landsat 2, Fourth Quarterly Report, ERTS Follow-on Program Study No. 2962A, NASA-CR-148982, Greenbelt, Md.

2. Other Landsat Publications

E.C.Barrett & C.K.Grant (in press):

"An appraisal of Landsat 2 imagery and its implications for the design of future meteorological observing systems", Journal of the British Interplanetary Society.

C.K.Grant (1977)

"The apparent shape of the sky and the estimation of cloud amount", Brycgstowe, University of Bristol Geographical Society, 11, p.37-43.

VI PROBLEMS

The chief problems encountered in this Study were of five kinds. They may be summarised as follows:

(a) The data coverage of the study area. It was pointed out in Section I that this was less complete than had been expected, and, more seriously, excepting in the case of the last Landsat Cycle in our study period, we had no advance information regarding those parts of the study area which might be covered in forthcoming cycles. Such difficulties affected especially the organisation of supporting *in situ* observations.

(b) The types of data received. Since the Landsat data were provided in image form the dependent studies were rather more general and less precise than they might have been had it been possible to analyse CCTs instead. A related problem was that the negatives received from NASA were too dense for positives to be printed from them on existing photographic equipment in the University of Bristol. Consequently, when further copies were required we were forced to produce them through the intermediate stage of a new contact negative.

(c) Available processing systems. As our requirements for access to sophisticated processing systems went far beyond our existing Departmental resources we had to rely more than we would have liked upon access to equipment owned by other establishments, and, in certain cases located in other cities. The most useful special facilities to which access was kindly granted by others included the Quantimet-720, the Photoscan P-1000, and the Harwell Image Processing System. In certain cases the pressure on the facilities was so great that our own use of them was more restricted than we might ideally have liked. Nevertheless we were deeply grateful to all those who gave practical assistance in such ways.

(d) Staffing. The Principal Investigator is a Lecturer in Geography in the University of Bristol, and his time for research is rather limited. Consequently it was fortuitous that the U.K. Natural Environment Research Council awarded a 3-year Studentship to the Department of Geography from 1 October 1975 to undertake analyses of Landsat MSS imagery. Mr. C. K. Grant was appointed to this Studentship and was able to devote most of his time from that date to the date of this Final Report to the ERTS Follow-on Study. Thus, through the 20 months of this Study some 24 man-months in total have been expended by the Principal Investigator and his Co-investigator to obtain the results reported here. Others have contributed time and expert advice on a more *ad hoc* basis. Acknowledgement of their services has been made from time to time in this Report, in addition to the statements in Section X. An associated problem was that of

(e) Time. Given the available research personnel, and the date by which the Final Report had to be presented, less work was possible than the intrinsic information of our Landsat data-file merited. This problem was exacerbated by the receipt of our final batch of images only 7 months before the termination of the study period. Thus,

although the spirit of the Study Agreement was met insofar as the earlier-mentioned problems permitted, it is expected that further results of interest will be gained from analyses of the Landsat 2 coverage of the British Isles after the termination of the formal agreement with NASA. Some suggestions as to the forms this work might take were listed in Section I; others are suggested in Section VIII.

It was as a result of these problems that such deviations as are evident from the original Statement of Work were made.

VII DATA QUALITY AND DELIVERY

Over a 12-month period we received a total of 491 Landsat frames from NASA, of which an overwhelming majority were of a high quality. On their arrival in Bristol a small number were somewhat spoiled by heavy finger-marking, but it was possible in most cases to reduce such effects on image-quality prior to processing and analysis.

The delay between the date of the Landsat imaging and our receipt of the resulting imagery in Bristol was approximately four months at first, lengthening to six months before we received the final batch. This did not hamper our programme excepting in its early and late stages: we were able to begin our serious research only after the date by which the First Quarterly Report was due, and some curtailment of our research was inevitable in the period leading up to the compilation of this Final Report on account of insufficient time for the last sets of data to be fully analysed.

VIII RECOMMENDATIONS

The following recommendations may be made as a result of the studies undertaken of Landsat 2 imagery for the British Isles:

1. Amendments to operational procedures

(a) The variable effect of shadow from clouds in Landsat images seems to have a sufficiently significant effect on image-processing, analysis and interpretation for many applications for it to be desirable for NASA to take account of this effect in assessing the quality and contents of images for reporting to the user community. It would seem worthwhile to propose that research be undertaken to formulate a general model relating cloud and cloud shadow, and that in Landsat Catalogs a column be included to indicate the percentage of each image which is affected by cloud shadows cast onto the ground. This would complement the column indicating the percentage of each image which portrays cloud-covered surfaces.

(b) Since rather constant relationships appear to exist between estimates of total cloud cover made from the ground at synoptic weather stations and estimates made objectively or semi-objectively from Landsat cloud images the feasibility of satellite-based, or surface-based and satellite-augmented, methods for broad-scale cloud mapping would not seem to be in question. It is recommended that such possibilities be further explored.

(c) It is recommended that the attention of meteorological officers and their field observers be drawn to the apparent errors that are common in their assessments of certain sky conditions as detailed in Sections II.2 & III.2, so that the results from the standard conventional procedures for evaluating total cloud amount might be improved.

2. Topics for further research

(a) Since it is highly desirable for several future operational programmes that a suitable method for automatic identification of clouds in satellite data be devised, and since different families of clouds appear to possess different spectral signatures even across the four wavebands investigated by Landsats 1 & 2, it is recommended that studies be undertaken to assess the further assistance that would be afforded to objective cloud mapping methods by the additional (thermal infrared) data expected from Landsat C. It is not impossible that the combination of channels in the Landsat C MSS system might be more informative in this respect than the different combination to be investigated by the AVHRR system of Tiros-N.

(b) The very high resolution data from Landsat satellites should be particularly beneficial in more extensive tests than were possible in this study of relationships between satellite image brightness, radar rain-echoes, and observed rainfall intensities. As expected, image brightness alone is poorly related to rainfall intensity

but it might prove possible, invoking cloud type assessments as well as radar and raingauge data, to develop schemes whereby more accurate rainfall maps might be prepared than any achieved currently in operational programmes. It is recommended that attention be given to this potentially valuable area of research.

(c) It would seem worthwhile to undertake extended studies of the relations between satellite-observed clouds and aircraft observations of their characteristics, cloud-top heights, and radiative properties. Maps of cloud-top altitude are being prepared already from Noaa imagery on a quasi-operational basis (Koffler et al., 1973), but no verifications of which the present authors are aware have been undertaken to check the accuracy of the resulting "3-dimensional nephanalyses". Synchronised aircraft operations, in conjunction with Noaa, Tiros-N, or Landsat passes, should afford valuable data for verification studies, and could provide data of use in rather detailed heat-budget and energy-budget studies.

(d) It is recommended that attention be given to the possibility that the needs of the total user community of environmental satellite data might be met better in the future by integrated systems of satellites less specifically designed and designated for separate agencies than has been generally the case until now. Manifestly, atmospheric scientists can derive much useful information from satellites like Landsat, designed for basic applications in other areas of environmental science. Indeed, the high spatial resolution of the Landsat imagery recommends it highly for certain meteorological purposes - but its low spatial resolution places restrictions presently upon its meteorological utility. In Section IX some suggestions are made as to ways in which the relative advantages of different satellites and satellite systems might be maximised to the benefit of many sections of the satellite data user community.

IX CONCLUSIONS

At the end of this quite lengthy study it is possible to summarise roadly our conclusions concerning the significance of Landsat 1 & 2 as remote sensing platforms for atmospheric studies in two ways. The first is fundamentally practical, and relates intimately to the programme of work we have completed. The second is more conceptual, and has arisen from experience with other satellite observing systems as well as Landsat.

1. The value of Landsat as a meteorological observatory

Although many allusions have been made in the past to a supposition that the first two Landsat satellites have offered little of interest to the meteorological community we believe that our studies, several and varied as they are, strongly refute that point of view. We would not deny the disadvantages of Landsat 1 & 2 as meteorological observing systems, associated most notably with the particular range of wavebands available in their multispectral scanners, the propensity of the MSS image data to become brightness-saturated by clouds too early, and the low frequency of the repetitive viewing of selected geographic locations. We would wish, however, to emphasise the advantages offered by Landsat 1 & 2 over and above those of the more familiar weather satellite systems through the much higher spatial resolution of their data (practically a whole order of magnitude better than that of the highest-resolution weather satellite data), and the unique multispectral capability in the visible and near-infrared. Although operational meteorology may have its immediate needs satisfied by data from systems like Noaa and the forthcoming Tiros-N, this is not always true of the research community. Because tomorrow's operations are influenced by today's research the availability of the spatially and spectrally more detailed Landsat data for meteorological research has been particularly welcome. It is significant that even this Study, with its various restrictions, has been able to point to certain modifications which might, with profit, be made to existing operational procedures.

2. Implications of Landsat for the design and operation of future Earth observation satellite systems

Elsewhere quite detailed consideration has been given to the roles and functions of satellites within the broader complex of Earth observation systems by conventional and/or remote sensing means (Barrett, 1976a). The arguments developed there were based in part upon an appreciation of the capabilities and potentialities of Landsat as well as other satellites. It would seem appropriate at this juncture to reproduce the final section of that paper, which was an attempt to sketch a future optimum system for observing Earth for many and diverse purposes. Perhaps the key background consideration is the fact that resolution (in space, time, or spectral bands) is easily degraded if the original data are too rich for a particular use, but cannot be generated beyond the design capabilities of the systems providing the original data. Since advanced remote sensing systems would be expensive to build, maintain, and support, it would seem

overlap in or between systems designed for different applications. The concluding suggestions seek to meet these ends.

The optimum system

This may be considered in terms of three of its basic attributes, namely its sensor systems, read-out systems, and the data products it provides.

First, concerning satellite sensor systems, it may be said that the practice of mission analysis which has been common hitherto may have involved approaching the problem from the wrong angle. In the design of multidisciplinary satellites it has been common to nominate those branches of environmental science which might be served thereby, then to specify the data requirements scientists in those fields might have, and finally to draw up a compromise package. Perhaps a more successful approach might be to design the sensor system first, and identify the full range of its potential applications afterwards. Now that the electromagnetic spectrum has been rather thoroughly and systematically explored the realisation is dawning that it affords far fewer opportunities for worthwhile observation of the Earth than once was hoped. Indeed, the ideal choice of wavebands for many phenomena coincide. A further development in recent months has been the tendency to feel that in multispectral monitoring data from a small number of channels (two, three or four) is often adequate - besides being much easier to use than data from more elaborate multiband sensors. So a manageable set of sensors might be designed for very general environmental use - including meteorological, oceanographic, and terrestrial - augmented only by sensors for more restricted applications where important data could not be provided by the general package (e.g. atmospheric depth-sounding units for weather studies).

So the specific needs of different branches of environmental science for satellite products would be met by the data processing systems, not by design constraints in the satellites. Products of the desired type and resolution would be prepared at major receiving stations, subject only to the final constraints of the resolution and frequency of the input from the satellites and elsewhere. For this, large, complex computing facilities would be required. However, supplementary data products for more specialised and/or more local use could be prepared cheaply at local receiving stations where cheap, hard-wired processors might be employed to exploit those data received from the satellite by direct read-out links.

Consequently we may conclude with the following propositions concerning the indicated satellite sensor systems, read-out methods, and data products for an optimum Earth observation satellite system operating in conjunction with an appropriate network of in situ sensors (see Fig.27):

(a) A satellite sensor system comprised of a basic (general purpose) package, with ancillary (limited purpose) sensors.

(b) A read-out system involving transmissions of recorded data to principal reception facilities for global or continental-scale programmes and direct read-out data to local reception facilities for more local use.

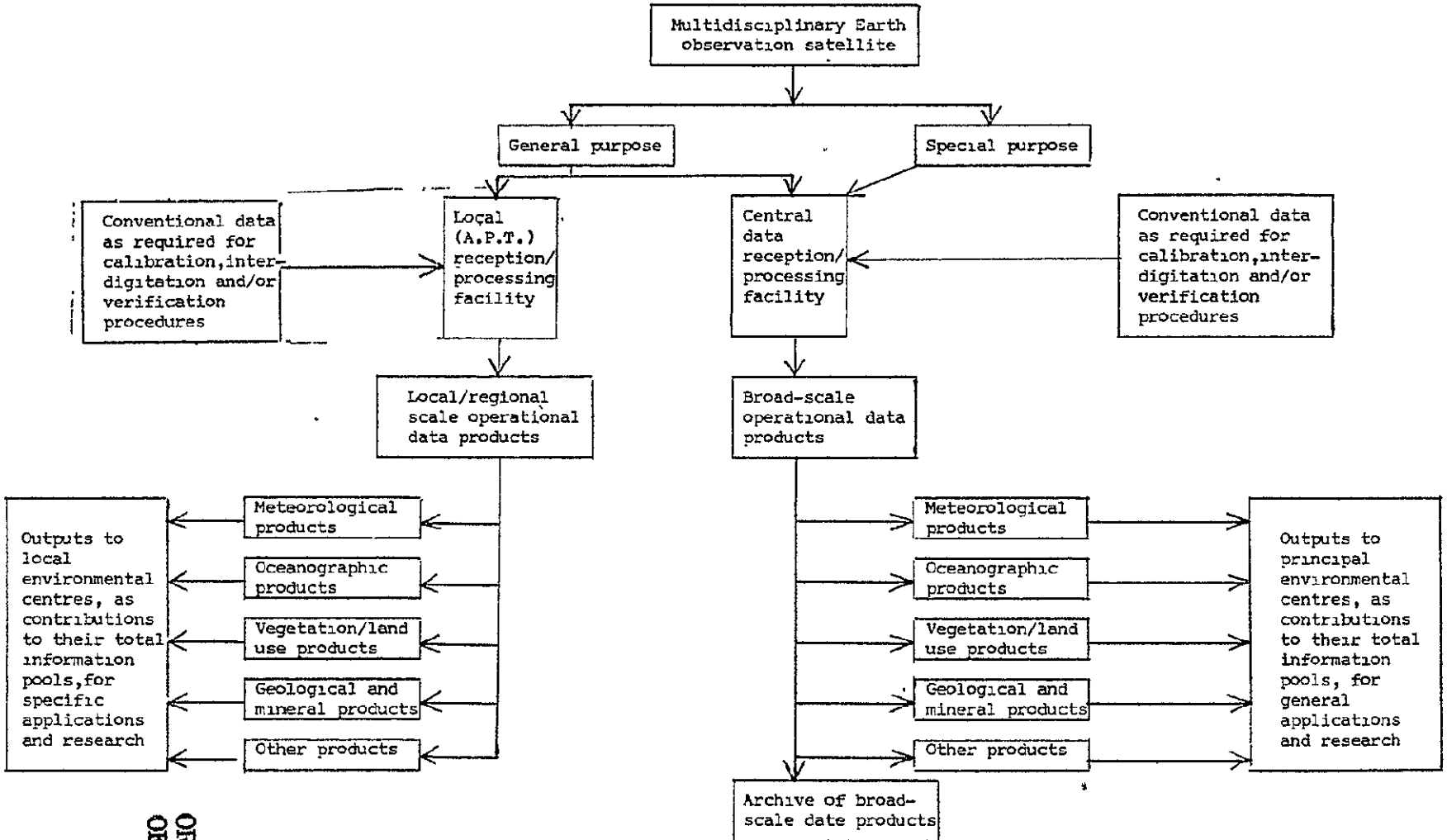

Fig. 27: A proposed pattern for an integrated Multidisciplinary Earth Observation Satellite system, in which the needs of specific users would be met at the data processing stage.

& (c) A central data-processing systems through which wide ranges of operational products for many different applications are prepared, a "total-systems" approach to the analysis of the satellite data. Simpler, and/or more specialised products could be prepared as required at local facilities.

Clearly such systems could not be implemented successfully without a global plan to which many nations should subscribe. So the over-riding need would seem to be for an international body - say a Global Environmental Monitoring Agency - to plan, co-ordinate and operate and maintain a suitable satellite service to meet the needs of many other national and international bodies for that information which is urgently required from remote sensing platforms to improve our knowledge and care of planet Earth.

X ACKNOWLEDGMENTS

Our thanks are due to many institutions and individuals for their help in making this Study possible. In particular we would like to thank the following: the National Aeronautics & Space Administration of the U.S.A. for accepting the initial Study proposals, and for their generous provision of imagery, free of charge, throughout the period of the Study; Dr. J. S. Theon, Discipline Leader for Meteorology, and Mr. H. Oseroff, Technical Monitor for Meteorology, both of NASA, Greenbelt, Md. for advice and practical help during the Study period; the U.K. Department of Industry, for financial assistance for the Study; Mr. D. D. Clark and Miss E. J. Lindsay of Space & Air Research, Division 2, D.O.I., London, for much moral and practical support; the U.K. Natural Environment Research Council for sponsoring the Co-Investigator's Research Studentship; the University of Bristol for permission for the work to be undertaken; the U.K. Agricultural Development & Advisory Service for access to the Quantimet-720 at ADAS, Cambridge, and to Mr.A. Hooper and Mr. T. S. Bell of that Unit for expert guidance on the use of the system; the U.K. Atomic Energy Authority for access to the Harwell Image Processing System, and to Dr. P. Carter for expert guidance on its use; the Molecular Enzymology Laboratory of the Department of Biochemistry, University of Bristol, for access to the Photoscan P-1000 system and neighbouring PDP-11 computer, and to Dr. H. Muirhead and Dr. H. C. Watson for expert guidance on the uses of these systems; the Director-General of the British Meteorological Office for the free provision of maps of hourly weather observations from synoptic weather stations across the British Isles in support of every Landsat pass, and to Mr. G. J. Day for making the practical arrangements; the Meteorological Research Flight, Royal Aircraft Establishment, especially Dr. D. G. James, for MRF Hercules data in support of a Landsat pass over East Anglia; the Procurement Executive, Royal Radar Establishment, Ministry of Defence, especially Dr. T. Harrold, for radar imagery synchronised with Landsat imagery of western England and Wales; the Meteorological Office, especially Mr. C. K. Folland; and the Department of Engineering, University of Bristol, especially Dr. T. Shaw, for access to MTER data files of continuously-recorded rainfall across the United Kingdom; the University of Bristol Computer Centre, especially N. Markovits, for aid with data retrieval; Dr. R. Harris, now of the Department of Geography, University of Durham, for assistance with problems of image analysis and computing; last, but not least, to many friends and colleagues in this University and elsewhere who have in any way helped in the furtherance of this Study to its present completion.

XI REFERENCES

American Society of Photogrammetry (1975): "Manual of remote sensing", Volume II, Chapter 14, "Fundamentals of Image Interpretation", American Society of Photogrammetry, Falls Church, Va., pp. 869-1072.

Anderson, R.K. et al., (1974) : "The use of satellite pictures in weather analysis and forecasting", W.M.O. Technical Note No. 124, World Meteorological Organization, Geneva, 275 pp.

Barnes, J.C., Beran, D.W., and Glaser, A.H. (1967) : "Cloud obscuration of Apollo landmarks derived from meteorological satellite observations", Final Report, Contract No. 1LB-2221B Allied Research Associates, Inc., Concord, Mass., U.S.A.

Barnes, J.C. and Chang, D. (1968) : "Accurate cloud cover determinations and its effects on albedo computations". Final Report, Contract No. NAS5-10478 Allied Research Associates, Inc., Concord, Mass, U.S.A., 82 pp.

Barrett, E.C. (1973) : "Forecasting daily rainfall from satellite data", Monthly Weather Review, 101, p. 215-22.

Barrett, E.C. (1974) : "Estimates of daily and monthly rainfall from weather satellite data", in Environmental Remote sensing and achievements (ed. E.C. Barrett and L.F. Curtis), Edward Arnold, London, p.241-266.

Barrett, E.C. (1976a) : "Identifying the optimum system for observing Earth", Paper presented to the NATO Advanced Research Institute on Earth Observation Systems, Bermuda, 15 pp.

Barrett, E.C. (1976b) : "Cloud and thunder", in The Climate of the British Isles (ed. T.J. Chandler and S. Gregory), Longmans, London, p.199-210.

Barrett, E.C. (1977a) : "Mapping rainfall from conventional data and weather satellite imagery across Algeria, Libya. Morocco and Tunisia", Desert Locust Satellite Application Project, Stage II, Consultant's Report to DLCC/FAO, Rome, Italy, 13 pp.

Barrett, E.C. (1977b) : "Applications of weather satellite data to mapping rainfall for the solution of associated problems in regions of sparse conventional data", in Remote sensing of the terrestrial environment", (eds. R.F. Peel, L.F. Curtis and E.C. Barrett), Butterworths, London. p. -

Barrett, E.C. and Grant, C.K. (1975) : "Mesoscale assessments of cloud and rainfall over the British Isles", ERTS Follow-on Programme Study No. 2962A, First Quarterly Report, NASA-CR-146033, Greenbelt, Md., 28 pp.

Barrett, E.C. and Grant C.K. (1976a) : "The identification of cloud types in Landsat MSS images", ERTS Follow-on Programme, Study No. 2962A, Second Quarterly Report, NASA-CR-146647, Greenbelt, Md., 50pp.

Barrett, E.C. and Grant, C.K. (1976b) : "Comparisons of cloud cover evaluated from Landsat imagery and meteorological stations across the British Isles", ERTS Follow-on Programme, Study No. 2962A, Third Quarterly Report, NASA-CR- 148216, Greenbelt, Md., 45pp.

Barrett, and Grant, C.K. (in press) : "An appraisal of Landsat 2 cloud imagery and its implications for the design of future meteorological observing systems", Journal of the British Interplanetary Society.

Barrett, E.C., Grant, C.K., and Harris, R. (1976) : "Multispectral characteristics of clouds observed by Landsat 2", ERTS Follow-on Programme, Study No. 2962A, Fourth Quarterly Report, NASA-CR-148982, Greenbelt, Md., 50 pp.

Barrett, E.C. and Harris, R. (1977) : "Infrared nephanalysis", Meteorological Magazine, 106, pp.11-20.

Carter, P. and Gardner, W.E. (1977) : "An image-processing system applied to Earth-resource imagery", in Environmental remote sensing: practices and problems, (ed. E.C. Barrett and L.F. Curtis), Edward Arnold, London, p.143-162.

Clapp, P.F. (1964) : "Global cloud cover for seasons using TIROS nephanalyses", Monthly Weather Review, 92, pp.495-507.

Coburn, A.R. (1971) : "Improved three dimensional nephanalysis model", AFGWC Technical Memorandum 71-2, Offutt Afb Nebr. 72pp.

Colvocoresses, A.P. (1973) : "Towards an operational ERTS - Requirements for implementing cartographic applications of an operational ERTS type satellite", 3rd ERTS-1 Symposium, Vol. 1, Paper L15, pp.539-557, G.S.F.C. Washington, D.C. (NASA SP-351).

Conover, J.H. (1962) : "Cloud interpretation from satellite altitudes", Research Note No. 81, Air Force Cambridge Research Laboratories, Cambridge, Mass., 55pp.

Conover, J.H. (1963) :"Cloud interpretation from satellite altitudes", Research Note No. 81, Supplement 1, Air Force Cambridge Research Laboratories, Cambridge, Mass., 18pp.

Cooley, D., Ball, J. and Pavlowitz, A. (1967) : "The objective analysis of cloud cover using satellite and surface data", Final Report, Contract No. N62306-1675, Travelers Research Center, Inc.

Danko, J.M. (1974) : "Meteorological utility of high resolution multi-spectral data", Final Report, No. E74-10635, Radio Corporation of America, 68pp.

Duda, R.O., Mancuso, R.L. and Serebreny, S.M. (1973) : "Automatic instrument systems for determining cloud amount", Journal of Applied Meteorology, 12, pp.537-542.

Fisher, C.F. (1971) : "The new Quantimet 720", Microscope, 19, pp.1-20.

Folk, R.L. (1965) : "Petrology of sedimentary rocks", Austin, Texas, Hemphill's.

Folk, R.L. and Ward, W.C. (1957): "Brazos River bar: a study in the significance of grain size parameters", Journal of Sedimentary Petrology, 27, pp.3-26.

Follansbee, W.A. (1976) : "Estimation of daily precipitation over China and the USSR using satellite imagery", Noaa Technical Memorandum NESS 81, 30pp.

GARP, (1975) : "The physical basis of climate and climate modelling", GARP Publications Series No. 16, ICSU/WMO, Geneva, 265pp.

Glaser, A.H., Barnes, J.C. and Beran, D.W. (1968) : "Apollo landmark sighting : An application of computer simulation to a problem in applied meteorology", Journal of Applied Meteorology, 7, pp. 768-779.

Godshall, F.A. (1971) : "The analysis of cloud amount from satellite data" Transactions of the New York Academy of Sciences, Series II, 33, No. 4, pp. 436-453.

Grant, C.K. (1977) L "The apparent shape of the sky, and the estimation of cloud amount", Brycgstowe, Univ. of Bristol Geographical Society, pp.37-43.

Greaves, J.R. (1973) : "Development of a global cloud model for simulating earth-viewing space missions", Journal of Applied Meteorology, 12, pp. 12-22.

Greenwood, B. (1972): "Modern analogues and the evaluation of a Pleistocene sedimentary sequence", Transactions of the Institute of British Geographers, 56, pp.145-169.

Harris, R. and Barrett, E.C. (1975) : "An improved satellite nephanalysis", Meteorological Magazine, 104, pp. 9-16

Higgitt, M. (1977) : "Seasonal variations in mid-latitude cloud brightness in multispectral Landsat imagery", Stage III Project Report, Univ. of Bristol, 57pp.

H.M.S.O. (1969) : Observers Handbook, Her Majesty's Stationery Office, London, 221pp.

Hopkins, M.M. (1967) : "An approach to the classification of meteorological satellite data", Journal of Applied Meteorology, 6, pp.164-78.

Imanco (1971) : "Quantimet 720 Image Analysing Computer, Operating Manual", 2nd Edition, Imanco, Cambridge Instruments, Royston, Herts., England.

James, D.G. and Nicholls, J.M. (1976) : "The current work of the meteorological research flight", Meteorological Magazine, 105, pp.86-89.

Koffler, R., de Cotiis, A.G. and Rao, P.K. (1973) : "A procedure for estimating cloud amount and height from satellite infrared radiation data", Monthly Weather Review, 101, pp.240-243.

Lee, R. and Taggert, C.I. (1969) : "A procedure for satellite cloud photo-interpretation, and appearance of clouds from satellite altitudes", in Satellite Meteorology, Bureau of Meteorology, Melbourne, Australia, pp.17(e) - (f).

Malberg, H. (1973) : "Comparison of mean cloud cover obtained by satellite photographs and ground-based observations over Europe and the Atlantic". Monthly Weather Review, 101, pp.893-897.

Martin, D.W. and Scherer, W.D. (1973) : "Review of satellite rainfall estimation methods", Bulletin of the American Meteorological Society, 54, pp.661-670.

Miller, A. and Neuberger, H. (1945) : "Investigations into the apparent shape of the sky", Bulletin of the American Meteorological Society, 26, pp.212-216.

Miller, D.B. (1971) : "Automated production of global cloud-climatology based on satellite data", Proceedings of the 6th Automated Weather Support Technical Exchange Conference, U.S. Naval Academy, Air Weather Service, U.S.A.F., Technical Report 242, pp.291-306.

Mott, P.G. and Chismon, H.J. (1975) : "The use of satellite imagery for very small scale mapping", Photogrammetric Record, 8(46), pp.458-475.

N.A.S.A. (1971) : "Data users handbook", NASA, Greenbelt, Md.

N.A.S.A. (1974) : Provision for participation in the Landsat Follow-on Programme, Mimeographed notes, N.A.S.A., Washington, D.C..

N.A.S.A. (1975) : "Proceedings of the NASA Earth Resources Survey Symposium", NASA TM-X-58168, NASA, Houston, Texas.

Neuberger, H. (1951) : "General meteorological optics", in Compendium of Meteorology, (ed. T.F. Malone), American Meteorological Society, Boston, Mass., pp.61-78.

Rosenfeld, A. (1970) : "A non-linear edge detection technique", Proceedings of the IEEE, 58, pp.814-816.

Ruff, I., Koffler, R.,Fritz, S., Winston, J.S. and Rao, P.K. (1968) : "Angular distribution of solar radiation reflected from clouds, as determined from Tiros 4 radiometer measurements", ESSA Technical Report, NESC-38, Washington, D.C., 64pp.

Sherr, P.E., Glaser, A.H., Barnes, J.C. and Willand, L.H. (1968) : "World-wide cloud cover distributions for use in computer simulations", NASA Contractor Report, NASA CR-61226, Contract NAS 8-21040, Allied Research Association, Inc., Concord, Mass., U.S.A., 272pp.

Sadler, J.C. (1969) : "Average cloudiness in the tropics from satellite observations", East-West Center Press, Honolulu, 22pp.

Werner, C. (1973) : "Automatic cloud cover indicator system", Journal of Applied Meteorology, 12, pp.1394-1400.

Winston, J.S. (1971) : "The annual course of mean zonal albedo as derived from Essa 3 and 5 digitized picture data", Monthly Weather Review, 104, pp.284-291.